A genetic system to study

the nuclear pore complex permeability barrier

of the yeast *Saccharomyces cerevisiae*

Dissertation

for the award of the degree
"Doctor rerum naturalium" (Dr. rer. nat.)
of the Georg August Universität Göttingen

submitted by

Michael Ridders

born in

Krefeld, Germany

Göttingen 2012

Affidavit

I hereby declare that this dissertation **"A genetic system to study the nuclear pore complex permeability barrier of the yeast *Saccharomyces cerevisiae*"** has been written independently with no other aids or sources than quoted.

This dissertation has not been submitted elsewhere for any academic award or qualification.

<div align="right">

Michael Ridders

April, 2012

Göttingen, Germany

</div>

However beautiful the strategy, you should occasionally look at the results.

WINSTON CHURCHILL

Contents

List of Figures

List of Tables

Acknowledgements - Danksagung

Darüber hinaus haben mich Susanne und Heike bei zahlreichen Klonierungen unterstützt. Besonders zu erwähnen ist auch Gabi, die für mich unzählige Midis präpariert hat und immer noch begeistert nach mehr verlangt, sowie Uwe und Elisabeth, die für uns alle stets fleißig autoklavierten, spülten, alliquotierten und sowieso Ordnung hielten. Ein Danke auch an Connie, die den Laden hier am Laufen hält.

Ohnehin möchte ich mich bei der gesamten Abteilung Görlich für die einmalige Arbeitsatmosphäre, die Diskussionen sowie die Anregungen und Ideen bedanken.

Darüber hinaus möchte meine Dankbarkeit gegenüber GGNB für seine finanzielle und administrative Unterstützung ausdrücken. Das Engagement der Beteiligten um den Aufbau einer großartigen Graduiertenschule kann man gar nicht genug hervorheben.

Ebenso bedanke ich mich bei allen, die meine Zeit in Göttingen zu mehr als zu reiner Arbeitszeit werden ließ.

Ganz besonders möchte ich meinen Eltern, Großeltern und Brüdern danken. Sie haben mir das mit auf den Weg gegeben, was man als Wissenschaftler unbedingt benötigt - innere Ruhe, Selbstvertrauen und die Kraft auch größte Frustrationen zu überstehen. Und auch wenn sie sich vielleicht nur schwer vorstellen können, was ich hier in Göttingen getan habe, so vermittelten sie mir doch immer das Gefühl, dass sie sich sicher sind, dass ich es schaffen werde.

Last but not least möchte ich mich von ganzem Herzen bei Katrin bedanken, die seit mehr als zwei Jahren an meiner Seite steht und mit ihrer Liebe mein Leben erhellt und bereichert.

Danke Euch allen!

Abstract

All nucleocytoplasmic transport occurs through nuclear pore complexes (NPCs). To hinder uncontrolled mixing of cytoplasmic and nuclear content, NPCs maintain the permeability barrier that suppresses passage of inert macromolecules but allows facilitated transloca- tion of even very large cargoes provided these are bound to nuclear transport receptors (NTRs). About a third of the proteins that built up the NPC contains so-called FG domains that are essential for establishing the NPC permeability barrier. NTRs bind to FG motifs and this interaction is essential for their privileged passage. How this binding accelerates NPC passage is one of the enigmas in the field.

FG domains are quite diverse, differing in their cohesiveness, in their FG motifs, their length, their charge distribution, and in the sequence of the spacers between the indi- vidual FG motifs. The biophysical and biochemical properties of individual FG domains have been well studied *in vitro*. The significance of most of the observed features for the functionality of the permeability barrier *in vivo*, however, so far remained unclear. Pre- viously, the *in vivo* significance of individual FG domains was studied by generating *S. cerevisiae* deletion strains lacking multiple FG domains in various combinations. We show that previously reported lethal phenotypes of the combined deletion of FG domains were not exclusively caused by the deletions but were a result of the previously applied dele- tion strategy. Moreover, with an alternative deletion strategy, we show that *S. cerevisiae* tolerates more FG domain deletions than expected so far.

The focus of my PhD work has been to elucidate which FG domain features are essential for permeability barrier function *in vivo*. We established an *in vivo* system allowing to analyze the functional contribution of individual FG domains by testing the consequences of mutations, deletions, or exchange of these domains for cell viability. Employing this *in vivo* system, we find that the very cohesive FG domains of Nup100p and Nup116p play a prominent role in maintaining the permeability barrier. We show that not all FG domains can functionally replace these prominent FG domains, suggesting that NTR binding alone is not sufficient to explain the functionality of the permeability barrier. Additionally, we show that the anchor points for FG domains within the NPC are not equivalent.

Our findings support models of permeability barrier functionality that rely on the cohe- siveness of FG domains. Based on our results, we, however, assume that both the excessive presence of cohesive FG mass as well as the absence of very cohesive FG domains is in- compatible with viability.

1 Introduction

Eukaryotic life is characterized by the separation of cellular processes into distinct compartments. Presumably, this compartmentalization was a prerequisite for the evolution of multicellular organisms as it allows a higher degree of organization and regulation.

A highly specialized compartments is the nucleus that gives eukaryotes their name[1]. It is surrounded by the double membrane of the nuclear envelope (NE) that separates nuclear processes, like transcription, from cytoplasmic processes, e.g. translation.

This spatial separation necessitates tremendous bidirectional transport processes, since on the one hand the proteins of the transcription machinery are synthesized in the cytoplasm whereas on the other hand the information for protein synthesis, i.e. the mRNA templates, originate from the DNA stored in the nucleus. Additionally, ribosomal subunits are assembled in the nucleus and need to cross the NE before they can fulfill their function in the cytoplasm.

These transport processes occur via nuclear pore complexes (NPCs) that perforate the nuclear envelope (Bahr and Beermann, 1954) and therewith provide the transport route between cytoplasm and nucleoplasm (Feldherr, 1962).

To avoid uncontrolled intermixing of cytoplasm and nucleoplasm, NPCs establish the so-called "permeability barrier" (Paine *et al.*, 1975). This barrier excludes inert macromolecules >40 kDa or $\geq$ 5 nm in diameter (Paine and Feldherr, 1972; Mohr *et al.*, 2009), but at the same time permits facilitated passage of even very large cargoes, provided these are bound to nuclear transport receptors (reviewed by Görlich and Kutay, 1999; Fried and Kutay, 2003).

NPCs are large structures of ∼66 MDa in the yeast *S. cerevisiae* (Rout and Blobel, 1993) and of ∼125 MDa in higher eukaryotes (Reichelt *et al.*, 1990) that exhibit an eight-fold rotational symmetry (Wischnitzer, 1958; Gall, 1967). They are build up by multiple copies

---

[1]from the Greek $\epsilon \upsilon$ (eu, "good") and $\kappa \alpha \rho \upsilon \omega \tau \sigma \varsigma$ (karyotos, "nut-like")

1

of ∼30 different proteins (Rout *et al.*, 2000; Cronshaw *et al.*, 2002), generally referred to as nucleoporins (Nups).

Electron microscopy studies visualized NPCs from *Xenopus laevis* (Hinshaw *et al.*, 1992; Akey and Radermacher, 1993; Stoffler *et al.*, 2003), *Saccharomyces cerevisiae* (Yang *et al.*, 1998; Kiseleva *et al.*, 2004), *Chironomus thummi* (Kiseleva *et al.*, 1998), and *Dictyostelium discoideum* (Beck *et al.*, 2004, 2007) and thereby showed that the overall structure of the NPC is evolutionary conserved. The central core of the NPC is formed by two nearly identical rings that are embedded in the NE. On the cytoplasmic side, filaments emanate from the NPC into the cytoplasm, whereas at the nucleoplasmic side filaments build up a structure called the nuclear basket (see figure 1.1 A for a consensus model).

Interestingly, the atomic structures from several Nups obtained in the recent past years (see e.g. Brohawn *et al.*, 2008; Nagy *et al.*, 2009; Whittle and Schwartz, 2009) show a striking similarity to the structural organization of membrane vesical-coating proteins (reviewed by Field and Dacks, 2009; Onischenko and Weis, 2011; Aitchison and Rout, 2012). These observations support the previously stated "protocoatomer hypothesis", which proposes a common ancestor of NPCs and coated vesicles (Devos *et al.*, 2004).

1.1 Composition of the *Saccharomyces cerevisiae* nuclear pore complex

In general, Nups can be divided into three groups: (i) Nups that are integrated into the membrane of the NE, (ii) structural Nups that form the NPC scaffold and (iii) FG Nups that enable proper NPC function by forming the NPC permeability barrier.

Most of the Nups are organized into distinct subcomplexes that are thought to be the building blocks of the NPC (for a schematic overview see figure 1.1 B).

Many Nups were originally discovered and studied in the yeast *Saccharomyces cerevisiae* (reviewed by Fabre and Hurt, 1997). In the following, the term "yeast" refers to the yeast *S. cerevisiae* if not otherwise stated.

For comparison, table 1.1 provides an overview of Nups from yeast and vertebrates.
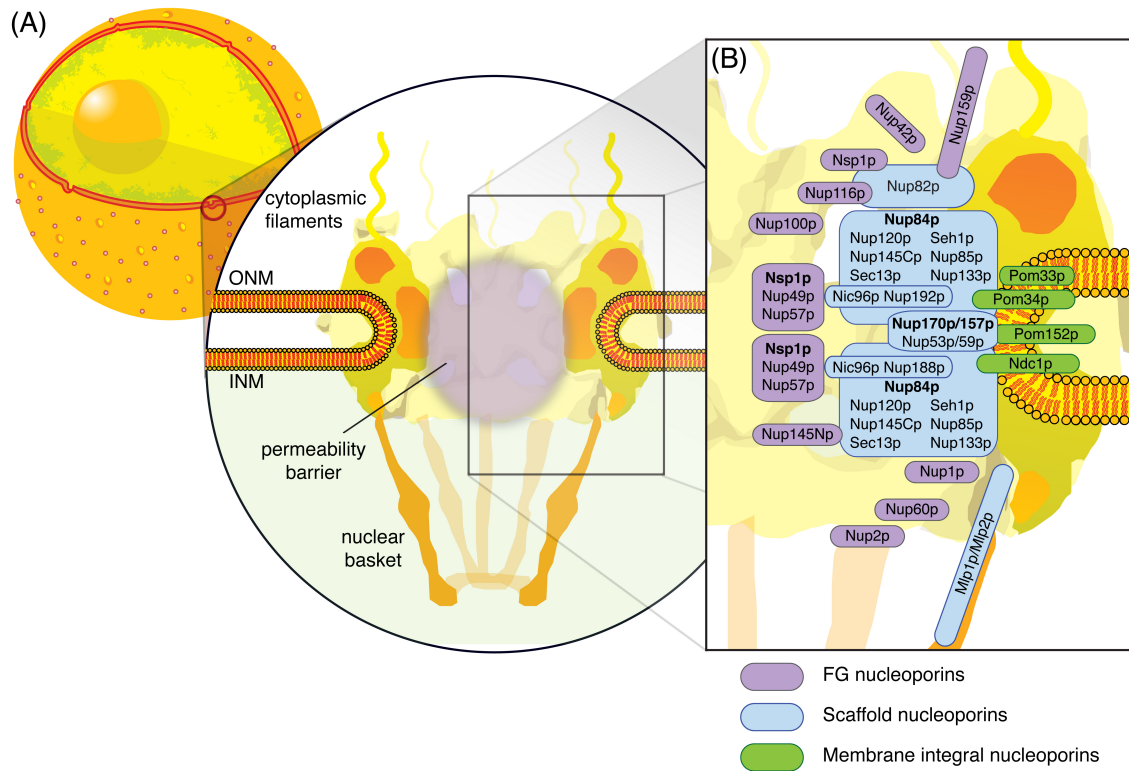
Figure 1.1: Schematic representation of the nuclear pore complex and individual Nups within the NPC. (A) The NPC is embedded in the nuclear envelope. Its main structural components include the core scaffold, the permeability barrier, the cytoplasmic filaments, and the nuclear basket. (ONM – Outer Nuclear Membrane, INM – Inner Nuclear Membrane)

(B) Nucleoporins can be sorted into three different groups: integral membrane nucleoporins (green), rigid scaffold nucleoporins (blue), and FG motif-containing nucleoporins (purple). The grouping of individual nucleoporins indicates their organization in biochemically characterized subcomplexes. Please note that the representation does not reflect the actual stoichiometric ratio nor the size of individual proteins or structures.

(The figure is based on an artwork created for Wikipedia by Mike Jones. This image is licensed under the Creative Commons Attribution-Share Alike 2.5 Generic license.)

Table 1.1: *S. cerevisiae* nups and their homologs in vertebrates. Summary of nups that constitute the NPC. Homology of yeast and vertebrate nups is listed according to Hetzer *et al.* (2005); D'Angelo and Hetzer (2008); Brohawn *et al.* (2009). "-" indicates that no homolog has been described.

S. cerevisiae	Vertebrates	Nucleoporin type	Subcomplex in yeast
Nup84p	Nup107	Scaffold nucleoporin	
Nup85p	Nup85/Nup75	Scaffold nucleoporin	
Nup120p	Nup160	Scaffold nucleoporin	
Nup133p	Nup133	Scaffold nucleoporin	Nup84 complex
Nup145Cp	Nup96	Scaffold nucleoporin	
Sec13p	Sec13	Scaffold nucleoporin	
Seh1p	Seh1	Scaffold nucleoporin	
Nic96p	Nup93	Scaffold nucleoporin	
Nup188p	Nup188	Scaffold nucleoporin	Nic96 complex
Nup192p	Nup205	Scaffold nucleoporin	
Nup53p	Nup35	Scaffold nucleoporin	
Nup59p	Nup35	Scaffold nucleoporin	Nup170 complex
Nup157p	Nup155	Scaffold nucleoporin	
Nup170p	Nup155	Scaffold nucleoporin	
Nup49p	Nup58 & Nup45	FG nucleoporin	Nsp1 complex
Nup57p	Nup54	FG nucleoporin	
Nsp1p	Nup62	FG nucleoporin	Nsp1 & Nup82 complex
Nup116p	Nup98	FG nucleoporin	
Nup82p	Nup88	Scaffold nucleoporin	Nup82 complex
Nup159p	Nup214/CAN	FG nucleoporin	
Mlp1p	Tpr	Scaffold nucleoporin	
Mlp2p	Tpr	Scaffold nucleoporin	Nuclear basket
Nup1p	Nup153	FG nucleoporin	forming complex
Nup2p	Nup50	FG nucleoporin	
Nup60p	-	FG nucleoporin	
Nup42p	NLP1/CG1	FG nucleoporin	
Nup100p	Nup98	FG nucleoporin	
Nup145Np	Nup98	FG nucleoporin	
Ndc1p	Ndc1	Integral membrane nucleoporin	
Pom33p	-	Integral membrane nucleoporin	
Pom34p	-	Integral membrane nucleoporin	
Pom152p	-	Integral membrane nucleoporin	
-	gp210	Integral membrane nucleoporin	
-	Pom121	Integral membrane & FG nucleoporin	
-	Aladin	Scaffold nucleoporin	
-	Nup37	Scaffold nucleoporin	
-	Nup43	Scaffold nucleoporin	
-	Ganp	FG nucleoporin	
-	Nup358/RanBP2	FG nucleoporin	

1.1.1 Integral Membrane Nucleoporins

Transmembrane Nups anchor the NPC into the NE. In yeast, these are Ndc1p (Thomas and Botstein, 1986), Pom152p (Wozniak *et al.*, 1994), Pom33p (Chadrin *et al.*, 2010), and Pom34p (Rout *et al.*, 2000).

Ndc1p localizes to the NPC and to the spindle pole body (Chial *et al.*, 1998) and it is essential for spindle pole body duplication (Winey *et al.*, 1993). The depletion of Ndc1p in interphase results only in a partial mislocalization of NPC components (Madrid *et al.*, 2006).

Pom33p was found to be dynamically associated with the NPC and a *POM33* deletion impairs NPC distribution (Chadrin *et al.*, 2010).

The deletion of genes of the other transmembrane Nups does not affect cell viability (Wozniak *et al.*, 1994; Giaever *et al.*, 2002). Those deletions are only synthetically lethal when combined with mutant alleles of a number of other Nups (Miao *et al.*, 2006; Chadrin *et al.*, 2010).

1.1.2 Scaffold Nucleoporins

The scaffold nucleoporins provide the structural framework of the NPC. They are interacting with both, the transmembrane Nups and the barrier forming Nups (see figure 1.1 B).

1.1.2.1 The Nup170 complex

Ndc1p, Pom34p, and Pom152p bind to Nup53p and Nup59 (both originally identified by Rout *et al.*, 2000). Nup53p and Nup59 then interact with Nup157p and Nup170p (Kenna *et al.*, 1996; Lusk *et al.*, 2002; Onischenko *et al.*, 2009).

NUP157 and *NUP170* are homologous genes and only one or the other is required for growth (Aitchison *et al.*, 1995b). Their deletion does not seem to affect existing NPCs but hinders formation of new pores. Thus, it was proposed that they are required for the assembly of newly forming NPCs (Makio *et al.*, 2009).

It was suggested that Nup170p and Nup157p may be part of a morphologically symmetrical but functionally distinct subcomplex of the NPC (Aitchison *et al.*, 1995b).

1.1.2.2 The Nup84 complex

A well characterized NPC subcomplex is the heptameric Nup84 complex that is build up by Nup84p, Nup85p, Nup120p, Nup133p, Nup145Cp, Seh1p, and Sec13p (Siniossoglou *et al.*, 1996, 2000; Lutzmann *et al.*, 2002). Structural similarities between Nup84 complex members and proteins of vesicle coating complexes suggest that all of these complexes have a common function in curving membranes (Devos *et al.*, 2004; Brohawn *et al.*, 2008; Nagy *et al.*, 2009).

The Nup84 complex exhibits a Y-shaped structure in negative staining transmission electron microscopy (Siniossoglou *et al.*, 2000; Fernandez-Martinez *et al.*, 2012) with Nup120p forming the one and a Seh1p-Nup85p heterodimer forming the other arm of the Y (Lutzmann *et al.*, 2002).

Although the Nup84 complex is essential for NPC formation (Siniossoglou *et al.*, 1996), individual genes encoding Nup84 complex members can be deleted resulting in mRNA export defects (Aitchison *et al.*, 1995a; Goldstein *et al.*, 1996; Siniossoglou *et al.*, 1996).

1.1.2.3 The Nic96 complex

The third subcomplex of the NPC scaffold is the Nic96 subcomplex constituted of Nic96p, Nup188p, and Nup192p (Grandi *et al.*, 1993; Nehrbass *et al.*, 1996; Zabel *et al.*, 1996; Kosova *et al.*, 1999).

Nic96p was originally identified by its interaction with the Nsp1 subcomplex (Grandi *et al.*, 1993, see section 1.1.3.1) and it is required for NPC formation (Gomez-Ospina *et al.*, 2000). Both, Nup188p and Nup192p were identified by their functional interaction with the C-terminus of Nic96p (Zabel *et al.*, 1996; Kosova *et al.*, 1999). *NUP192* is essential (Kosova *et al.*, 1999), whereas *NUP188* is not essential but shows synthetic lethality when its deletion is combined with a mutant allele of *NIC96* (Zabel *et al.*, 1996).

No direct interaction of Nup188p and Nup192p was found so far, thus it was proposed that both associate independently with distinct copies of Nic96p (Alber *et al.*, 2007).

1.1.2.4 The nuclear basket forming complex

Besides the previously mentioned structural subcomplexes of the NPC core, other structural elements are represented by Mlp1p (Kölling *et al.*, 1993) and Mlp2p (de Castillia *et al.*, 1999).

Mlp1p and Mlp2p are thought to assemble the yeast nucleoplasmatic basket structure by

forming filamentous structures that reach into the nucleoplasm (de Castillia *et al.*, 1999; Feuerbach *et al.*, 2002; Kiseleva *et al.*, 2004). This basket structure is presumably anchored to the NPC core via Nup60p (Feuerbach *et al.*, 2002).

MLP1 and *MLP2* can be deleted simultaneously without affecting cell viability (de Castillia *et al.*, 1999). They are homologs to the vertebrate gene coding the nuclear basket protein Tpr (Cordes *et al.*, 1997; de Castillia *et al.*, 1999).

1.1.3 Barrier-forming Nucleoporins

Approximately one third of all nucleoporins comprise domains with multiple repeats of phenylalanine (F) glycine (G) dipeptide motifs that are separated by hydrophilic spacer sequences. These domains are referred to as "FG repeat domains" or "FG domains". FG domains represent $\sim$12% of the NPC mass (Yamada *et al.*, 2010) and can be sorted according to the exact amino acid composition of an FG motif, with "FG", "GLFG", "FxFG", or "FxF" (where "x" stands for any amino acid) being the most prominent ones in yeast (Rout and Wente, 1994; Strawn *et al.*, 2004).

In total, eleven Nups with FG domains were identified in yeast (Rout *et al.*, 2000, see figure 1.2).

FG domains are considered to adopt a non-globular structure (Denning *et al.*, 2002, 2003). However, based on the amino acid composition of the FG domains, distinct categories of intrinsically disordered structures were proposed (Yamada *et al.*, 2010).

In contrast to the scaffold Nups or the non-FG domains of barrier-forming Nups, the amino acid sequences surrounding FG motifs are poorly conserved among eukaryotes. It was therefore proposed that they evolved roughly five times faster compared to structured domains (Denning and Rexach, 2007).

FG domains provide the binding sites for nuclear transport receptors (NTRs) and binding of NTRs to FG motifs is essential for facilitated NPC passage (Iovine *et al.*, 1995; Radu *et al.*, 1995; Bayliss *et al.*, 1999, 2000; Bednenko *et al.*, 2003; Isgro and Schulten, 2005).

Aside from binding NTRs, FG domains were shown to form intramolecular and intermolecular interactions (Frey *et al.*, 2006; Patel *et al.*, 2007; Frey and Görlich, 2009; Ader *et al.*, 2010; Yamada *et al.*, 2010). The interactions of Nsp1p FG domains are best characterized. Recombinantly expressed Nsp1p FG domain was found to form macroscopic hydrogels by hydrophobic inter-repeat interactions (Frey *et al.*, 2006; Ader *et al.*, 2010). Additionally, the asparagine-rich spacer regions of the N-terminal FG domain of Nsp1p are engaged in amyloid-like intermolecular β-sheets (Ader *et al.*, 2010).
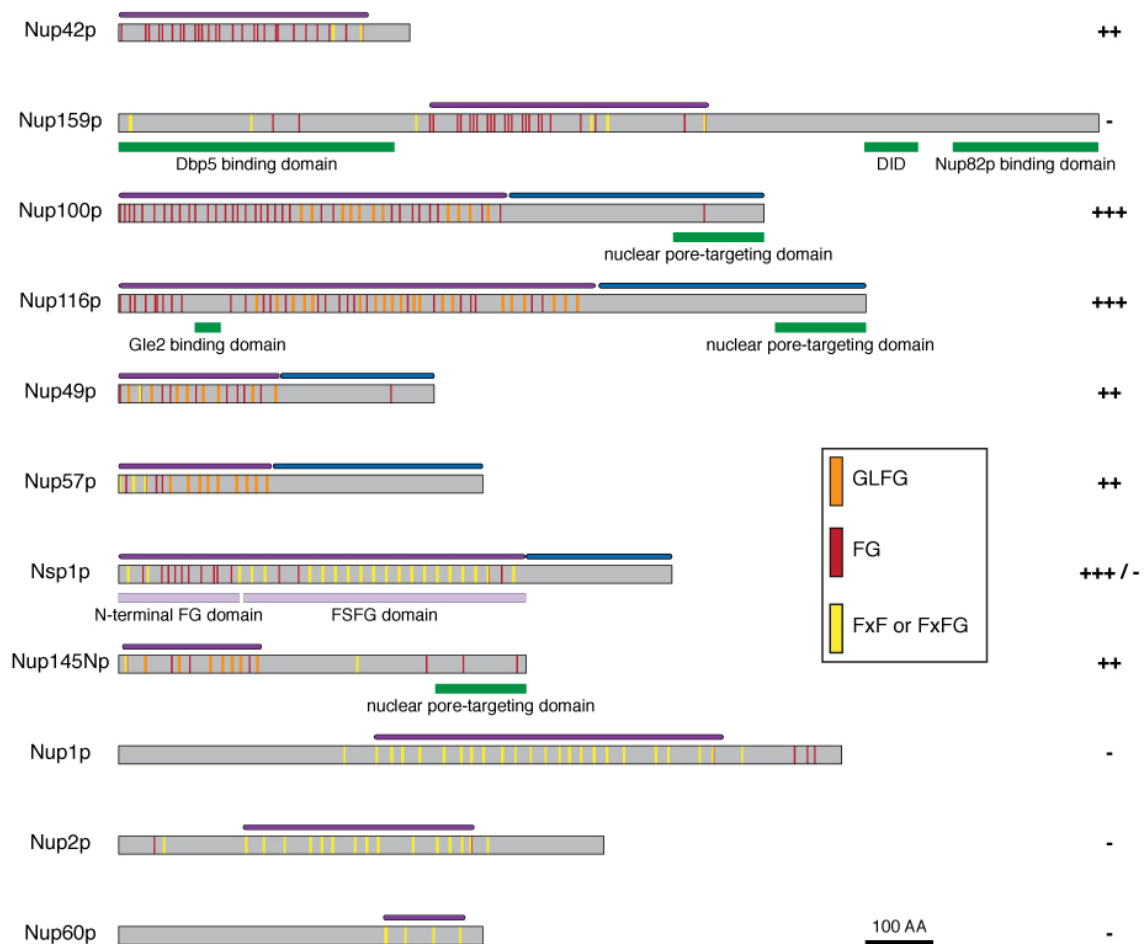
Figure 1.2: Schematic representation of *S. cerevisiae* FG nucleoporins: FG nucleoporins (grey boxes) were drawn to scale. Individual FG motifs are indicated as colored vertical strokes according to their exact sequence. FG domains (purple) and NPC anchor domains (blue) are indicated according to their definition in this study. Additional nucleoporin domains mentioned in the text are depicted as green boxes and the FG subdomains of Nsp1p are shown as lilac boxes. The cohesiveness of depicted FG domains was extrapolated from Frey *et al.* (2006); Patel *et al.* (2007); Frey and Görlich (2009); Ader *et al.* (2010); Yamada *et al.* (2010) and is indicated with (+++) very cohesive, (++) less cohesive, (+) slightly cohesive, and (-) non-cohesive. DID: dynein light chain interacting domain

Anchored to the NPC scaffold by smaller structured domains, FG domains radiate into the central channel of the NPC (Grote *et al.*, 1995) and are thought to form the permeability barrier that controls nucleocytoplasmic translocations (Ribbeck and Görlich, 2001; Frey and Görlich, 2007, 2009). It has been estimated that more than 1000 copies of FG repeats are within one NPC, and that their local concentration in the interior of the central channel approximates 50 mM (Bayliss *et al.*, 1999).

FG domains are essential for cell viability (Strawn *et al.*, 2004). However, the deletion of individual FG Nup coding genes give rise to a variety of transport defects (reviewed e.g. in Fabre and Hurt, 1997).

1.1.3.1 The Nsp1 complex

The Nsp1 subcomplex was the first identified NPC subcomplex in yeast (Grandi *et al.*, 1993, 1995). It is composed of the essential proteins Nsp1p (Hurt, 1988), Nup49p (Wimmer *et al.*, 1992; Wente *et al.*, 1992), and Nup57p (Grandi *et al.*, 1995). Assembly of the complex occurs via the C-terminal coiled-coil domains of the complex members (Grandi *et al.*, 1995; Schlaich *et al.*, 1997; Bailer *et al.*, 2001). These domains bind to the N-terminus of Nic96p and thereby attach the complex to the central part of the NPC scaffold (Grandi *et al.*, 1995; Schrader *et al.*, 2008, see figure 1.1 B). Notably, the NPC-binding site for Nsp1p on Nic96p is not required for cell viability, even though its deletion results in a severe growth defect (Schrader *et al.*, 2008).

The FG domain of Nsp1p can be divided into two parts, namely (i) the highly cohesive N-terminal part with a low content of charged amino acids consisting mainly of "FG" motifs, and (ii) the more C-terminal part of the FG domain with a higher content of charged amino acids and "FSFG" being the predominant motif (Ader *et al.*, 2010; Yamada *et al.*, 2010). The FG domains of Nup49p and Nup57p both belong to the "GLFG" family, being cohesive with a low content of charged amino acids (Wente *et al.*, 1992; Yamada *et al.*, 2010) (see figure 1.2). Nsp1p, but not Nup49p or Nup57p, is additionally part of the Nup82p complex (Belgareh *et al.*, 1998, see below).

1.1.3.2 Yeast homologs of vertebrate Nup98

Nup145Np is generated *in vivo* by self-cleavage of the precursor protein Nup145p (Teixeira *et al.*, 1997). The resulting C-terminal protein is Nup145Cp which is incorporated

into the Nup84 subcomplex (Teixeira *et al.*, 1997). The autocatalytic cleavage site within Nup145p is conserved throughout evolution (Teixeira *et al.*, 1997) and allows the identification of homologous in virtually all eukaryotes (Broder Schmidt, personal communication and Neumann *et al.*, 2010).

The vertebrate homolog of *NUP145* is *NUP98* (Powers *et al.*, 1995; Radu *et al.*, 1995). Like Nup145Np, Nup98 is generated by self-cleavage of a precursor protein (Fontoura *et al.*, 1999). Moreover, *S. cerevisiae* possesses two additional homologs of *NUP98*, namely *NUP100* and *NUP116* (Fabre *et al.*, 1994; Wente and Blobel, 1994; Powers *et al.*, 1995). But Nup100p and Nup116p are not generated by self-cleavage of a precursor protein. *NUP100* and *NUP116* are both flanked by a histidine tRNA gene and a transposon element suggesting that they arose by gene duplication (Wente *et al.*, 1992).

Nup100p, Nup116p, Nup145Np, and Nup98 share an N-terminally localized "GLFG" type FG domain (Wimmer *et al.*, 1992; Wente *et al.*, 1992; Wente and Blobel, 1994; Fabre *et al.*, 1994) and the conserved autocatalytic domain, which functions as nuclear pore-targeting domain (Bailer *et al.*, 1998; Ho *et al.*, 2000; Hodel *et al.*, 2002).
However, Nup100p, Nup116p and Nup145Np do not anchor into the NPC via the same proteins. Nup145Np was shown to bind to the Nup84 subcomplex through Nup145C (Ratner *et al.*, 2007; Lutzmann *et al.*, 2005) and a biochemical analysis implied that neither Nup100p nor Nup116p can attach to this binding partner *in vivo* (Ratner *et al.*, 2007).
Nup116p binds to the Nup82 subcomplex (Ho *et al.*, 2000; Bailer *et al.*, 2000). Additionally, a yet unknown binding site for Nup116p was proposed, since the deletion of its nuclear pore-targeting domain leads to a reduced but still observable localization at the nuclear rim, indicative for NPC incorporation (Yoshida *et al.*, 2011). This assumption is well in line with the observation that a simultaneous deletion of all three nuclear pore-targeting domains results only in a severe temperature sensitive phenotype (Fabre *et al.*, 1994).
The binding site of Nup100p within the NPC could not be identified so far. However, it is considered to bind to the same location within the NPC as Nup116p (Ho *et al.*, 2000). In line with this assumption, Nup100p and Nup145Np were found to bind to Nup116p's binding site on Nup82p in a mutually exclusive manner *in vitro* (Yoshida *et al.*, 2011).

Deletion of *NUP116* was shown to result in morphological changes of the nuclear envelope accompanied by a severe growth delay and temperature sensitivity (Wente and Blobel,

1993; Wente *et al.*, 1992). These phenotypes could partially be attributed to the concomitant deletion of the conserved Gle2p binding site (GLEBS domain) that intervenes the FG domain of Nup116p (Bailer *et al.*, 1998). Likewise, Nup98 harbors a binding site for Rae1, the vertebrate homolog of Gle2p (Pritchard *et al.*, 1999).

Gle2p is a conserved RNA export factor (Brown *et al.*, 1995; Murphy *et al.*, 1996) and its interaction with Nup116p is crucial for Gle2p *in vivo* function (Bailer *et al.*, 1998). Notably, Bailer *et al.* (1998) functionally transplanted the GLEBS domain from Nup116p to Nup100p and therewith rescued an observed Nup116pΔGLEBS phenotype. In contrast, transplantation of the GLEBS domain to Nup49p or Seh1p did not rescue the phenotype.

In a *Xenopus* egg extract system, Nup98 was found to predominantly establish the permeability barrier of vertebrate NPCs (Hülsmann *et al.*, manuscript submitted). Especially, its cohesive FG domain is sufficient to maintain a permeability barrier. Remarkably, replacing the Nup98 FG domain by the FG domains of Nup100p or Nup116p results in functional pores *in vitro*.

1.1.3.3 The Nup82 complex

The Nup82 subcomplex comprises Nup82p, Nsp1p, Nup116p, and Nup159p (Belgareh *et al.*, 1998; Hurwitz *et al.*, 1998; Ho *et al.*, 2000; Bailer *et al.*, 2000). Dbp5p, a DEAD-box RNA helicase involved in termination of mRNA export, associates with the complex by binding to Nup159p (Weirich *et al.*, 2004).

Nup82p is located exclusively at the cytoplasmic side of the NPC (Hurwitz *et al.*, 1998) and seems to serve as a platform to attach the FG Nups Nsp1p, Nup116p, and Nup159p to the NPC scaffold (Yoshida *et al.*, 2011).

1.1.3.4 Peripheral FG Nups

The FG domains of the peripheral FG Nups do not preferentially radiate into the NPC channel. Instead, they constitute filamentous structures observed on both, the nucleoplasmic and the cytoplasmic, sides of the NPC (see figure 1.1).

Cytoplasmic filaments

Nup159p is an essential protein (Gorsch *et al.*, 1995). It is a component of the Nup82 subcomplex that is thought to form filamentous structure at the cytoplasmic side of the NPC (Belgareh *et al.*, 1998; Hurwitz *et al.*, 1998). It consists of several domains with

distinct functions. The N-terminal domain functions in mRNA export by tethering the helicase Dbp5p to the NPC (Priore *et al.*, 1997; Weirich *et al.*, 2004). The centrally localized domain is rich in FG motifs (Gorsch *et al.*, 1995). C-terminal of this FG domain is the dynein light chain interacting domain (DID) that binds Dyn2p, which is thought to project the Nup159p FG domain from the structural core of the Nup82 complex (Stelter *et al.*, 2007). Nup159p is anchored to the Nup82 subcomplex via its C-terminal domain that folds into an amphipathic α-helix (Priore *et al.*, 1997; Yoshida *et al.*, 2011).

The second FG Nup that localizes exclusively to the cytoplasmic side of the NPC is Nup42p, also known as Rip1p. It was originally identified in a screen as being a yeast target of the HI-Virus protein Rev (Stutz *et al.*, 1995). It is not essential and was proposed to specifically function in the export of heat shock mRNAs (Saavedra *et al.*, 1997), even though the deletion of its FG domain has no effect on mRNA export (Stutz *et al.*, 1997).

Nucleoplasmic filaments

Nup1p is essential for cell viability, and its over-expression inhibits cell growth (Davis and Fink, 1990). Notably, some yeast strains bear a natural occurring suppressor that renders Nup1p to be non essential (Belanger *et al.*, 1994). Nup1p is anchored to the NPC via its N-terminal domain probably by binding to Nup157p and Nup170p (Kenna *et al.*, 1996). Nup1p and Nup60p were found to localize exclusively to the nucleoplasmic side of the NPC, and together with Nup2p, Mlp1p, and Mlp2p they are thought to form the nuclear basket structure of the yeast NPC (Rout *et al.*, 2000; Kiseleva *et al.*, 2004).

The localization of Nup2p is less defined: It was found to be a nucleo-cytoplasmic shuttling protein that dynamically associates with the nucleoplasmic side of the NPC (Dilworth *et al.*, 2001). It binds the NPC via Nup60p in dependence of the intranuclear concentration of Gsp1p–GTP, the yeast homolog to the vertebrate GTPase Ran (Denning *et al.*, 2001). The FG domains of Nup1p, Nup2p, and Nup60p belong to the "FxF" type FG domains. They were found to be non-essential and can be deleted simultaneously without affecting viability (Strawn *et al.*, 2004).

1.2 Models of nucleocytoplasmic transport across the NPC permeability barrier

The permeability barrier of NPCs excludes inert macromolecules >40 kDa (Paine *et al.*, 1975) or ≥ 5 nm in diameter (Mohr *et al.*, 2009). At the same time it permits facilitated passage of even very large cargoes, provided these are bound to NTRs (reviewd e.g. by Görlich and Kutay, 1999; Fried and Kutay, 2003). NTRs bind to FG motifs (e.g. Iovine *et al.*, 1995; Radu *et al.*, 1995; Bayliss *et al.*, 2000) and this binding was found to be essential for facilitated NPC passage (Bayliss *et al.*, 1999). Actually, this binding even accelerates NPC passage of the NTR·cargo complex by a factor of up to 1000 compared to the passage of an inert objects of similar size (Ribbeck and Görlich, 2001). It is however not trivial to explain this phenomenon, since a binding should instead cause the retention of the NTR·cargo complex and therefore delay the NPC passage.
In the past years, several models were proposed that try to resolve this paradox.

1.2.1 The reduction of dimensionality model

The "reduction of dimensionality" model (Peters, 2005, 2009) assumes that FG domains line the channel of the NPC but leave a free transit way in the middle of the NPC that allows the diffusion of small molecules. However, this channel is so narrow that free transit of molecules with a diameter above a certain limit is restricted. In this model, NTRs act as "ferries" for their bound cargos. They slide along the FG layer of the channel surface by a two dimensional random walk. This sliding is thought to be considerably faster than a three dimensional random diffusion of inert material. This model is well in line with the observation that cells are viable after deletion of more than half of the FG mass (Strawn *et al.*, 2004), assuming that the remaining FG domains are still sufficient to form a thin layer of FG mass but inconsistent with the observed permeability of the NPC. Given that ribosomes with a diameter of ∼25 nm can pass, the central channel cannot be narrower than 25 nm. Such wide channel can however not significantly hinder passage of 5 nm-sized objects.

1.2.2 The virtual gating model

The "virtual gate" model (Rout *et al.*, 2000, 2003) assumes that the NPC forms an aqueous central channel that is surrounded by FG domains. This channel is so narrow that molecules larger than the size limit are unlikely to enter. However, FG domains at the

cytoplasmic and at the nucleoplasmic side of the NPC provide initial docking sites for NTRs, increasing the residence time of NTR·cargo complexes at the entrances to the central channel. This initial docking is thought to increase the probability of the complexes to enter the channel and to subsequently diffuse through it.

Inert macromolecules are repulsed by FG domains from entering the NPC channel whereas small objects can easily lurch through this entropic barrier.

However, the model does not explain how NTR·cargo complexes with a diameter larger than the diameter of the narrow channel can cross the NPC.

1.2.2.1 The reverse collapse model

The "virtual gate" model was extended by the observation that some FG domains collapse from their natively unfolded protein structures into a more collapsed-coil configuration (Lim *et al.*, 2006, 2007). In this "reversible collapse model", NTR·cargo complexes are thought to move across the barrier via contracting FG domains.

However, a recent study did not observe collapse of FG domains in the presence of NTRs (Eisele *et al.*, 2010) and the authors argue that the previously observed collapse can be attributed to the low density of FG domains in the experimental setup. Thus reversible collapse is unlikely to occur in the central region of the NPC (Eisele *et al.*, 2010).

1.2.3 The selective phase model

In contrast to the previously described models, the "selective phase" model (Ribbeck and Görlich, 2001; Frey and Görlich, 2007) relies on interactions between FG motifs that cross-link the FG domains into a sieve-like meshwork. And free diffusion of inert molecules is controlled only by the mesh size. NTRs overcome this size limit by binding to FG motifs. The binding results in an opening of the FG meshes. Due to the fact that NTRs harbor multiple binding sites for FG motifs (Bayliss *et al.*, 2000, 2002b; Bednenko *et al.*, 2003; Isgro and Schulten, 2005) they subsequently become a part of the meshwork.

The "selective phase" model is supported by the observation that cohesive FG domains spontaneously form macroscopic hydrogels by creating inter-repeat contacts (Frey *et al.*, 2006; Frey and Görlich, 2009; Milles and Lemke, 2011). The needed concentration for hydrogel formation was found to be in the range of the calculated concentration of FG domains within nuclear pores (Bayliss *et al.*, 1999; Frey *et al.*, 2006).

A macroscopic hydrogel displays permeability properties very similar to those of authentic NPCs. It effectively suppresses the influx of inert macromolecules, while the uptake of

NTRs occurs so rapidly that it is only limited by the rate of their diffusion to the barrier (Frey and Görlich, 2007). Strikingly, the selectivity of macroscopic hydrogels increase when they are pre-incubated with NTRs (Frey and Görlich, 2009). Additionally, the ability of FG domains to form such hydrogels is conserved during evolution (A. Labokha & B. Schmidt, personal communication).

Since yeast NPCs contain numerous cohesive FG repeat domains (Patel *et al.*, 2007; Frey and Görlich, 2007, 2009; Yamada *et al.*, 2010), it is plausible to assume that hydrogel formation occurs in authentic NPCs. A recent study directly showed that multivalent cohesion between FG repeats is indeed required (Hülsmann *et al.*, manuscript submitted). However, it is still unclear whether hydrogels mimic the situation in NPCs *in vivo*.

1.2.4 The forest model

Like the "selective phase" model, the recently proposed "forest" model (Yamada *et al.*, 2010) relies on hydrophobic interactions. However, not all FG domains were found to be cohesive (Patel *et al.*, 2007; Yamada *et al.*, 2010). Thus, inter-repeat cohesions might not be the only defining features. Based on measured stoke radii and molecular dynamic simulations, Yamada *et al.* (2010) proposed the existence of two distinct conformations of FG domains. FG domains that adopt a proposed collapsed coil conformation place the hydrophobic FG motifs in direct proximity to the anchoring domains. These "shrubs" thus line the wall of the NPC channel. In contrast, some FG domains, the "trees", allocate FG motifs to the central part of the channel by partially adopting an extended coil conformation. Only the tops of the "trees" form a hydrogel like structure in the central part of the channel. Here, large objects like ribosomal subunits pass the NPC according to principles described by the "selective phase" model. The "shrubs" act more like an entropic gate, as proposed by the "virtual gate" model. Smaller NTR·cargo complexes preferentially move through this zone.

1.3 Yeast genetics to study the NPC permeability barrier

Yeast genetics has been extensively used to study the protein composition of the NPC and the contribution of individual nucleoporins in protein and RNA transport (reviewed by Fabre and Hurt, 1997). Thus the general involvement of FG Nups and their crucial function in nucleo-cytoplasmic transport is generally established (reviewed e.g. by Terry and Wente, 2009).

Additionally, yeast genetic studies are a useful tool to test predictions of transport models *in vivo*. As an example, it was suggested that the asymmetric localization of discrete Nups might be in part responsible for conferring directionality of protein import (Ben-Efraim and Gerace, 2001). Addressing this issue, Zeitler and Weis (2004) showed that an asymmetric distribution of FG domains between the nucleoplasmic and the cytoplasmic side of the NPC is not required for bulk protein import *in vivo*. Even though they genetically swapped the FG domains from Nup1p and Nup159p, protein import was not impaired.

An other yeast genetic study systematically analyzed relationships between all FG domains in the NPC. Strawn *et al.* (2004) reported the generation of deletion strains deficient in various combinations of FG domains. The authors first defined every FG domain of the NPC and then genomically removed it. All but one possible single FG domain deletions resulted in viable strains. Only deletion of the entire Nup116p FG domain was lethal. Thus, for subsequent steps only the Nup116p FG subdomain was removed which is located C-terminal of the GLEBS domain (figure 1.2).
As a next step, mutants for the centrally localized Nups were combined in all possible pair-wise combinations. Since only the combined deletion of Nup100p and Nup116p FG domains resulted in a non viable strain, a third - and where possible a fourth - deletion was added to each double mutant. Additionally, the authors analyzed specific transport pathways in their mutant strains.
In the end, Strawn *et al.* came to several conclusions: (i) not all FG domains are functionally equivalent, (ii) the remaining FG domain mass is insufficient to predict viability and transport efficiency, and (iii) NTRs have different requirements for individual FG domains.

For the generation of their multi FG domain deletion strains, Strawn *et al.* applied a strategy based on a selection marker gene flanked by loxP sites (see figure 1.3 A). After successful integration of this deletion cassette in diploid yeast cells and thereby replacing one allele of the targeted gene, Cre recombinase (Sauer, 1987) was expressed. The recombinase activity led to excision of the selection marker (figure 1.3 C), allowing its reuse in further rounds of deletion.
Cre-driven recombination of loxP sites is a common technique in mouse genetics (for review see e.g. Sauer, 1998). For this application, loxP sites are targeted to non-coding regions flanking an exon. Normally, targeted exons are chosen in a way that their excision finally results in a frame shift mutation. Thus no functional protein can be produced. The
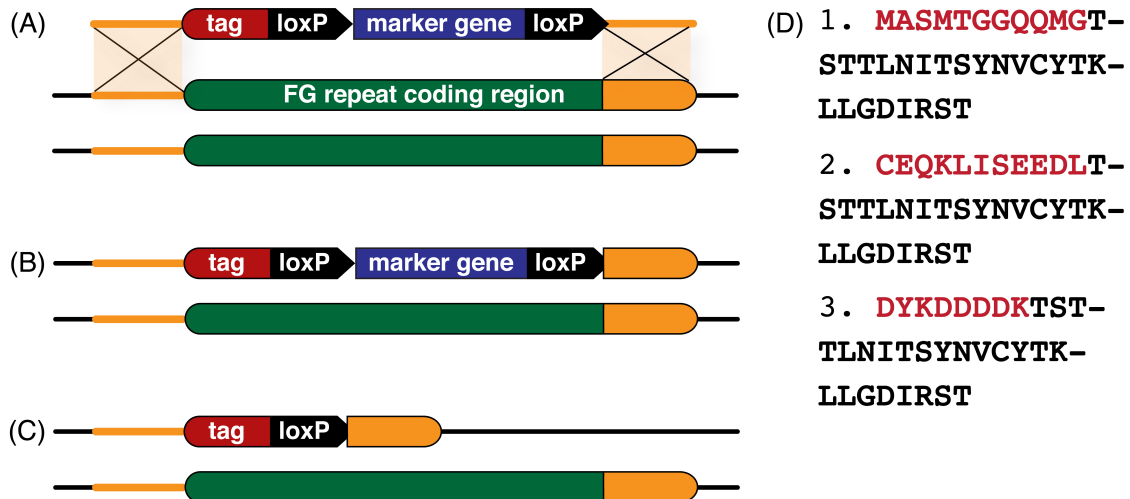
Figure 1.3: Genetic strategy to genomically delete coding regions of FG domains using Cre recombinase as applied by Strawn *et al.* (2004) (A) A deletion cassette harboring a selection marker (blue) flanked by loxP sites (black) is targeted to the coding region of a specific FG domain (green) by homologous DNA regions (orange). Note that coding regions are depicted as rounded boxes. (B) Integration of the deletion cassette in diploid cells results in the substitution of the FG domain coding sequence by the deletion cassette on one allele. A wild type protein can still be expressed from the remaining second allele. (C) After expression of Cre recombinase, the selection marker is excised. DNA coding for an N-terminal tag and one loxP site persists in the coding sequence, being in frame with the remaining protein coding sequence (orange box). (D) Expressed amino acid sequences from the integrated tag (red) followed by the amino acids that are coded by the loxP sequence (black) for three different deletion cassettes including different tags: 1. t7 tag, 2. myc tag 3. flag tag

Cre loxP system was also applied in yeast genetics to completely delete a gene.

In contrast to the previously described approaches, Strawn *et al.* only targeted a part of the gene. As a consequence, the remaining loxP site became part of the coding region that was later on translated into the encoded protein. In combination with an additionally integrated N-terminal tag this led to the attachment of 32-35 additional amino acids to the remaining domain of the protein (figure 1.3 D).

1.4 Aim of this study

FG hydrogels reproduce the permeability properties of NPCs almost perfectly. However, it is still unclear whether FG hydrogels form in authentic NPCs and are required for *in vivo* NPC function.

The obvious solution to address this issue would be to introduce point mutations that change the cohesive FG domains into non-cohesive ones that do not form hydrogels *in vitro* and test the effects of such mutations on viability and transport. However, this requires more than point mutations, since FG domains consist of many divergent repeat motifs. In addition, not only in the sequences of the repeat motifs differ within a given FG domain but also the sequences of the intervening spacers. Likewise, FG domains differ from one nucleoporin to another. And in total yeast possesses 11 different Nups with FG domains (Rout *et al.*, 2000).

However, the significance of most of these observed differences among FG domains for the functionality of the permeability barrier *in vivo* so far remained unclear.

The focus of my PhD work has been to elucidate which FG domain features are essential for permeability barrier function *in vivo*. Therefore, the immediate aim of this project has been to establish a genetic assay that allows us to test individual FG domains, motifs or artificial FG domains for their ability to support NPC function and viability. We want to know which features of FG domains are important for NPC selectivity and, concomitant with that, for viability.

By relocating FG domains from one anchor point to an other one and monitoring the viability of resulting cells, we want to answer questions such as whether the anchoring and thereby the relative position of a domain within the NPC influences its overall functionality and whether FG domains are functionally equivalent.

If we find a strains that relies on the presence of a given FG domain for viability, we will change the length, the NTR binding sites or the cohesiveness of the FG domain and test

whether this influences the viability of the strain. By doing so we will answer questions about what FG domain features are important for NPC functionality.

Overall, we want to be able to extrapolate determinant features of FG domains, beside cohesiveness and NTR binding, for permeability barrier function.

2 Results

FG domains have been known for being the building blocks of the NPC permeability barrier for many years. *In vitro* studies accumulated data about properties of individual FG domains from a variety of organisms and allowed the proposal of models for barrier function. However, information about the *in vivo* contribution of individual FG domains are still insufficient and experimental systems to test predictions from proposed models for *in vivo* functionality are missing.

We set out to establish such a system that not only allows the analysis of an *in vivo* permeability barrier but also offers the potential to simultaneously manipulate components of the barrier *in vivo*.

The yeast *Saccharomyces cerevisiae* was chosen as a model system since (i) methods for its genetic manipulations are well established, (ii) it is one of the best studied model organism in cell biology, and (iii) the FG nucleporins of *S. cerevisiae* belong to a group of biochemically well characterized FG Nups.

As a first step, we wanted to establish a genetic assay that allows to evaluate the importance of a given FG domain for viability. For this assay, a mutant strain with a maximal number of genomically deleted FG domains is needed. The according anchor domains (that anchor the FG Nups to the rigid NPC scaffold) should not be impaired in this strain. Deletion of a next FG Nup should then be lethal and supplying the anchor domain of this Nup alone should not be sufficient to restore viability. In such a strain, the *in vivo* functionality of any FG domain can be assayed by transforming a plasmid that codes for a fusion of this FG domain with the anchor domain of the completely deleted Nup.

Based on the previous observation that a triple deletion of the FG domains of Nup49p, Nup57p, and Nsp1p is lethal and that viability can be restored with either FG domains of the Nup49p, Nup57p, or Nsp1p (Strawn *et al.*, 2004), these combinations of deletions were chosen as starting points.

2.1 The combined deletions of FG domains from Nsp1p, Nup49p, and Nup57p are not lethal

Lethality in the previously created triple ΔFG mutant strain (Strawn *et al.*, 2004) is rescued by a Nsp1p wild type coding vector. In principal, this strain could already be used to test FG domains fused to the Nsp1p anchor domain. However, problematic in that strain is the residual existence of a genomically encoded Nsp1p anchor domain. With this genomic copy there are in total three genetic sources of Nsp1p anchor domains: (i) the genomically coded one (Nsp1p^{anchor}), (ii) Nsp1p wild type originating from the rescuing vector, and (iii) Nsp1p anchor domain fused to the FG domain to be tested (Test^{FG}-Nsp1p^{anchor}). The composition of the NPC at a given time is thus not precisely controllable.

The obvious solution for the generation of a Nsp1p, Nup49p, Nup57p triple FG domain deletion strain was to completely delete one of these three FG nucleoporins in a background where the two other corresponding FG domains were already genomically deleted.

2.1.1 Remaining scar domains result in a deleterious effect

Strawn *et al.* (2004) reported the generation of several combinations of double FG domain deletion strains. For the generation of their strains with multi FG domain deletions, the authors applied a recombinase strategy. The used recombinase recognition site remained in the amino acid coding region of the anchor domain. In combination with an additionally integrated N-terminal tag this resulted in the attachment of 32-35 amino acids to the anchor domain (see section 1.3 and figure 1.3 D).

Three new strains with combined FG domain deletions of Nsp1p, Nup49p, and Nup57p including one complete gene deletion, respectively, were generated on the basis of these strains. Due to the recombinase based deletion strategy of parental strains, the resulting strains have the following genotypes:

Δ*nup49 flag-loxP-nsp1ΔFG myc-loxP-nup57ΔFG + NUP49 URA3 CEN*

Δ*nup57 t7-loxP-nup49ΔFG flag-loxP-nsp1ΔFG + NUP57 URA3 CEN*

Δ*nsp1 t7-loxP-nup49ΔFG myc-loxP-nup57ΔFG + NSP1 URA3 CEN*

The expected lethality caused by the complete deletion of one of the Nups is rescued by a vector coding the corresponding wild type Nup and the *URA3* selection marker gene. This allows the use of the FOA based complementation assay (4.2.2.9). With that assay

we tested whether the anchor domain of the completely deleted Nup alone is sufficient to rescue loss of the wild type coding rescue vector.
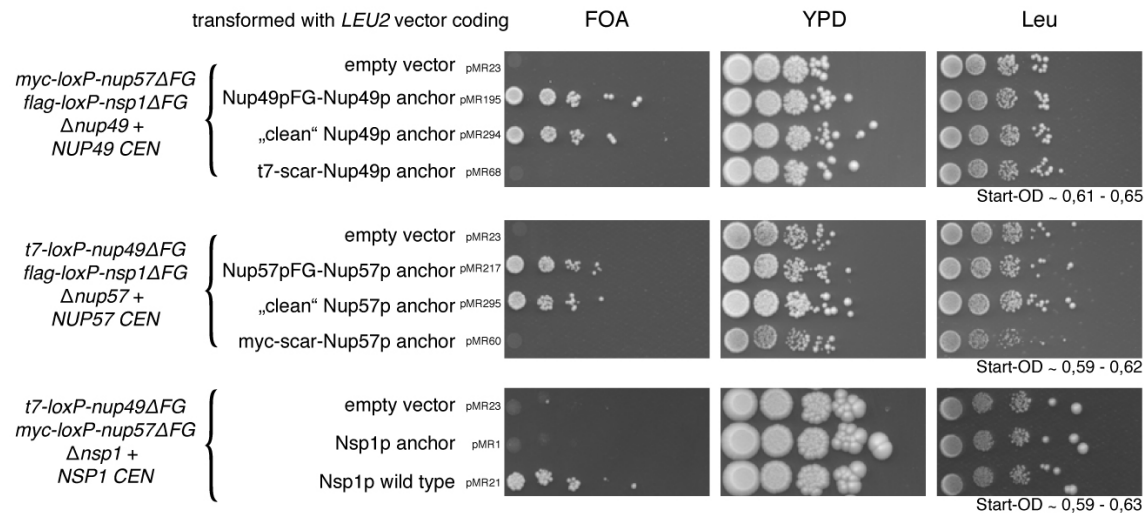
Figure 2.1: Effect of a deletion scar: Plasmids encoding the specified proteins were transformed into strains with genetic backgrounds as indicated (from top to bottom: YMR27, YMR28, YMR26). Additionally the strains contained a *URA3* harboring plasmid that encoded an essential wild type protein. In this so-called FOA Assay, the ability of the encoded fusion protein to functionally replace the according wild type protein is assayed by monitoring cell growth on FOA containing plates. If the fusion protein cannot functionally replace the wild type protein, cells depend on the presence of the wild type coding plasmid. However, in such a case cell growth is prevented since the *URA3* gene product converts FOA in an toxic compound. For details see section 4.2.2.9. Cells were incubated for 5 days (top and middle panel) or 8 days (bottom panel) at 25 °C, respectively. The exact amino acid composition of the fusion proteins can be found in section 4.1.10.

In contrast to published data (Strawn *et al.*, 2004), it turned out that already the Nup49p anchor domain alone was able to complement the loss of the *NUP49* gene in the *nsp1ΔFG nup57ΔFG* background (see figure 2.1 "clean Nup49p anchor"-construct). Likewise the Nup57p anchor domain complemented for the loss of the *NUP57* gene in a *nsp1ΔFG nup49ΔFG* background. Only the Nsp1p anchor domain, as previously reported, was not sufficient to complement the loss of the *NSP1* gene in a *nup49ΔFG nup57ΔFG* background.

We could reproduce the reported lethal phenotype, when we mimicked the exact coding region of the published triple FG deletion strains including the genetic "scar" that originated from the recombinase based deletion strategy (see constructs "t7-scar-Nup49p anchor" and "myc-scar-Nup57p anchor" in figure 2.1 respectively).

The deletion of a single FG domain by recombinase driven excision might not show a different phenotype compared to a "clean" deletion (Strawn *et al.*, 2004). But unexpectedly, the combination of deletions created by this method finally results in a dominant negative effect.

To avoid such a artificial effect, we had to start from scratch to generate strains with multiple clean FG domain deletions. In such strains a generated phenotype should only show the effect due to the loss of the FG domains.

2.2 *S. cerevisiae* tolerates more FG domain deletions than expected

We focused on deleting the FG domains of Nups that are thought to be centrally localized within the NPC, namely Nsp1p, Nup49p, Nup57p, Nup100p, Nup116p, and Nup145Np, in order to efficiently weaken the NPCs permeability barrier. For genomic deletions, we defined the respective FG domains as follows:

Nsp1p FG repeat domain   amino acid 3-602
Nup49p FG repeat domain   amino acid 2-236
Nup57p FG repeat domain   amino acid 2-223
Nup100p FG repeat domain   amino acid 2-576
Nup116p FG repeat domain   amino acid 2-714
Nup145Np FG repeat domain amino acid 10-209

Applying the strategies described in 4.2.2.4, we obtained several viable strains carrying combinations of FG domain deletions that previously had been described as lethal (Strawn *et al.*, 2004):

 nsp1ΔFG nup49ΔFG nup57ΔFG
 nsp1ΔFG nup49ΔFG nup145ΔFG
 nsp1ΔFG nup57ΔFG nup145ΔFG
 nup49ΔFG nup57ΔFG nup145ΔFG
 nsp1ΔFG nup49ΔFG nup57ΔFG nup100ΔFG
 nsp1ΔFG nup49ΔFG nup100ΔFG nup145ΔFG

All strains generated in this study are summarized in table 4.1, page 65.

Even though some triple ΔFG mutant strains generated by the recombinase strategy do
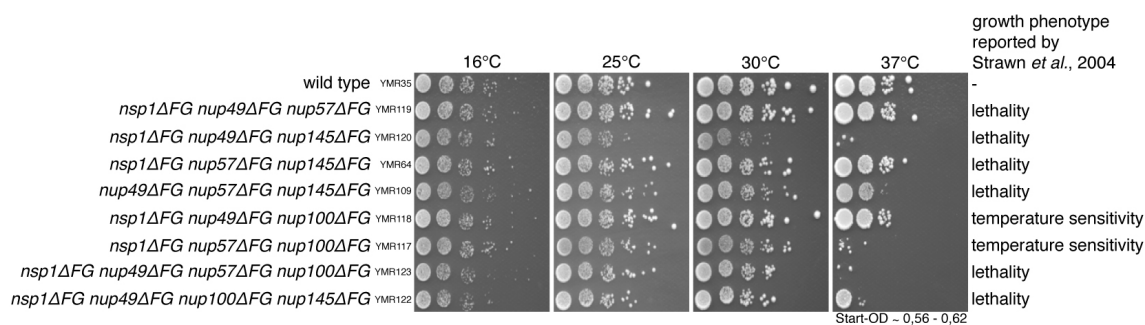
Figure 2.2: Temperature sensitivity assay of multiple ∆FG mutant strains: Multiple FG domain deletion strains were subjected to a temperature sensitivity assay as described in 4.2.2.10. Cells were allowed to grow for 5 days at 25 ℃, 30 ℃, and 37 ℃ and for 8 days at 16 ℃. For comparison, the growth phenotypes reported by Strawn *et al.* (2004) are summarized.

not show a lethal phenotype, they were shown to be temperature sensitive at 37℃ (Strawn *et al.*, 2004). To test if strains with multiple clean FG domain deletions share such a temperature sensitive phenotype, all strains with three or more FG domain deletions generated in this study where subjected to a temperature sensitivity assay (figure 2.2).

Cold sensitivity or reduced growth at 30℃ were not observed for any of the strains. Only two of the triple ∆FG mutants exhibited reduced growth at 37℃. This phenotype was previously reported (Strawn *et al.*, 2004) for the *nsp1∆FG nup57∆FG nup100∆FG* strain. Hence, no difference caused by the scar domains could be observed here.
Remarkably, the quadruple ∆FG mutant strain *nsp1∆FG nup49∆FG nup100∆FG nup145∆FG* only showed reduced growth at 37℃ even though only the Nup57p- and Nup116p FG domains remain in the central part of the NPC. The *nsp1∆FG nup49∆FG nup57∆FG nup100∆FG* mutant failed to grow at 37℃.
Obviously, *S. cerevisiae* tolerates more FG domain deletions than previously reported (Strawn *et al.*, 2004).

2.3 Multi ∆FG mutant strains can be used to assay *in vivo* functionality of FG domains at a given NPC anchor point

As demonstrated in the previous chapter, we already massively reduced the number of FG domains, but the resulting cells showed no severe phenotype. It appears that the

permeability barrier is either built up in a highly redundant manner or the really crucial constituents of the barrier have not been affected so far.

2.3.1 FG domains at Nup98 homologous anchor position are essential

Experiments by Hülsmann *et al.* using a *Xenopus* egg extract system strongly support the idea that the main component of the vertebrate permeability barrier is the FG domain of Nup98 (manuscript submitted). As summarized in the introduction, there are three Nup98 homologous proteins in *S. cerevisiae*, namely Nup100p, Nup116p, and Nup145Np. A deeper insight into the functions of FG domains from Nup98 homologs in yeast required simultaneous genetic manipulation of all of these FG nucleoporins.

2.3.1.1 The GLEBS domain can be functionally transplanted to Nsp1p

The investigation of Nup116p FG repeat domain function is hampered by the presence of the GLEBS domain, which intervenes the FG domain of Nup116p. Deleting the complete FG domain including the GLEBS domain results in a loss of NPC function (Iovine *et al.*, 1995). And removing just the FG regions of the domain and thereby relocating the GLEBS domain directly to the N-terminus of the anchor domain was also lethal (see figure 2.4 A, upper part).

Bailer *et al.* (1998) successfully transplanted the GLEBS domain from Nup116p to Nup100p, which rescued the phenotype caused by the removal of the GLEBS domain from Nup116p. However, this transplantation would not ease the genetic analysis of FG domain functions of yeast Nup98 homologs, since Nup100p is one these homologs.

To gain genetic access to all Nup98 homolog FG domains, we tested the effect of transplanting the GLEBS domain to Nsp1p.

Nsp1p was chosen for two reasons: First, like Nup116p, Nsp1p places a relatively large FG domain to the central part of the NPC so that the GLEBS domain would be positioned into an environment that should mimic its natural surrounding. Second, the Nsp1p FG domain is the only FG domain in the central part of the NPC that does not belong to the "GLFG" type of FG domains. To specifically analyse contribution of "GLFG" type FG domains to NPC function it would be crucial to have genetic access to all of the "GLFG" type Nups. Thus, if transplantation of the GLEBS domain to Nsp1p does not effect its function, reduction of FG mass contributed by "GLFG" type FG domains is possible.

Transplantation of the GLEBS domain from Nup116p to Nsp1p has to meet two demands:

It should not interfere with normal Nsp1p function and it should enable normal GLEBS domain activity.

Nsp1-GLEBSp fusion does not interfere with Nsp1p function

We tested the effect of an Nsp1-GLEBSp fusion construct (figure 2.3 C) on Nsp1p function in two genetic backgrounds: (i)Δ*nsp1* (YMR54) and (ii) Δ*nsp1 t7-loxP-nup49ΔFG myc-loxP-nup57ΔFG* (YMR26).

In a Δ*nsp1* background (YMR54) no obvious phenotype could be detected by a temperature sensitivity assay (figure 2.3 A). Cells grew nearly equally well at all temperatures tested with either the wild type Nsp1p, the Nsp1p anchor domain only, or the Nsp1-GLEBSp fusion protein being present. Furthermore we tested the effect of the Nsp1-
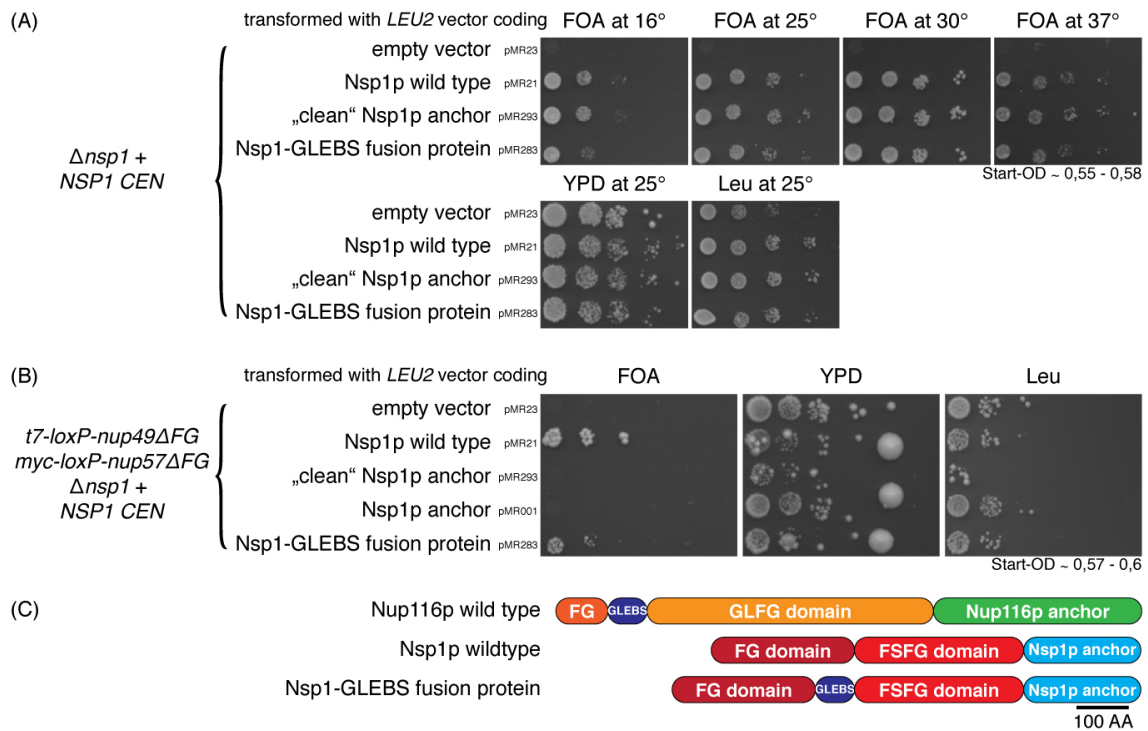
Figure 2.3: Nsp1-GLEBSp fusion does not interfere with Nsp1p function: Constructs were transformed into strains with genetic backgrounds as indicated (panel A: YMR54, panel B YMR26). The ability of the transformed constructs to complement the loss of an Nsp1p wild type protein was monitored by an FOA Assay. (A) Cells on FOA plates were grown for 3 days at 23 °C, 30 °C, and 37 °C and for 8 days at 16 °C. Cells on control plates (YPD, Leu) were grown at 23 °C. Additional controls grown at 16 °C, 30 °C, and 37 °C behave normal (data not shown). (B) Cells were incubated for 12 days at 25 °C. (C) Schematic representation of Nup116p wild type protein, Nsp1p wild type protein, and the Nsp1-GLEBSp fusion protein. Exact amino acid composition of all fusion proteins can be found in section 4.1.10.

GLEBSp fusion protein in YMR26. This strain was chosen since its growth is already severely reduced by scar domains present in FG domain deleted Nup49p and Nup57p (figure 1.3 D). A possible additional negative effect of the GLEBS-Nsp1 fusion protein should therefore be easily detectable.

After 12 days of incubation on FOA, comparable growth behavior was observed both with wild type Nsp1p and with the Nsp1-GLEBSp fusion protein (figure 2.3 B).

No phenotype of the Nsp1-GLEBSp fusion protein could be detected. So we concluded that the GLEBS domain does not interfere with Nsp1p function *in vivo*.

GLEBS domain is functional on Nsp1p

In a next step, we integrated the coding sequence of the Nsp1-GLEBSp fusion protein at the genomic locus of *NSP1*. Then phenotypes of a *NUP116* deletion in a wild type background versus a background with integrated *NSP1-GLEBS* fusion construct were compared. By doing so, we evaluated if the GLEBS domain is functional when transplanted to Nsp1p (figure 2.4).

As expected, the loss of Nup116p in a wild type background resulted in lethality and could not be complemented by the presence of Nup116p anchor domain or the GLEBS domain directly fused to the anchor domain alone (figure 2.4 A, upper part). In contrast, in an *NSP1-GLEBS* fusion background, cells were viable after the loss of wild type Nup116p (figure 2.4 A, lower part). In this background *NUP116* is no longer essential.

These results indicate the functionality of the GLEBS domain after transplantation to Nsp1p. Additionally we demonstrated that *NUP116* becomes dispensable after transplantation.

(A)

transformed with *LEU2* vector coding	FOA	YPD	Leu

∆nup116 + NUP116 CEN

Nup116p wild type ₚMR82
empty vector ₚMR23
Nup116p anchor ₚMR336
GLEBS-Nup116p anchor ₚMR279
Nup116p ∆GLEBS ₚSF1191
Nup116∆GLFG-Spacer-Nup116p anchor ₚSF1196

∆nup116 NSP1-GLEBS + NUP116 CEN

Nup116p wild type ₚMR82
empty vector ₚMR23
Nup116p anchor ₚMR336
GLEBS-Nup116p anchor ₚMR279
Nup116p ∆GLEBS ₚSF1191
Nup116∆GLFG-Spacer-Nup116p anchor ₚSF1196

Start-OD ~ 0,56 - 0,68

(B)

Nup116p wild type — FG GLEBS GLFG domain Nup116p anchor

Nup116p anchor — Nup116p anchor

GLEBS-Nup116p anchor — GLEBS Nup116p anchor

Nup116p ∆GLEBS — FG GLFG domain Nup116p anchor

Nup116∆GLFG-Spacer-Nup116p anchor — FG GLEBS Spacer Nup116p anchor

100 AA

Figure 2.4: Nup116p becomes dispensable after GLEBS transplantation: (A) Indicated constructs were transformed into YMR58 (upper part) and YMR73 (lower part). The ability of the transformed constructs to complement the loss of Nup116p wild type protein was monitored by an FOA Assay. Cells were incubated for 3 days at 25 °C. The exact amino acid composition of fusion proteins can be found in section 4.1.10. (B) Schematic representation of Nup116p mutant proteins. The spacer sequence consists of 16 repeats of the following amino acid sequence: NSGSGTGSSG.

Resulting strains

Transplantation of Nup116p's GLEBS domain into the Nsp1p FG domain led to dispensability of Nup116p. Thus the genetic analysis of Nup98 homologs in *S. cerevisiae* is no longer hindered by the presence of the GLEBS domain on Nup116p.

We used the transplantation background to generate the following ΔFG mutants:

nup100ΔFG

nup145ΔFG

nup100ΔFG nup145ΔFG

nup116ΔFG nup145ΔFG

An additional deletion either of *NUP100* in the *nup116ΔFG nup145ΔFG* background or of *NUP116* in the *nup100ΔFG* background resulted in lethality that could not be rescued by the presence of the corresponding anchor domain alone (figure 2.5). Effects of other additional deletions are not tested so far.
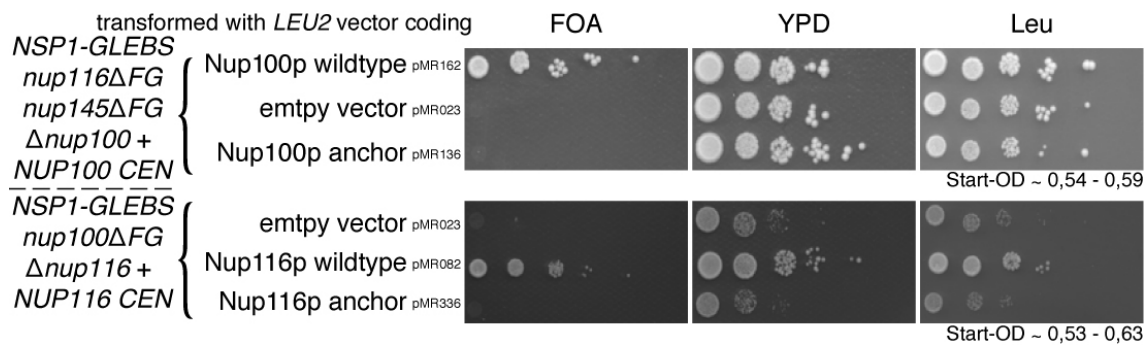
Figure 2.5: Effect of Nup100p and Nup116p deletion: Constructs were transformed into strains with genetic backgrounds as indicated (upper panel YMR128, lower panel YMR127). The ability of the transformed constructs to complement the loss of an according wild type protein was monitored by an FOA Assay. Cells were incubated for 5 days (YMR128) or 2 days (YMR127) at 25 °C, respectively. The exact amino acid composition of the fusion proteins can be found in section 4.1.10.

2.3.1.2 Only Nup116p FG domains can functionally replace the Nup100p FG domain

The deletion of *NUP100* in a *nup116ΔFG nup145ΔFG* mutant background resulted in lethality. This phenotype was rescued by plasmid coded Nup100p wild type protein. And replacing Nup100p only by the Nup100p anchor domain did not rescue lethality (figure 2.5). Obviously, viability was only maintained when Nup100p FG domain was present.

This genetic background offered for the first time the possibility to assay the effect of changing a given FG domain on viability.

With more than 570 amino acids, Nup100p FG domain is the third longest FG domain (after the FG domains of Nup116p and Nsp1p) in *S. cerevisiae*. To test whether the entire FG domain of Nup100p is essential for viability in this mutant background, shortened mutants of the FG domain were tested (figure 2.6).
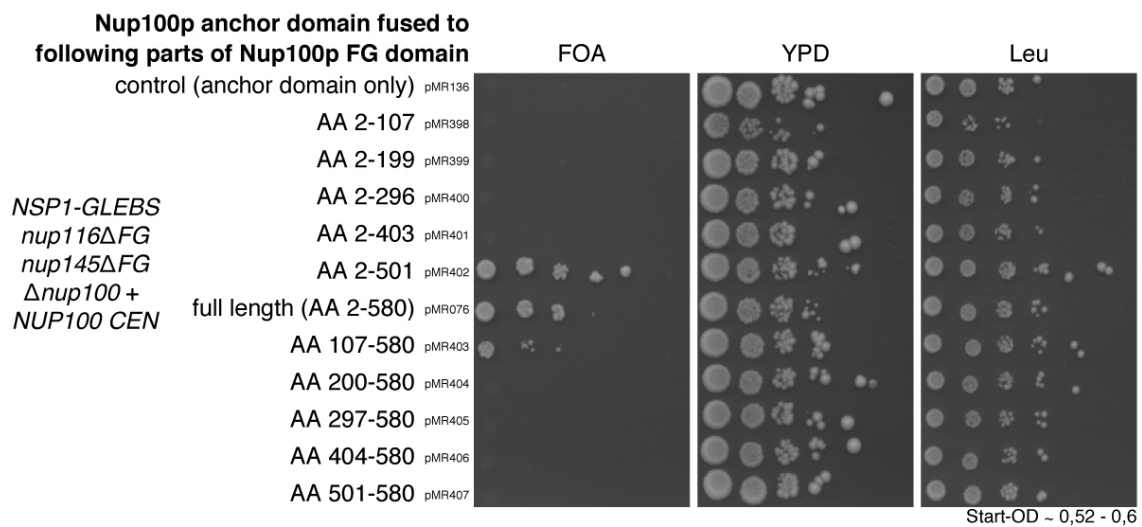
Figure 2.6: Effect of a shortened Nup100p FG domain: Nup100p FG domain was nearly equally divided into five parts. To generate mutant constructs, Nup100p's FG domain was shortened either from the N- or the C-terminus. The constructs were transformed into YMR128. The ability of the transformed constructs to complement the loss of Nup100p wild type protein was monitored by an FOA Assay. Cells were incubated for 7 days at 25 °C. The exact amino acid composition of the fusion proteins can be found in section 4.1.10.

Most of Nup100p's FG mass was needed to maintain viability. Only a minor fraction of around 100 amino acids could be deleted. It was not important whether the FG domain was shortened from its N- or C-terminus.

In a next step, we wondered whether FG domains of other Nups can substitute the Nup100 FG domain. Assuming that a certain FG mass at the Nup100p anchor position is needed, only FG domains from Nup116p and Nsp1p would be long enough to compensate for the loss of the Nup100p FG domain. By contrast, if not the quantity of the fused FG domain is relevant, at least some shorter FG domains should result in viable cells. Additionally, this kind of experiment would address the question to what extent variety of FG domains

is needed.

Thus we assayed the ability of all other endogenous *S. cerevisiae* FG domains to restore viability in this background when they were genetically fused to the Nup100p anchor domain. Out of the endogenous *S. cerevisiae* FG domains, only the FG domain of Nup116p

Figure 2.7: Effect of endogenous *S. cerevisiae* FG domains fused to the Nup100p anchor domain: Indicated FG domains were genetically fused to the Nup100p anchor domain. Their ability to complement the loss of Nup100p wild type was monitored after transformation into YMR128 via FOA Assay. Cells were incubated for 7 days at 25 °C. The exact amino acid composition of the fusion proteins can be found in section 4.1.10.

could replace the FG domain of Nup100p (figure 2.7). Even though the FG domain of Nsp1p has approximately the same length, Nsp1p^{FG}-Nup100p^{anchor} was not able to complement the loss of Nup100p wild type. Apparently the type of the FG domain anchored at this position has a great influence on viability.

2.3.1.3 Only Nup100p FG domains can functionally replace the Nup116p FG domain

As described above, we first investigated the *in vivo* effects of fusing FG domains to the Nup100p anchor position. Only those FG domains originating from Nup100p and Nup116p maintained viability when fused to the Nup100p anchor domain.

To test whether this is a particular peculiarity of the Nup100p anchor domain, we next studied the effects of fusing all endogenous FG domains to the Nup116p anchor domain in the Δ*nup116 nup100*Δ*FG* mutant strain.

Nup116p anchor domain fused to	FOA	YPD	Leu
control (anchor domain only) pMR311			
Nsp1p FG domain pMR315			
Nup49p FG domain pMR313			
Nup57p FG domain pMR314			
Nup100p FG domain pMR316			
Nup116p FG domain pMR82			
Nup145Np FG domain pMR317			
Nup1p FG domain pMR408			
Nup2p FG domain pMR409			
Nup60p FG domain pMR412			
Nup42p FG domain pMR410			
Nup159p FG domain pMR411			

NSP1-GLEBS nup100ΔFG Δnup116 + NUP116 CEN

Start-OD ~ 0,54 - 0,59
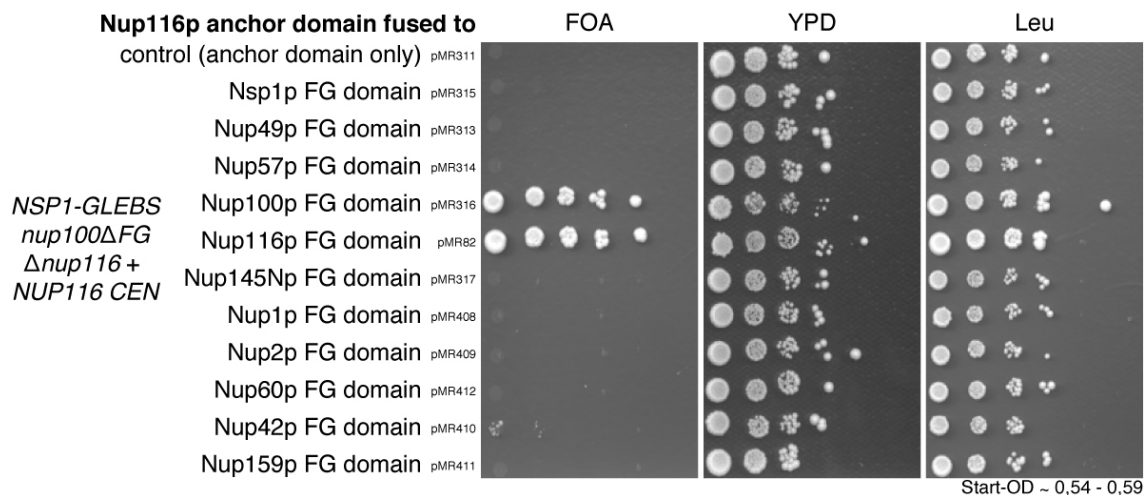
Figure 2.8: Effect of endogenous *S. cerevisiae* FG domains fused to the Nup116p anchor domain: Indicated FG domains were genetically fused to the Nup116p anchor domain. Their ability to complement the loss of Nup116p wild type was monitored after transformation into YMR127 via FOA Assay. Cells were incubated for 7 days at 25 °C. The exact amino acid composition of the fusion proteins can be found in section 4.1.10.

Again, cells were only viable when either wild type Nup116p or Nup100p^{FG}-Nup116p^{anchor} were present (figure 2.8).

Surprisingly, the FG domain of Nup145Np, the third *S. cerevisiae* homolog of vertebrate Nup98, did not rescue viability although its relative amino acid composition is comparable to the Nup100p- and Nup116p FG domain, respectively. One obvious difference is the length of Nup145Np FG domain, which is just 200 amino acids. This is roughly only one third of the length of the Nup100p- or Nup116p FG domain. We therefore assayed whether a multimerized Nup145Np FG domain mutant would enable cell viability.

As shown in figure 2.9, a quadrupled Nup145Np FG domain rescued cell viability after fusion to the anchor domain of Nup100p or Nup116p. But even though viability was achieved with the 4×Nup145Np FG fusion constructs, cells grew much slower as compared to Nup100p- or Nup116p FG domain fusion constructs.

Apparently, a mere substitution of FG mass is not sufficient to maintain cell viability at this anchor domain. However, the experiment in figure 2.6 argues for the importance of FG mass fused to the Nup100p anchor domain. Taken together these data point to the idea that not only the FG mass is important to constitute a functional permeability barrier but that FG domains have to meet more criteria.
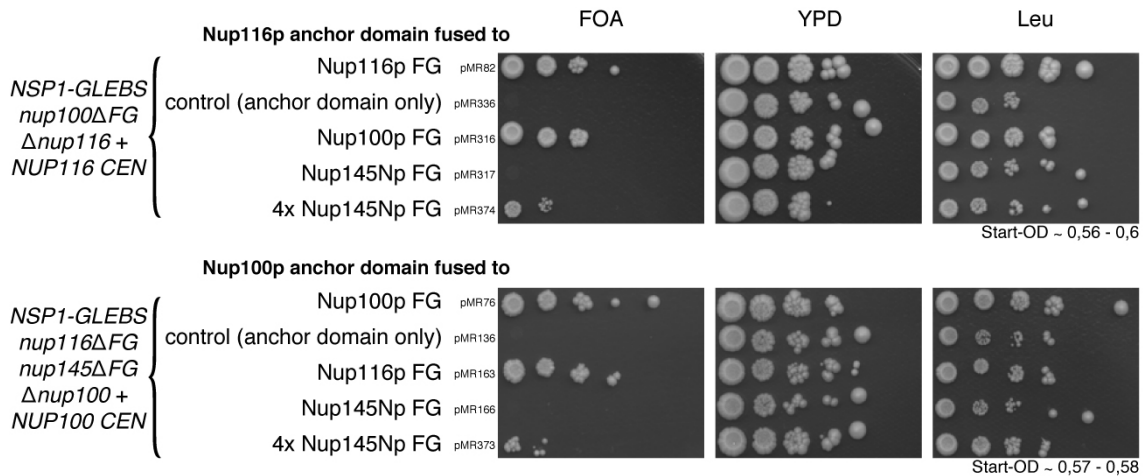
Figure 2.9: Effect of a quadruplicated Nup145N FG domain: Constructs were transformed into strains with genetic backgrounds as indicated (upper panel: YMR127, lower panel: YMR128). The ability of the transformed constructs to complement the loss of an according wild type protein was monitored by an FOA Assay. Cells were incubated for 11 days at 25 °C, respectively. The exact amino acid composition of the fusion proteins can be found in section 4.1.10.

It was shown that cohesive FG domains are important for maintaining the vertebrate permeability barrier (Hülsmann *et al.*, manuscript submitted). Therefore we assume that the presence of a very cohesive FG domain at Nup100p and Nup116p anchor points is likewise crucial for permeability barrier function in yeast.

2.3.2 Endogenous FG domains can functionally replace the Nsp1p FG domain

As shown in the previous chapter, the NPC anchoring domains of Nup100p and Nup116p are quite restrictive concerning which anchored FG domains are able to preserve the integrity of NPC permeability barrier as indicated by cell viability. We wondered whether other anchor domains behave in the same manner. Do they only constitute a functional barrier when anchoring their endogenous FG domain, analogous to Nup100p and Nup116p anchor domain? Or can some anchor domains incorporate any FG domain into the NPC such that cell viability is preserved?

To answer these questions, we tested the effects of additional gene deletions in the multi ΔFG mutant strains. It turned out that the deletion of *NSP1* in the *nup49ΔFG nup57ΔFG nup145ΔFG* mutant strain was lethal and viability could not be restored by providing the Nsp1p anchor domain alone (figure 2.10).
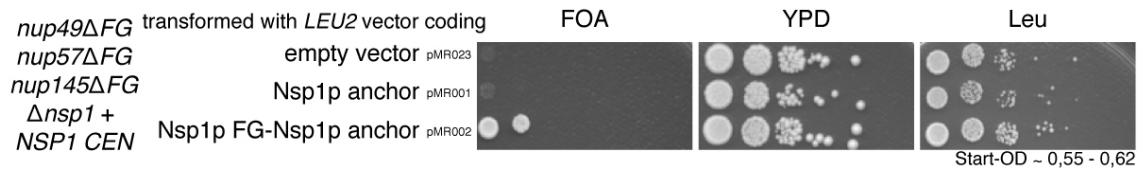
Figure 2.10: FG domains fused to the Nsp1p anchor domain are needed: The ability of the transformed constructs to complement the loss of Nsp1p wild type protein was monitored in YMR113 via FOA Assay. Cells were incubated for 5 days at 25℃. The exact amino acid composition of fusion proteins can be found in section 4.1.10.

Since the Nsp1p FG domain is only cohesive at its distal end, the Nsp1p anchor domain positions an FG domain within the NPC that is non-cohesive around the anchor point (Ader *et al.*, 2010; Yamada *et al.*, 2010). This distinguishes Nsp1p from Nup100p or Nup116p, since their FG domains are entirely cohesive (Patel *et al.*, 2007; Yamada *et al.*, 2010). Thus, this strain allowed us to study the consequences of fusing various FG domains to an anchor domain which endogenously positions a non-cohesive FG domain within the NPC.
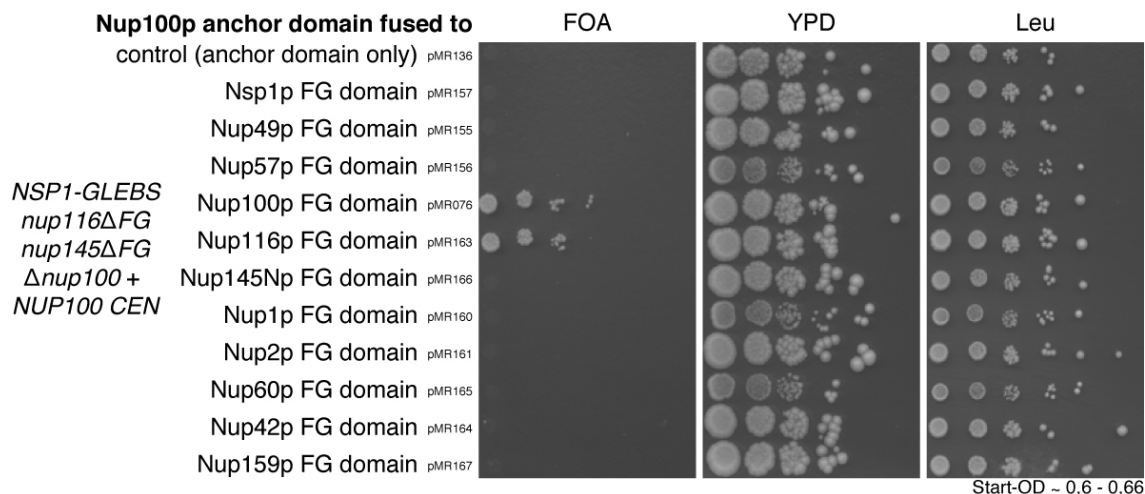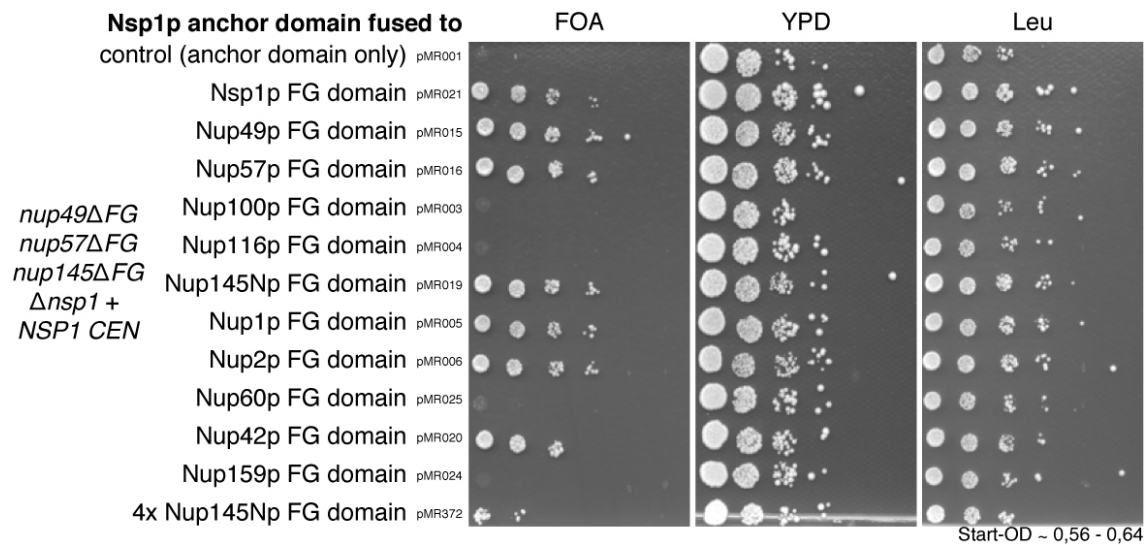

Figure 2.11: Effect of endogenous *S. cerevisiae* FG domain fused to the Nsp1p anchor domain: Indicated FG domains were genetically fused to the Nsp1p anchor domain. Their ability to complement the loss of Nsp1p wild type was monitored after transformation into YMR113 via FOA Assay. Cells were incubated for 5 days at 25℃. The exact amino acid composition of fusion proteins can be found in section 4.1.10.

In contrast to the Nup100p- or Nup116p anchor point, a much higher diversity of fused FG domains was functional at the Nsp1p anchor point (figure 2.11), as indicated by cell

viability. Out of all 11 endogenous *S. cerevisiae* FG domains only those derived from Nup100p, Nup116p, Nup60p, and Nup159p did not rescue cell viability. Irrespective of the FG domains from Nup60p and Nup159p, which cannot functionally replace any tested FG domain, the Nsp1p anchor domain thus tolerates the fusion of a complementary set of FG domains. Even more striking, the fusion protein containing a quadrupled Nup145Np FG domain rescued viability, albeit with a delay in growth. This artificial FG domain seems to be a compromise in terms of supporting viability between the two complementary groups of FG domains.

Obviously the permeability barrier can tolerate a remarkable degree of FG domain substitutions. However, a functional substitution, i.e. resulting in viable cells, is not possible at every anchor domain and with every FG domain respectively. With these result we show for the first time that FG domain anchor points are not equivalent.

2.4 The Nup100p FG domain causes a dominant negative effect at various anchor points

Nup100p and Nup116p FG domains are important for viability. A simultaneous deletion results in lethality. Furthermore, we showed that no other endogenous FG domain can maintain cell viability when substituting Nup100p or Nup116p FG domain at their anchor domains. Therefore, it is remarkable that they did not rescue viability when fused to the Nsp1p anchor domain. One simple explanation for this effect would be that the fusion constructs are not incorporated into the NPC. Thereby the essential Nsp1p anchor domain would not be present in the pore, resulting in a lethal phenotype. This possibility was tested in the following experiment.

2.4.1 Nup100p FG domain fusion constructs are incorporated into the NPC

We generated Citrine labeled fusion constructs to monitor their incorporation into the NPC by confocal microscopy. Citrine is an enhanced version of the yellow fluorescent protein (Griesbeck *et al.*, 2001). Like with the unlabeled constructs, we expected a non viable phenotype after selection for these constructs in the $\Delta nsp1\ nup49\Delta FG\ nup57\Delta FG\ nup145\Delta FG$ mutant strain. Thus, the effect of the fusion protein (Nup100p^{FG}-Citrine-Nsp1p^{anchor}) was evaluated in a $\Delta nsp1$ strain without any further deletions. Nup100p^{FG}-Citrine-Nup49p^{anchor} and Nup100p^{FG}-Citrine-Nup57p^{anchor} chimeric proteins were additionally tested in respective deletion strains (figure 2.12 A).

Though fusion of the Nup100p FG domain to the anchor domains resulted in a decreased cell growth, cells were viable. This argues already for a correct insertion of fusion proteins into the NPC. To further prove their incorporation, fluorescence was monitored by confocal microscopy (figure 2.12 B).

Clearly, rim staining was observed for all constructs, indicating their incorporation into the NPC. Nevertheless, we cannot fully exclude the possibility that fusion proteins only attached to the nuclear envelope or sticked to the NPC without being incorporated.
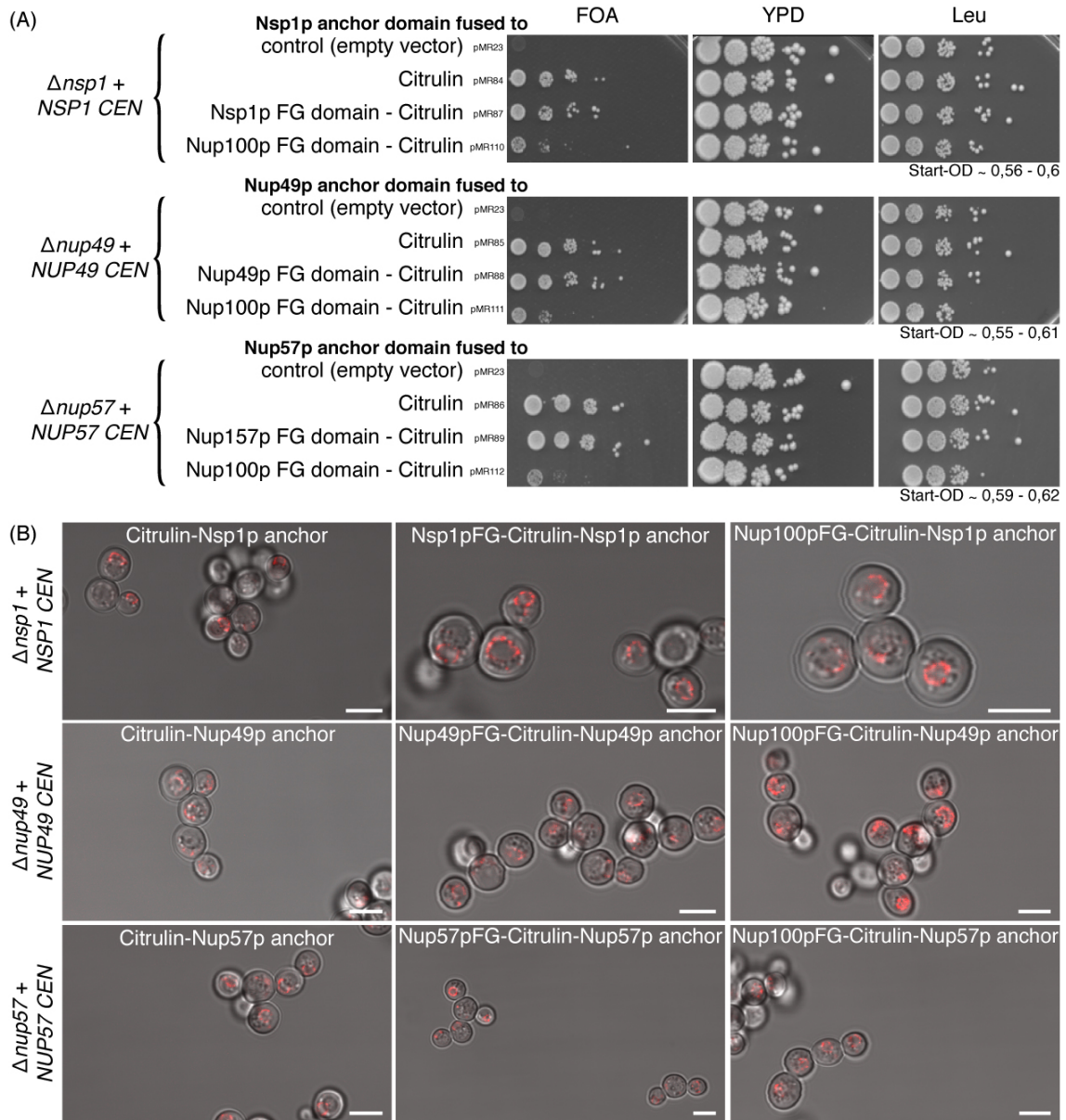
Figure 2.12: Nup100p FG domain fusion proteins incorporate into the NPC: (A) Constructs were transformed into strains with genetic backgrounds as indicated (from top to bottom: YMR29, YMR30, YMR31). The ability of the transformed constructs to complement the loss of an according wild type protein was monitored by an FOA Assay. Cells were incubated for 4 days at 25 °C. The exact amino acid composition of the fusion proteins can be found in section 4.1.10. (B) Cells grown on FOA plates from the assay shown in (A) were analyzed by confocal microscopy as described in section 4.2.3. An overlay of the scattered light image with the fluorescence signal by Citrulin (red) is shown. Scale bars represent 5 µm.

2.4.2 Nup100p FG domain reduces cell growth at various anchor domains

The Nup100p FG domain fused to various Citrine labeled anchor domains was incorporated into the NPC even though transformed cells showed decreased growth rates. We wondered whether the reduction in growth rate observed was an effect of the Citrine labeling or whether the presence of the Nup100p FG domain interfered with normal growth behavior. Hence, we tested various fusions of the Nup100p FG domain to anchor domains in such genetic backgrounds, where the presence of the endogenous FG domain fused to its respective anchor domain is not essential for cell viability (figure 2.13).

In a $\Delta nsp1$ strain, the Nsp1p anchor domain is essential, and its sole presence, i.e. without its FG domain, restored cell growth comparable to a wild type situation. In contrast, cells provided with Nup100p^{FG}-Nsp1p^{anchor} showed reduced growth compared to the presence of the anchor domain alone.

An analogous phenotype was observed in a $\Delta nup49$ strain and in a $\Delta nup57$ strain. Clearly, the reduction in growth rate can be attributed to the presence of the Nup100p FG domain. This dominant negative phenotype of the Nup100p FG domain was even more pronounced in a $\Delta nup57$ $nsp1\Delta FG$ $nup49\Delta FG$ $nup145\Delta FG$ background. Here, the fusion protein Nup100p^{FG}-Nup57p^{anchor} was not able to rescue viability at all.

On the other hand, in a $\Delta nup57$ $nsp1\Delta FG$ $nup49\Delta FG$ $nup100\Delta FG$ background Nup100p^{FG}-Nup57p^{anchor} rescued viability to a similar extent as the wild type protein did. Notably, in this background the Nup100p FG domain was genomically deleted so that it was only supplied by the transformed fusion protein.

2.4.3 The negative effect is not caused by exceeding FG mass

The FG domain of Nup100p is 579 amino acids long ($\sim$58 kD). To test whether exceeding FG mass incorporated at the Nsp1p anchor domain was the cause of lethality, we generated chimeric FG domains and anchored them via the Nsp1p anchor domain in the NPC. The chimeric FG domains were Nup57p^{FG}-Nup49p^{FG} with a total length of 470 amino acids ($\sim$45 kD) and the triple fusion Nup57p^{FG}-Nsp1p^{FG}-Nup49p^{FG} with a total length of 1073 amino acids ($\sim$107 kD) (figure 2.14).

None of these fusions resulted in a dominant negative effect. This argues against the hypotheses that exceeding FG mass fused to the Nsp1p anchor domain negatively impacts viability.
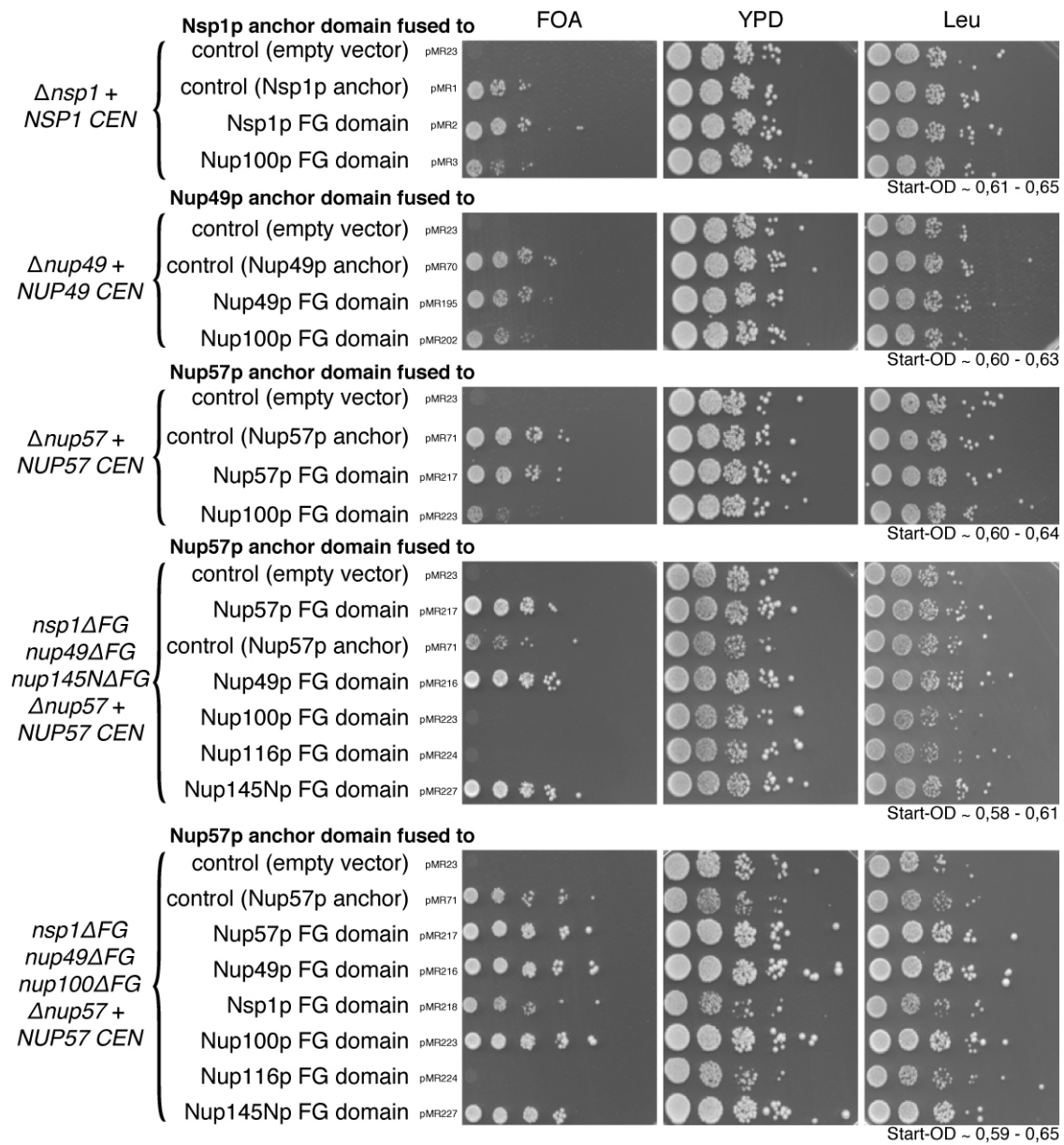
Figure 2.13: Nup100 FG domain fusion proteins show a dominant negative effect: Constructs were transformed into strains with genetic backgrounds as indicated (from top to bottom: YMR29, YMR30, YMR31, YMR78, YMR81). The ability of the transformed constructs to complement the loss of an according wild type protein was monitored by an FOA Assay. Cells were incubated for 3 days (YMR29-YMR31), 4 days (YMR81), or 5 days (YMR78) at 25 °C, respectively. The exact amino acid composition of the fusion proteins can be found in section 4.1.10.
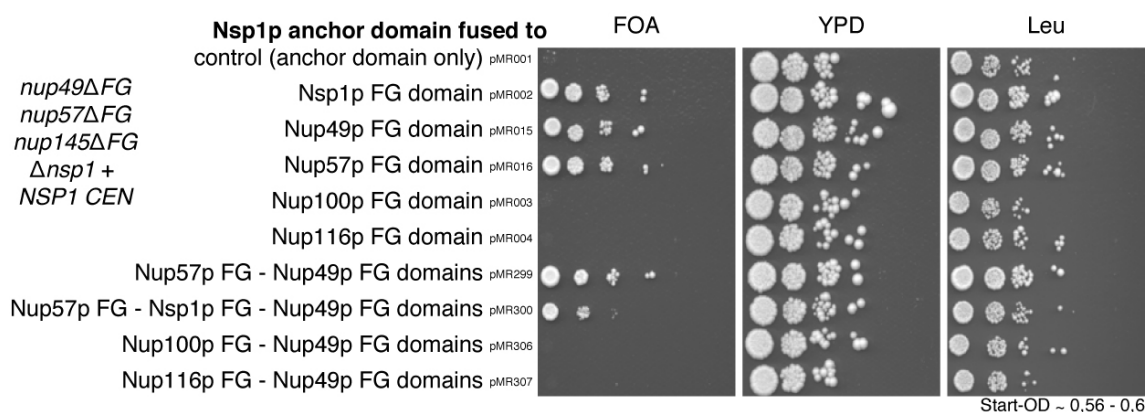
Figure 2.14: Increasing FG mass and junction spacer constructs at the Nsp1p anchor point:
The ability of the transformed constructs to complement the loss of Nsp1p wild type protein was monitored in YMR113 via FOA Assay. Cells were incubated for 6 days at 25 °C. The exact amino acid composition of fusion proteins can be found in section 4.1.10.

2.4.4 The negative effect is not caused by an inappropriate connection to the anchor domain

An alternative explanation for the dominant negative effect of Nup100p^{FG}-Nsp1p^{anchor} on cell growth would be that the artificial connection at the fusion point of the Nup100p- or Nup116p FG domain with the Nsp1p anchor domain is deleterious.

We already knew that Nup49p^{FG}-Nsp1p^{anchor} rescues lethality. So we tested the hypotheses by using parts of the Nup49p FG domain as a "spacer" in between the FG domain of Nup100p or Nup116p and the Nsp1p anchor domain. Again, the presence of Nup100p- or Nup116p FG domain caused a lethal phenotype (figure 2.14).

2.5 FG domain mass is insufficient to predict viability

One main conclusion by Strawn *et al.* (2004) was that remaining FG domain mass is insufficient to predict viability or transport efficiency of a given strain. However, we showed that strains lacking multiple FG domains in some combinations, previously reported to be non-viable, remained viable when the FG domains were cleanly deleted.

Thus it is challenging to ask, whether remaining FG mass is a predictive value for viability when re-evaluated with results from our deletion study. We recalculated therefor the remaining FG mass in the NPC for each of the mutant strains. In table 2.1, data are included that result from screening the effect of an additional gene deletion in the multi ΔFG mutant strains (see section 2.3.2). Like Strawn *et al.* we were not able to predict

Table 2.1: Remaining FG mass in multi ΔFG mutant strains: Strains are sorted according to their remaining FG mass. Remaining FG mass (in MDa) was calculated for each mutant strain on the basis of the FG domain boundaries defined in section 2.2 or according to Strawn *et al.* (2004). The abundance of each FG nucleoporin in the NPC was estimated based on the stoichiometry reported by Rout *et al.* (2000) and on described FG Nup binding sites in the NPC (8 copies of Nup42p, Nup159p, Nup1p, Nup2p, Nup60p, Nup100p, and Nup116p; 16 copies of Nup49p, Nup57p, and Nup145Np; and 24 copies of Nsp1p). ● indicates the presence of the according FG domain in the strain whereas an empty box indicates that the FG domain was deleted.

$Nsp1p^{FG}$	$Nup49p^{FG}$	$Nup57p^{FG}$	$Nup100p^{FG}$	$Nup116p^{FG}$	$Nup145Np^{FG}$	$Nup1p^{FG}$	$Nup2p^{FG}$	$Nup60p^{FG}$	$Nup42p^{FG}$	$Nup159p^{FG}$	FG mass (in MDa)	strain/comment
●	●	●	●	●	●	●	●	●	●	●	4,98	wild type
●	●	●	●			●	●	●	●	●	4,09	YMR77*
●	●	●			●	●	●	●	●	●	3,95	YMR127* ‡
●			●	●		●	●	●	●	●	3,96	YMR109 †
●	●		●			●	●	●	●	●	3,67	(1)
●		●	●			●	●	●	●	●	3,65	(1)
●	●	●				●	●	●	●	●	3,63	YMR128* ‡
●		●			●	●	●	●	●	●	3,62	(1)
●	●			●		●	●	●	●	●	3,61	(1)
●		●		●		●	●	●	●	●	3,59	(1)
●				●	●	●	●	●	●	●	3,57	(1)
●	●	●	●	●	●						3,29	(1)
●	●	●	●		●						2,97	(2)
●	●		●	●	●						2,95	(2)
●	●	●		●	●						2,89	(2)
	●	●	●			●	●	●	●	●	2,85	YMR64 †
		●	●			●	●	●	●	●	2,83	YMR120 †
●	●	●		●	●						2,83	(1)
		●	●	●	●	●	●	●	●	●	2,80	YMR119 †
	●		●	●	●	●	●	●	●	●	2,70	YMR117
		●	●	●	●	●	●	●	●	●	2,68	YMR118
●	●	●		●							2,62	(2)
	●	●	●			●			●	●	2,59	(1)
	●		●		●	●	●	●	●	●	2,56	(1)
		●	●		●	●	●	●	●	●	2,54	(1)
	●	●			●	●	●	●	●	●	2,53	(1)
		●	●		●	●	●	●	●	●	2,49	YMR68 †‡
	●	●	●	●					●	●	2,49	(1)
		●		●		●	●	●	●	●	2,37	YMR122 †
				●	●	●	●	●	●	●	2,34	YMR123 †
	●	●	●	●	●						1,87	(1)
					●	●	●	●	●	●	1,77	YMR124 ‡

● FG domain present / not deleted

* strain with transplanted GLEBS domain, see section 2.3.1.1

† strain non-viable when generated by recombinase strategy, but viable in this study

‡ viability assayed by FOA assay

(1) strain generated by Strawn *et al.* (2004), genotype not reproduced in this study

(2) strain generated by Terry and Wente (2007), genotype not reproduced in this study

▮ viable strain

▮ non-viable strain

viability of cells based on remaining FG mass.

However, it was argued that avidity effects due to cohesion mediated by the FG domains contribute to the incorporation of FG Nups into the NPC (Griffis *et al.*, 2003, Hülsmann *et al.*, submitted). Therefore it might well be that an FG domain deleted Nup is not able to bind to its endogenous binding site within the NPC any longer and that this free binding site is consequently occupied by an other FG Nup. For example, it was shown that Nup100p and Nup145Np can attach to the binding site of Nup116p *in vitro* (Yoshida *et al.*, 2011). Such possible replacements were not considered for the calculation of remaining FG mass.

3 Discussion

Nuclear pore complexes (NPCs) provide the transport route for nucleocytoplasmic exchange (Feldherr, 1962). They establish the permeability barrier (Paine *et al.*, 1975) that excludes inert macromolecules (Paine and Feldherr, 1972; Mohr *et al.*, 2009) but permits facilitated passage of even very large cargoes, provided these are bound to nuclear transport receptors (NTRs, reviewed e.g. by Görlich and Kutay, 1999).

There is strong evidence that FG domains are the building blocks of the permeability barrier:

(i) NTRs bind to FG motifs (e.g. Iovine *et al.*, 1995; Radu *et al.*, 1995; Bayliss *et al.*, 2000, 2002a,b) and this binding was found to be essential for facilitated NPC passage (Bayliss *et al.*, 1999). Even more, this binding accelerates NPC passage of the NTR·cargo complex by a factor of 100-1000 compared to the passage of an inert objects of similar size (Ribbeck and Görlich, 2001).

(ii) FG domains radiate into the central channel of the NPC (Akey and Goldfarb, 1989; Grote *et al.*, 1995). It has been estimated that more than 1000 copies of FG repeats are within one NPC, and that their local concentration in the interior of the central channel approximates 50 mM (Bayliss *et al.*, 1999), which would be sufficient to establish a functional barrier (Ribbeck and Görlich, 2001; Frey and Görlich, 2007).

(iii) FG domains spontaneously form macroscopic hydrogels when a critical protein concentration is exceeded (Frey *et al.*, 2006), and these macroscopic hydrogels reproduce permeability barrier properties of authentic NPCs (Frey and Görlich, 2007, 2009; Milles and Lemke, 2011).

(iv) With the onset of *Aspergillus nidulans* closed mitosis, all FG Nups disperse throughout the cell, whereas the majority of the structural Nups remain at the NPC (Souza *et al.*, 2004; Osmani *et al.*, 2006). Concomitant, proteins that exclusively locate either to the nucleoplasm or the cytoplasm during interphase equilibrate between the two compartments (Suelmann *et al.*, 1997; Ovechkina *et al.*, 2003). Likewise, phosphorylation of vertebrate

Nup98 was suggested to be crucial for mitotic disassembly of the permeability barrier and inhibition of phosphorylation retards NE permeabilization (Laurell *et al.*, 2011).

(v) Upon infection with poliovirus, nuclear proteins leak into the cytoplasm (Belov *et al.*, 2004) and the active import of proteins is suppressed (Gustin and Sarnow, 2001). Associated with this perturbation is the observation that several FG Nups are released from the NPC by the activity of viral proteases (Gustin and Sarnow, 2001, 2002; Park *et al.*, 2008).

3.1 Experimental systems for the analysis of the permeability barrier

Even though the role of FG domains as main building blocks of the permeability barrier is well established, the question how FG domains achieve selectivity while allowing very fast translocation of transport complexes is a central issue in the field. However, addressing this question is challenging since it is not obvious which features of FG domains are important for permeability barrier functionality *in vivo*.

3.1.1 Differences among FG domains

The *S. cerevisiae* permeability barrier is constituted of FG domains originating from 11 distinct nucleoporins (Rout *et al.*, 2000). Thus, heterogeneity is a prominent feature *in vivo*. Besides the fact that several Nups with distinct binding sites within the NPC contribute FG domains, FG domains themselves are also very heterogeneous since they can differ in a multitude of features: (i) their exact FG motif, with "FG", "GLFG", "FxFG", or "FxF" being the prominent ones in yeast, (ii) their length, ranging from around 100 amino acids for the Nup60p FG domain to more than 700 amino acids for the FG domain of Nup116p, (iii) the sequence of their inter-repeat spacer, or (iv) the distribution and frequency of individual amino acids. For example, even though most of the FG domains do not exhibit an overall net charge, they differ in the relative number of charged amino acids[1]. It was proposed that the ratio of charged to hydrophobic amino acids relates to different proposed categories of intrinsically disordered structures for FG domains (Yamada *et al.*, 2010).

However, it is not known whether any of this diverging features is of functional significance

---

[1]More than 20% of the amino acids from the FG domains of Nsp1p, Nup1p, Nup2p, Nup60p, and Nup159p comprise charged amino acids (Asp, Glu, Lys, Arg) whereas the other yeast FG domains exhibit less than 5% charged amino acids.

or whether heterogeneity as such is an essential feature for *in vivo* NPC function.

We know that binding of NTRs to FG motifs is not only essential for facilitated NPC passage (Bayliss *et al.*, 1999) but also accelerates NPC passage of an NTR·cargo complex (Ribbeck and Görlich, 2001). Therefore, NTR binding sites are a crucial functional feature of FG domains.

The hydrophobic clusters of FG domains not only bind NTRs but they also create inter-repeat contacts (Frey *et al.*, 2006; Patel *et al.*, 2007; Frey and Görlich, 2009; Ader *et al.*, 2010; Yamada *et al.*, 2010). Intermolecular interaction between FG domains is determined by their overall cohesiveness. Additionally, it was observed that FG domains bind to non-FG domains of Nups *in vitro* (Patel *et al.*, 2007; Schrader *et al.*, 2008).

In addition to the listed characteristics, there may be more yet unknown but functionally important features.

3.1.1.1 Limits of current experimental systems

So far several types of experimental setups analyzed aspects of FG domain features for permeability barrier functionality.

Recombinantly expressed FG domains were found to form macroscopic hydrogels (Frey *et al.*, 2006). These FG hydrogels display selectivity properties very similar to authentic nuclear pores (Frey and Görlich, 2007, 2009). Using FG hydrogels as a model system allows to study facilitated and passive transport *in vitro*. The system was e.g. used to quantify and compare partition coefficients and entry rates of different molecules in hydrogels derived from distinct FG domains (Frey and Görlich, 2009). Additionally it was shown that hydrogel formation not only depends on hydrophobic interactions but as well on hydrophilic contacts (Ader *et al.*, 2010) specifying further the molecular basis of FG domain cohesiveness. Thus, hydrogels can be a very powerful tool to evaluate the effect of FG domain mutations on transport processes.

However, so far hydrogels were only formed by one kind of FG domain or by a chimeric fusion protein of up to three FG domains, therewith limiting the system for the analysis of heterogeneity. Even more, it is unclear whether hydrogel formation occurs in authentic NPCs and whether it is required for *in vivo* NPC function.

The significance of heterogeneity was addressed by genetic studies in yeast deleting FG domains *in vivo* (Fabre *et al.*, 1995; Strawn *et al.*, 2004; Terry and Wente, 2007). These

studies showed that FG domains build up the permeability barrier in a highly redundant manner, and further indicated that FG domains are not equivalent to each other. Thus, a certain degree of heterogeneity seems to be essential for NPC functionality *in vivo*. However, previous studies did not further specify the need for heterogeneity, neither they addressed the question whether the anchoring points of FG domains within the NPC are of functional significance.

Artificial nanopores that were thought to resemble certain characteristics of NPCs were used to observe transport events or behavior of an ensemble of FG domains (Jovanovic-Talisman *et al.*, 2009; Kowalczyk *et al.*, 2011). In theory, such a system would combine the possibility to manipulate FG domains - and thus to test the effect of changing FG domain features - with the potential to create a "pore" that consists of several distinct FG domains. In hitherto presented systems, FG domains were however immobilized on surfaces and it was assumed that they radiate into the generated channel. This is problematic for two reasons: First, such a model does not accurately mimic the situation in the NPC, where FG domains are grafted inside the translocation channel. Second, the FG domain covered surface provides a multitude of additional binding sites for NTR·cargo complexes. Even more, the systems presented so far did not accomplish selectivity that is in the range of selectivity provided by authentic NPCs.

Computational studies simulating NPCs tried to "observe" transport events *in silico* (e.g. Miao and Schulten, 2009; Mincer and Simon, 2011; Moussavi-Baygi *et al.*, 2011). These studies can be grouped into two categories. All atom molecular dynamics simulations (Miao and Schulten, 2009) allow to accurately study interactions between NPC components but are limited to a very short time scale of nanoseconds to microseconds. However, transport events occur in the range of several milliseconds (Kubitscheck *et al.*, 2005; Yang and Musser, 2006). In contrast, other simulations model longer time scales but to do so they have to reduce the complexity of the system by making prior assumptions[2]. For example, FG domains are modeled as inert filaments interacting solely via FG motifs[3]

---

[2]For a simulation of transport reactions it would be necessary to calculate interactions of more than 800000 atoms for the FG mass plus the mass contributed by multiple NTR·cargo complexes. This is not feasible since computing power is still a limiting factor

[3]Hitherto, binding of FG motifs was simulated with one defined FG-FG off rate. Doing so does not account for the fact that NTR binding to FG motifs increases the off rate.

neglecting interactions mediated by the spacer sequences (Mincer and Simon, 2011).

In summary, all these studies are limited or biased to a certain extent. To clarify the nature of the permeability barrier without a prior bias, the significance of distinct FG domain features and predictions from transport models have to be tested in the context of real NPCs. This might be done by analyzing living cells, native NPCs in permeabilized cells, or NPCs in an engineered system.

To test hypotheses about the significance of FG domain features it is not only necessary to delete individual FG domains but also to integrate artificial FG domains with modified domain features into the NPC. Therefore, a more modular and flexible experimental system is needed.

Experiments performed in such a modular system should allow to clearly evaluate the significance of distinct FG domain features for the functionality of the permeability barrier *in vivo*.

3.1.2 New experimental systems to study the NPC permeability barrier

The development of such a system was very recently reported by Hülsmann *et al.* (manuscript submitted). This system is based on *in vitro* assembled nuclei from *Xenopus laevis* egg extract and allows the incorporation of artificial FG domains into authentic NPCs. Selectivity and tightness are then tested by simultaneously challenging the modified permeability barrier with inert molecules and NTR·cargo complexes.

Here, we report the development of a complementary system based on genetically modified *Saccharomyces cerevisiae* strains. We employed this *in vivo* yeast system to evaluate FG domain features for barrier functionality and to test central predictions of the proposed permeability barrier models.

Like the system by Hülsmann *et al.*, the *in vivo* yeast system allows to incorporate artificial FG domains at various anchor points in the NPC. Functionality of the permeability barrier is assayed by testing cell viability.

In our system, living cells are indicative for the proper function of all physiologically essential nuclear import and export pathways. Living cells allow to additionally test the consequences of cell stress on barrier function. More over, the yeast based system does not rely on recombinantly expressed proteins. Thus, it allows to analyze synthetic FG

domains that cannot be expressed or purified for usage in the *Xenopus* system.

However, the *in vivo* yeast system has one disadvantage compared to the *X. laevis* egg extract system. So far, we cannot distinguish whether a resulting lethal phenotype of an integrated FG domain is caused by (i) a non-selective barrier that results in uncontrolled mixing of cytoplasmic and nuclear content, (ii) a barrier that is too tight so that any transport is prevented, (iii) by the blockade of one specific transport pathway.

In summary, both systems can be used to assay the consequences of fusing any FG domain to one specific anchor point for barrier functionality in authentic NPCs.

3.1.3 Establishment of the yeast genetic system

Our strategy to develop an *in vivo* yeast system relied on the use of previously described FG domain deletion strains (Strawn *et al.*, 2004). We needed a strain with a lethal combination of deleted FG domains. Viability in such a strain should only be re-established by the presence of one specific FG domain. By genetically replacing this FG domain with modified FG domains and testing the consequences for viability we wanted to extrapolate critical features of FG domains for viability.

For the generation of their FG domain deletion strains, Strawn *et al.* (2004) applied a strategy that eventually resulted in an N-terminal extension of the FG domain-deleted nucleoporin. These additional amino acids (the "scar domain" of the deletion strategy) are coded by a remaining recombinase recognition site. We showed here that this scar is causative for a cumulatively deleterious effect in multi ΔFG mutant strains. Furthermore, we demonstrated that the addition of a single scar domain could convert a normally viable multi ΔFG mutant strain into a non-viable strain.

For this reason, the previously generated multi ΔFG mutant strains were not suitable as starting point for our genetic assay. If we had used them, we would not have been able to differentiate between a phenotype caused by the scar domain and a phenotype related to a modification within the FG domain of interest.

We thus had to start generating "clean" multi ΔFG mutant strains.

3.1.3.1 A new FG domain deletion strategy was needed

The generation of "clean" deletion strains useful for the above mentioned assay was faced with two general challenges.

(i) The yeast *S. cerevisiae* harbors 11 FG Nups. To analyse all possible combinations of FG domain deletions, we would have needed to generate 2047 strains[4]. Generating this number of strains seemed unfeasible.

However, Strawn *et al.* (2004) reported that the deletion of all peripherally localized FG domains, namely Nup1p, Nup2p, Nup42p, Nup60p, and Nup159p, results in a viable strain. Furthermore, these FG domains were proposed to primarily function in the disassembly of import or export complexes (Wälde and Kehlenbach, 2010). We therefore assumed that these FG domains do not considerably participate in establishing the peremability barrier. For the generation of a starting strain for our intended assay, we thus focused on deleting only the centrally localized FG domains, namely Nsp1p, Nup49p, Nup57p, Nup100p, Nup116p, and Nup145Np. This reduced the number of possible combinations to 64. Even more, Strawn *et al.* (2004) reported that nearly all ΔFG mutant strains deficient in only one or two FG domains were viable. Thus we did not need to generate all possible double FG domain deletions[5], reducing the number of strains to be generated to 43 at most.

(ii) Two general strategies seem to allow the efficient generation of strains lacking multiple FG domains in various combinations. The strains can be generated either by using a recombinase system or by applying an elaborated scheme of combining ΔFG mutant alleles via mating and sporulation. However, in this study we showed that the use of a recombinase based strategy previously resulted in a cumulatively lethal effect. On the other hand, deficiency in some nucleoporins was shown to result in cell division phenotypes (Baï *et al.*, 2004). Thus a strategy based on mating and sporulation seemed not feasible either.

We decided to employ a strategy based on yeast integration plasmids in combination with selection marker recovery via "loop-out" (for details see section 4.2.2.4). This strategy allows to successively delete any number of FG domains without being limited by the number of available selection marker.

3.1.3.2 FG domains operate in a redundant manner

Pursuing this strategy, we generated a set of new multi ΔFG domain deletion strains that have "clean" genomic deletions, i.e. just the FG domain coding sequence is removed and

---

[4]Any FG domain can either be present or deleted. These two possibilities apply to all of the 11 FG Nups, resulting in 2^{11} possible combinations. However, we do not need to generate the wild type strain, resulting in $2^{11}\text{-}1 = 2047$ combinations.

[5]The number of possible combinations is calculated by the binomial coefficient $\binom{n}{k}$ with n being the total number of considered FG domains and k being the number of combined deletions. There are $\binom{6}{1} = 6$ possible single deletions and $\binom{6}{2} = 15$ combinations for double deletions.

no additional sequences are inserted.

In contrast to previous reports (Strawn *et al.*, 2004), four triple combinations of FG domain deletions resulted in viable strains when the FG domains were "cleanly" deleted. Additionally we reported the viability of three quadruple ΔFG domain strains (see table 2.1 on page 41).

Thus, we enlarged the number of viable multi FG domain deletion strains and therewith corroborated the previous statement that FG domains function in a highly redundant manner (Fabre *et al.*, 1995; Strawn *et al.*, 2004). We conclude that remaining FG mass is insufficient to predict viability or transport efficiency of a given strain. Therefore, FG mass *per se* seems not to be an essential criterium for permeability barrier functionality.

We next assayed the effects of additional complete gene deletions in the multi ΔFG mutant strains. If viability of a strain depends on the presence of the FG domain coded by the previously deleted gene, we can use this strain to assay the effect on viability when this FG domain is replaced by other domains. By doing so, we identified three strains, which fulfill this criterion and could thus be used for the *in vivo* yeast assay.

3.1.3.3 FG domains of the Nsp1 subcomplex are not essential

We show that all FG domains of the Nsp1 subcomplex, i.e. Nsp1p, Nup49p, and Nup57p, can be deleted simultaneously without affecting cell viability.

Fabre *et al.* (1995) already concluded the viability of such a triple FG domain deletion strain whereas Strawn *et al.* (2004) concluded the opposite.

However, there were several differences between these studies: First, Fabre *et al.* only partially deleted the FG domain from Nsp1p. Additionally, the first 12 amino acids of Nup49p were not deleted. Second, Strawn *et al.* performed chromosomal deletions of the FG domains with all mutant alleles being under the control of their endogenous promoters. Fabre *et al.* expressed FG domain deficient Nup49p and Nup57p from a plasmid, with *nup57ΔFG* being under the control of the *NOP1* promoter. And third, the studies differ in the genetic background of the used yeast strains. It was therefore argued that the discrepancy in the observed phenotypes could be due to a difference in the deleted sequences, protein expression levels, or yeast strain background (Strawn *et al.*, 2004).

It is known that *NUP1* becomes non essential in the presence of a suppressor mutant background (Belanger *et al.*, 1994). Thus, the background of a deletion might strongly

influence its phenotype.

We chose the same genetic background as Strawn *et al.* and deleted nearly the same sequences. Only the deleted sequence for Nsp1p slightly varies (Δ3-602 in this study versus Δ13-591 in Strawn *et al.*, 2004). We therefore expected to reproduce the phenotype previously described by Strawn *et al.* (2004).

However, we could show that the lethal phenotype of a *nsp1ΔFG nup49ΔFG nup57ΔFG* strain observed by Strawn *et al.* is only caused by a deleterious effect of the "scar domain". If generated with "clean" FG domain deletions, this combination of deletions results in a viable strain.

This result is in line with the previous observation that the NPC-binding site for Nsp1p on Nic96p is not required for viability, even though deletion of this binding site results in a severe decrease in growth rate (Schrader *et al.*, 2008).

We have not evaluated the mechanism of how the additional amino acids of the "scar domain" negatively impact cell viability further.

It is, however, tempting to speculate about the mechanism. More than one third of the amino acids of the "scar domains" are hydrophobic. It is well possible that scar domains somehow interact with parts of the FG domains or with themselves. Thereby they could form a conglutination that clogs the transport channel of the NPC. This would also explain why a single FG domain deletion via recombinase-driven excision has no detectable effect but the combination of such deletions results in cell death.

3.1.3.4 Re-evaluation of former results is needed

We showed that more FG domains can be simultaneously deleted without affecting viability than previously reported (Strawn *et al.*, 2004; Terry and Wente, 2007). We could attribute the partially drastic differences in reported phenotypes to the presence of a "scar domain" in previously generated yeast strains.

As a consequence, it seems reasonable to re-evaluate conclusions that were drawn by making use of ΔFG mutant strains created by Strawn *et al.* (2004) (ΔFG$^{\mathrm{scar}}$ strains).

For a re-evaluation, three kinds of conclusions need to be distinguished as exemplified in the following: (i) Strawn *et al.* (2004) concluded that FG domains function in a highly redundant manner as a third of the yeast FG mass can be deleted without affecting cell viability. This conclusion, even though obtained by ΔFG$^{\mathrm{scar}}$ strains, holds true since strains should be viable when the same combinations of FG domains are cleanly deleted as compared to viable ΔFG$^{\mathrm{scar}}$ strains.

(ii) By comparing which FG domains are present in viable ΔFG$^{\text{scar}}$ and non-viable ΔFG$^{\text{scar}}$ strains, Strawn *et al.* extrapolate requirements for minimal functional NPCs. This kind of conclusion needs to be reevaluated since some ΔFG$^{\text{scar}}$ strains are viable when cleanly generated (see table 2.1 on page 41).

(iii) Transport of NTR·cargo complexes or reporter constructs was studied to reveal defects in specific transport pathways (Strawn *et al.*, 2004; Terry and Wente, 2007; Meinema *et al.*, 2011). An observed decrease in transport rates was attributed to the absence of a specific subset of FG domains. However, it might as well be attributed to the presence of the scar domain that might strongly bind NTR·cargo complexes or reporter constructs. Thereby the complexes would be retained in the NPC. In this case, the experiments should be repeated in clean multi ΔFG strains to evaluate whether the presence of additional amino acids impacts the results.

3.2 Role of FG domain anchor points

We identified three strains, in which a lethal combination of deleted FG domains was only rescued by the presence of one specific FG domain. These strains allowed to test the effect of fusing any FG domains to the anchor domains of Nup100p, Nup116p, and Nsp1p on viability.

We first employed these strains to test whether endogenous FG domains can functionally substitute each other. In summary, we observed that endogenous FG domains can be grouped into three classes:

(i) The FG domains of Nup60p and Nup159p do not rescue cell viability at any of the tested anchor domains. With only four FG motifs within its 116 amino acids, the Nup60p FG domain might be too short or too low in FG motifs density to functionally replace any other FG domain. But these arguments do not apply to the FG domain of Nup159p. However, the FG domains of Nup60p and Nup159p are the only yeast FG domains with a negative net charge[6] (for amino acid composition analysis see e.g. Patel *et al.*, 2007). Thus the negative net charge might be the cause for the inability of Nup60p$^{\text{FG}}$ and Nup159p$^{\text{FG}}$ to functionally replace other FG domains. To test this assumption, we could generate FG domain mutants, in which Asp and Glu are exchanged to Lys and Arg and vice versa and test their effect on viability when fused to various anchor domains. We further could analyze mutants, in which Asp and Glu are mutated to non-charged amino acids.

---

[6]Nup60p FG domain: 5 Asp, 9 Glu, 10 Lys, 2 Arg; Nup159p FG domain 5 Asp, 6 Glu, 7 Lys, 0 Arg

(ii) FG domains from Nup100p and Nup116p only result in viable cells when fused to the anchor domains of Nup100p or Nup116p.

(iii) All other endogenous FG domains can functionally replace the Nsp1p FG domain.

Both of the two last-mentioned classes comprise FG domains that were shown to provide nuclear transport receptor (NTR) binding sites (Iovine *et al.*, 1995; Bayliss *et al.*, 1999, 2000, 2002a,b; Bednenko *et al.*, 2003; Isgro and Schulten, 2005). Nevertheless, fused FG domains are either functional at one or the other anchor domain. This indicates that the ability of an FG domain to bind NTRs is not sufficient to functionally replace any other FG domain.

Furthermore, we show with these result for the first time that FG domain anchor points are not equivalent. Thus, FG domain function not only depends on properties of the FG domain itself but additionally on its anchor point within the NPC.

3.3 Role of FG domain cohesion for *in vivo* permeability barrier functionality

The "selective phase" model assumes that permeability barrier-forming FG domains mediate multivalent intra- and inter molecular interactions via their cohesive parts. Thereby they create a sieve-like meshwork that prevents diffusion of molecules with a diameter above a size limit defined by the mesh size. NTR·cargo complexes bind to FG motifs and as a consequence disengage FG meshes. This allows their passage through the meshwork (Ribbeck and Görlich, 2002; Frey and Görlich, 2007).

According to the "selective phase" model, cohesiveness and the ability to bind NTRs are thus central features of FG domains.

Previous experiments demonstrated that recombinantly expressed and purified cohesive FG domains indeed form a macroscopic hydrogel that reproduces main properties expected for authentic NPCs (Frey and Görlich, 2007, 2009).

3.3.1 Cohesive FG domains are essential for *in vivo* permeability barrier function

Very recently it was shown that the Nup98 FG domain is the main constituent of the vertebrate's permeability barrier (Hülsmann *et al.*, manuscript submitted). Moreover, the highly cohesive nature of the Nup98 FG domain was shown to be the crucial determinant for a functional barrier and Nup98 FG domain-deficient NPCs failed in establishing an

efficient barrier. This phenotype could only be rescued by re-addition of the Nup98 FG domain or by presence of other cohesive FG repeats (Hülsmann *et al.*, manuscript submitted).

We observed that most triple combinations of FG domain deletions resulted in viable strains. However, in line with the results by Hülsmann *et al.*, already the deletion of the FG domains from two yeast homologs of Nup98, Nup100p and Nup116p resulted in non-viable cells, as reported previously (Iovine and Wente, 1997).
The FG domain of Nup116p harbors the so-called GLEBS domain and it was shown that a strain with a *nup116ΔGLEBS* mutant allele exhibits clusters of herniated NPCs and is temperature sensitive (Bailer *et al.*, 1998). However, in contrast to Iovine and Wente (1997) we can exclude that the lethal phenotype of the double deletion (*nup100ΔFG nup116ΔFG*) is partially caused by the deletion of the GLEBS domain as we functionally transplanted it to Nsp1p prior to the deletion of the Nup116p FG domain. This suggests a prominent functional role of the FG domains of Nup100p and Nup116p for cell viability.

By shortening of the Nup100p FG domain, we learned that a critical FG mass at the Nup100p anchor domain is needed for cell viability when assayed in a *nup116ΔFG* background. However, FG mass fused to the Nup100p anchor alone is not sufficient to constitute a functional permeability barrier (see section 2.3.1.2).
The FG domains of Nup100p and Nup116p are very cohesive, probably even more cohesive than the FG domain of Nup98 (K. Kirli, personal communication). Analogous to the vertebrate NPC, we therefore assume that the FG domains of Nup100p and Nup116p are main constituents of the yeast permeability barrier.

The FG domains of Nup100p and Nup116p cannot be functionally be replaced by any other endogenous FG domain. Nevertheless, an artificially elongated version of the Nup145Np FG domain was able to functionally replace them partially. We predict that also other endogenous cohesive FG domains could functionally replace the FG domains of Nup100p or Nup116p *in vivo* when artificially elongated.
For example, the N-terminal FG subdomain of Nsp1p (Nsp1p$^{2\text{-}175}$) was found to be very cohesive (Ader *et al.*, 2010; Yamada *et al.*, 2010) and preliminary data indeed indicated that this FG subdomain can functionally replace the Nup116p FG domain when a quadrupled mutant of the Nsp1p$^{2\text{-}175}$ FG subdomain is fused to the Nup116p anchor domain. This experiments remains to be repeated and the results carefully analyzed.

3.3.2 Can the NPC channel be blocked by an excessive presence of cohesive FG mass?

We observed that the FG domains of Nup100p and Nup116p inhibit cell growth when fused to the anchor domain of nucleoporins that are part of the Nsp1 subcomplex, i.e. Nsp1p, Nup49p or Nup57p. However, this growth inhibition only becomes apparent in strains where Nup100p^{FG} and Nup116p^{FG} are present at their endogenous anchor points. In contrast, cell growth with a Nup100p^{FG}-Nup57p^{anchor} construct was normal when analyzed in a *nup100ΔFG* background (see figure 2.13, lowest panel, page 39).

One explanation for this phenomenon is that the fusion of FG domains from Nup100p or Nup116p to anchor domains of Nsp1 subcomplex proteins created a permeability barrier that simply was too tight to allow nuclear transport. We suggest that an excessive presence of these cohesive FG domains in the central part of the NPC clogs the pores in a way that facilitated transport is delayed or restricted.

To test this assumption, we will generate two sets of Nup100p FG domain mutants and assay whether they can functionally replace the FG domain of Nsp1p. In one set, the Nup100p FG domain will be gradually shortened. Thus, the incorporated cohesive FG mass will be reduced. For the second set of mutations, we want to reduce the cohesiveness of the Nup100p FG domain e.g. by exchanging hydrophobic amino acids to non-hydrophobic amino acids.

We expect that at least some of these mutants can functionally replace the FG domain of Nsp1p so that cell growth is not inhibited.

3.4 Role of FG domain heterogeneity

In this study, we reason that the FG domains of Nup100p and Nup116p are main constituents of the yeast permeability barrier. But what is the function of the nine other endogenous FG domains if mainly Nup100p and Nup116p FG domains build up the permeability barrier?

It was previously proposed that FG domains from the peripheral Nups might primarily function in the disassembly of import or export complexes (reviewed by Wälde and Kehlenbach, 2010). Even though the peripheral FG Nups might therefore not be involved in maintaining the permeability barrier, yeast features six distinct FG Nups that are thought to localize to the central channel of the NPC and thus are thought to have a primary role in formation of the permeability barrier (Terry and Wente, 2009).

3.4.1 Do less cohesive FG domains regulate the tightness of the yeast permeability barrier?

The Nup100$^{\text{FG}}$-Nsp1$^{\text{anchor}}$ construct provoked only a slight delay of growth when assayed in a $\Delta nsp1$ background. (Please note that in this genetic background all other endogenous FG domains were unaffected and thus present in the NPC.) However, the same construct caused a much more severe phenotype, i.e. non-viability, when assayed in a background where several FG domains were genomically deleted ($\Delta nsp1$ $nup49\Delta FG$ $nup57\Delta FG$ $nup145\Delta FG$). If it is the addition of FG mass that caused this effect, we would however expect exactly the opposite behavior, since addition of cohesive FG mass would more likely result in a blocked NPC channel when the channel is already completely equipped with the endogenous FG domains.

We can overcome this conflict by the following assumption. The permeability barrier of yeast is mainly constituted by the cohesive FG domains of Nup100p and Nup116p. But such a permeability barrier is too tight to allow the transport of very large NTR·cargo complexes due to the strong cohesive properties of these domains. To modulate the barrier, less cohesive or non-cohesive FG domains could "dilute" the barrier.

In an FG domain deletion background the supplemental added FG domain of Nup100p cannot be sufficiently blended by the other remaining FG domains, resulting in the lethal phenotype.

A similar mechanism of "permeability blending" was previously observed in macroscopic hydrogels formed by the FG domain of Nsp1p. A hydrogel formed by the very cohesive N-terminal FG subdomain was so tight that NTR·cargo complexes only accumulated at the surface of the gel and diffusion into the gel was blocked. The regular "FSFG" subdomain alone did not form a hydrogel (Ader *et al.*, 2010). In contrast, both domains together formed a hydrogel that restricted diffusion of inert molecules but highly enriched NTR·cargo complexes thus resembling permeability properties of authentic NPCs (Frey and Görlich, 2007; Ader *et al.*, 2010).

3.4.2 Vertebrates regulate the tightness of their permeability barrier

The hypothesis that yeast NPCs regulate the tightness of their permeability barrier by "blending" too cohesive FG domains with less cohesive FG domains is well in line with other findings. The vertebrate homolog of yeast Nup100p and Nup116p is Nup98. Its FG

domain was found to be highly cohesive and it can form an extremely dense macroscopic hydrogel which is restrictive towards inert molecules. However, this *in vitro* hydrogel is so dense that even NTR·cargo complexes are not allowed to efficiently enter the gel (A. Labokha *et al.*, manuscript in preparation).

It is known that Nup98 is glycosylated *in vivo* (Snow *et al.*, 1987; Davis and Blobel, 1987; Finlay and Forbes, 1990). Labokha *et al.* showed that hydrogels formed of *in vitro*-glycosylated Nup98 FG domain are still restrictive towards inert molecules but allow the enrichment of NTR·cargo complexes in a selective manner. The authors therefore assume that vertebrates titrate the density of their permeability barrier by glycosylation.

In contrast, glycosylation of FG domains is not described in yeast. A regulation of the permeability barrier by glycosylation is thus not expected. However, yeast possesses FG domains that are less-cohesive.

It seems thus reasonable to assume that yeast balanced the cohesiveness of its permeability barrier in the course of evolution by two means. First, the main constituent of the permeability barrier, an evolutionary ancestor of Nup98, was adapted resulting in three distinct homologs with partly differing properties. Second, several less-cohesive FG domains were employed to lower and balance the tightness of the barrier.

3.5 Implications for proposed permeability barrier models

FG domain exhibit a multitude of features. However, the significance of most of the features for functionality of the permeability barrier remained unclear. An essential feature is the binding of NTRs to FG motifs, which is not only essential for translocation but also accelerates NPC passage (Ribbeck and Görlich, 2001). It is unclear how such binding can accelerate translocation since one would expect that a binding delays passage of a molecule.

Several models have been proposed to resolve this enigma (reviewed by Terry and Wente, 2009; Wälde and Kehlenbach, 2010; Yang, 2011).

In general these models can be distinguished by their assumptions concerning the mode of interaction among FG domains. The "selective phase" model and the "forest" model explain barrier characteristics by the ability of FG domains to engage in inter-repeat contacts. On the other side, if the "entropic gate" or the "reduction of dimensionality" model faithfully described NPC selectivity, then inter-FG domain cohesion would not be required. It was recently found that in *Xenopus* NPCs the multivalent cohesion between FG do-

mains is required for a functional permeability barrier (Hülsmann *et al.*, submitted). In line with that we showed that in yeast indeed cohesiveness is an essential feature of FG domains for *in vivo* permeability barrier function.

In the "entropic gate" and the "reduction of dimensionality" model, translocation of NTRs only depends on the presence of NTR binding sites. The models would predict that an exchange of FG domains has no consequences as long as the inserted FG domain provides NTR binding sites.

However, we showed that not all FG domains harboring NTR binding sites can functionally replace the FG domains of Nup100p and Nup116p. On the other side, these two domains, even though they bind NTRs (Iovine *et al.*, 1995; Bayliss *et al.*, 2002b), cannot functionally replace the Nsp1p FG domain. The ability to replace FG domains was thus not related to NTR binding. Neither the "entropic gate" nor the "reduction of dimensionality" model can explain this observation.

The models predict different consequences concerning the deletion of FG domains. In the "reduction of dimensionality" model, deletions would have no effect as long as enough FG mass is present to line the inner wall of the channel. And the deletion of FG mass above a critical value would result in a collapse of facilitated transport. According to the "entropic gate" model, a stepwise deletion of FG domains should result in a stepwise reduction of selectivity because less FG domains would be present to repulse inert macromolecules. And like for the "reduction of dimensionality" model, the deletion of FG mass above a critical value would result in a collapse of facilitated transport. In contrast, according to the "selective phase" or the "forest" model, the effect of deletions would depend on the kind of deleted FG domains. The deletion of non-cohesive FG mass should have no effect whereas the excessive deletion of cohesive FG domains should lead to a collapse of the FG meshwork.

We observed that the simultaneous deletion of the cohesive FG domains from Nup100p and Nup116p results in lethality. Together, these FG domains provide approximately 20% of the total FG mass. If the "entropic gate" or the "reduction of dimensionality" model correctly described NPC functionality, then the deletion of more FG mass would not be compatible with viability. However, a strain with only ∼40% of its FG mass being left over was found to be viable.

Due to these argument, we consider the "entropic gate" and the "reduction of dimension-

ality" model to be refuted.

On the other side, all phenotypes observed in this study are in line with predictions from the "selective phase" model and from the "forest" model. So how can we experimentally distinguish these two models?

The "selective phase" model assumes a homogenous meshwork. In contrast, the "forest" model assumes that FG domains adopt distinct "disordered structures" that create two distinct transport zones within the NPC channel. If the "forest" model correctly predicted NPC functionality, and if we simultaneously deleted all FG domains that are predicted to build up one of these transport zones, then the resulting NPC would not be functional. However, this remains to be tested.

3.6 Perspectives

In this study we developed a new experimental system that allows to manipulate the NPC permeability barrier *in vivo*. We showed that the postulated necessity of cohesiveness, according to the "selective phase" model, is indeed an essential feature of FG domains *in vivo*. However, we assume that both the excessive presence as well as the absence of cohesive FG mass is incompatible with the *in vivo* functionality of the permeability barrier. Furthermore we demonstrated that neither FG domains nor the FG domain anchor points within the NPC are equivalent. Thus, heterogeneity seems to be a crucial for *in vivo* NPC function.

To further analyze predictions by the "selective phase" model and to distinguish them from predictions by other models, we need to extend and exploit our system. Four main directions are obvious.

(i) So far, we did not "cleanly" generate and test all triple and quadruple combinations of FG domain deletions. Doing so would probably pave the way for the creation of new anchor domain test strains which would broaden our understanding of requirements for the anchoring of FG domains. Furthermore, we concentrated so far on the centrally localized FG domains. Is was previously shown that all peripherally localized FG domains can be deleted simultaneously in addition to the deletion of one central FG domain (Strawn *et al.*, 2004; Terry and Wente, 2007). It is provoking to test if our triple of quadruple ΔFG mutants would be viable in a background where all peripherally localized FG domains are

deleted. A viable strain would confirm the assumption that peripherally localized FG domains mainly function in other processes than permeability barrier formation.

(ii) Our system allows to assay the consequences of fusing one FG domain to a given anchor domain. However, we are not yet able to fuse a second FG domain to an unrelated anchor domain. In order to obtain a homogenous permeability barrier, it will be crucial to exchange more than one FG domain.

(iii) To date we only tested the effect of fusing endogenous FG domains to distinct anchor domains. However, to better understand FG domain properties, it is essential to modify and evaluate existing FG domains. Maybe it is possible to balance FG domain cohesiveness in such manner that it is functional at every anchor domain. This artificial FG domain could then be characterized in detail by biophysical and biochemical methods. The artificial quadrupled FG domain of Nup145Np described in this study might serve as a useful starting point for the development of such a universally functional FG domain. It is the only domain so far that is functional at all tested anchor points. However, this artificial domain has to be further optimized since cell growth is seriously delayed when FG domains are replaced by this domain.

(iv) So far, our experimental *in vivo* does not allow to distinguish whether a resulting lethal phenotype of an integrated FG domain is caused (i) by a non-selective barrier that results in uncontrolled mixing of cytoplasmic and nuclear content (ii) by a barrier that is too tight so that any transport is prevented or (iii) by the blockade of one specific transport pathway.
To resolve this issue, two experimental approaches needs to be combined. We need to establish *in vivo* transport assays that allow to monitor the intracellular distribution of very large transport cargos (like ribosomal subunits) and of small inert molecules (like GFP). By comparing steady-state distributions of molecules in wild type strains versus strains with modified FG domains we should be able to evaluate changes in barrier tightness. However, to evaluate the cause of a lethal phenotype such transport assays need to be combined with the ability to induce changes of the barrier. If we put the gene encoding a modified FG Nup under the control of an inducible promotor, we can follow the onset of lethal effects.

4 Materials and Methods

4.1 Materials

4.1.1 Chemicals

If not stated otherwise, laboratory reagents were purchased from Calbiochem (San Diego, CA, USA), GibcoBRL-Life Technologies (Paisley, UK), Merck (Darmstadt, Germany), MoBiTech (Göttingen, Germany), Pharmacia (Uppsala, Sweden), Promega (Madison, WI, USA), Roche Diagnostics (Mannheim, Germany), Carl Roth (Karlsruhe, Germany), or Sigma-Aldrich (St. Louis, MO, USA).

4.1.2 Software

Software	Website
Adobe CS4	https://www.adobe.com/de/products/creativesuite.html
Lasergene 8	http://www.dnastar.com/t-products-lasergene.aspx
Freemind	http://freemind.softonic.de/
BibTeX	http://www.bibtex.org/
ImageJ	http://rsbweb.nih.gov/ij/
LaTeX	http://www.latex-project.org/
Microsoft Office	https://office.microsoft.com
Oligo 6	http://oligo.net/
GeneDesigner	https://www.dna20.com/genedesigner2/
Papers	http://www.mekentosj.com/papers/
"Epson Scan" Software Vers. 3.28A	http://www.epson.de/
Mac OS X Vers. 10.6.8	http://www.apple.com/

4.1.3 Instruments

Research pro multi channel pipette	Eppendorf AG, Hamburg, Germany
Set of "Pipetman" pipettes	Gilson, Middleton, WI, USA
SensoQuest lab cycler	SensoQuest, Göttingen, Germany
GenePulser™	BioRad, Hercules, CA, USA
NanoDrop ND-2000	PEQLAB Biotechnologie GmbH, Erlangen, Germany
Biophotometer plus	Eppendorf AG, Hamburg, Germany
Rotator SB3	Stuart, Stone, Staffordshire, UK
Thermomixer plus	Eppendorf AG, Hamburg, Germany
5415R cooled tabletop centrifuge	Eppendorf AG, Hamburg, Germany
5424 tabletop centrifuge	Eppendorf AG, Hamburg, Germany
Multifuge 3L-R with 75006445 Rotor	Thermo Scientific, Waltham, MA, USA
Liebherr Premium fridge	Liebherr, Biberach, Germany
Liebherr Comfort freezer	Liebherr, Biberach, Germany
Thermostatic cabinet	AquaLytic, Dortmund, Germany
Ecotorn incubator	Infors AG, Basel, Switzerland
Incubator Climo-Shaker ISF1-X	Kuhner AG, Basel, Switzerland
Ultra low freezer	Sanya, Osaka, Japan
Intas Gel Documentation System	Intas Science Imaging Instruments GmbH, Germany
Perfection V700 Photo Scanner	Epson, Tokio, Japan
Micromanipulator MSM System Series 300	Singer Instruments, Roadwater, Somerset, UK
BX50 Microscope	Olympus, Tokio, Japan
TCS SP5 microscope	Leica Microsystems, Wetzlar, Germany
iMac 2,4GHz Intel Core 2 Duo	Apple, Cupertino, CA, UAS

4.1.4 buffers & solutions

10× Ligation buffer:
500mM Tris (pH7,5), 100mM $MgCl_2$, 100mM DTT, 10mM ATP, 250μg/mL BSA
10× PfuS buffer:
200mM Tris-HCl (pH9), 250mM KCl, 100mM $(NH_4)_2SO_4$, 15mM $MgSO_4$, 1% Tween20, 1mg/mL BSA
10× Tth buffer:
100mM Tris-HCl (pH8,9), 15mM $MgCl_2$, 1M KCl, 500μg/mL BSA, 0,5% Tween20
Orange G DNA loading buffer:
10mM Tris-HCl (pH8), 10mM EDTA (pH8), 50% Glycerol (w/v), 0,25% OrangeG (w/v)
LiAc/TE solution:

0,1M Lithiumacetat in 1×TE buffer

10× TE (<u>T</u>ris-<u>E</u>DTA) buffer:

100mM Tris/HCl (pH 8,0), 5mM EDTA

PEG/LiAc/TE solution:

40% (w/v) PEG6000, 1M Lithiumacetat in 1×TE buffer

50× TAE (<u>T</u>ris-<u>A</u>cetat-<u>E</u>DTA) buffer:

242g Tris base, 57,1mL acetic acid, 100mL 0,5M EDTA (pH8) in total 1L

4.1.5 *Escherichia coli* Media

2YT liquid medium		**2YT plates**	
16g	Trypton	16g	Trypton
10g	Yeast Extract	10g	Yeast Extract
5g	NaCl	5g	NaC
20mL	Glycerol 85%	20mL	Glycerol 85%
H_2O	up to 1L	14g	Agar
		H_2O	up to 1L

The ingredients were mixed and autoclaved. Before the plates were poured, 10mL 2M K_2HPO_4 and 10mL of 40% (w/v) glucose were additionally added.

For the selection and culturing of bacteria after transformation, plates or liquid medium were supplemented with the appropriate antibiotics in a final concentrations of $100\mu g/mL$ ampicillin or $25\mu g/mL$ kanamycin.

4.1.6 *Escherichia coli* Strains

Strain	**relevante genotype**	**origin**
NEB5α F´	F´ {$proA^+B^+$ $lacI^q$ $\Delta(lacZ)$M15 zzf::Tn10 (Tet^R)} $fhuA2\Delta(argF\text{-}lacZ)$U169 $phoA$ $glnV44$ $\Phi80\Delta(lacZ)$M15 gyrA96 recA1 relA1 endA1 thi-1 hsdR17	New England Biolabs (Beverly, MA, USA)
TOP10 F´	F´ {$lacI^q$ $Tn10$ (Tet^R)} mcrA $\Delta(mrr\text{-}hsd$RMS-mcrBC) $\Phi80lac$ZΔM15 lacX74 recA1 araD139 $\Delta(ara\text{-}leu)$7697 galU galK rpsL endA1 nupG	Invitrogen (Karlsruhe, Germany)
GM2163	F$^-$ dam-13::Tn9 dcm-6 hsdR2 mcrA mcrB leuB6 his-4 thi-1 ara-14 lacY1 galK2 galT22 xyl-5 mtl-1 rpsL136 tonA31 tsx-78 supE44i	Palmer and Marinus (1994)

4.1.7 *Saccharomyces cerevisiae* Media

Standard yeast media were used (Sherman, 2002). Plates contained 2% (w/v) agar additionally. Media were autoclaved for sterilization and glucose was added afterwards in form of an autoclaved 40% (w/v) glucose solution.

Agar was purchased from Invitrogen (Karlsruhe, Germany), yeast extract and tryptone from Serva (Heidelberg, Germany). CSM-mixes and yeast nitrogen base without ammonium sulfate (YNB) were obtained from MP Biomedicals (Santa Ana, CA, USA).

YPD medium (<u>y</u>east extract, <u>p</u>eptone, <u>D</u>-glucose):

1% (w/v) yeast extract, 2% (w/v) tryptone, 2% (w/v) glucose

CSM medium (<u>c</u>omplete <u>s</u>upplement <u>m</u>ixture):

0,17% (w/v) yeast nitrogen base without ammonium sulfate, 5% ammonium sulfate, 2% (w/v) glucose, CSM-mix according to needs as follows:

CSM complete	790mg/L	(= 0,079% (w/v))
CSM -Leu	690mg/L	(= 0,069% (w/v))
CSM -Ura	770mg/L	(= 0,077% (w/v))
CSM -His	770mg/L	(= 0,077% (w/v))
CSM -Ura -Leu	670mg/L	(= 0,067% (w/v))

Sporulation plates:

1% (w/v) potassium acetat, 0,1% (w/v) yeast extract, 2% (w/v) agar, 0,0204% (w/v) adenine hemisulfate, 0,018% (w/v) tryptophan, 0,03% (w/v) L-leucine, 0,03% (w/v) L-lysine. Potassium acetat, yeast extract, and agar were autoclaved before the remaining ingredients were added in form of a sterile filtered solution.

FOA plates (5-<u>f</u>luoro-<u>o</u>rotic-<u>a</u>cid):

0,17% (w/v) yeast nitrogen base without ammonium sulfate, 5% ammonium sulfate, 2% (w/v) glucose, 0,079% (w/v) CSM complete mix, 1% (w/v) FOA, 2% (w/v) agar.

Yeast nitrogen base without ammonium sulfate, ammonium sulfate, CSM complete mix, and agar were prepared and autoclaved. After the solution was cooled down to ~50°C, glucose in form of a 40% (w/v) autoclaved solution and 100×FOA solution in DMSO

(Zymo Research, Irvine, CA, USA) were added. Before the plates were poured, the pH was adjusted to ∼4,4 by addition of 10M NaOH (∼100μL for 500mL of medium).

4.1.8 *Saccharomyces cerevisiae* Strains

All *Saccharomyces cerevisiae* strains in this study originate from a W303 strain background (originally constructed by Rodney Rothstein).

Table 4.1: *S. cerevisiae* **strains used in this study.** Starting with strain YMR35, all strains below are *MATa △ade2 his3-11, 15 leu2-3, 112 LYS2 trp1-1 ura3 can1-100* and were generated as described in 4.2.2.3 and 4.2.2.4. Please note that numbers given in parentheses indicate deleted amino acids compared to the wild type protein.

Strain	Relevante genotype	Parental strain / Reference
RJY358	*MATa ade2-1 his3-11, 15 leu2-3, 112 LYS2 trp1-1 ura3 can1-100*	provided by R.P. Jansen
SFY401	*MATa ADE2 his3-11, 15 leu2-3, 112 LYS2 trp1-1 ura3 can1-100*	RJY358 / provided by S. Frey
SWY2284	*MATα ade2-1::ADE2 his3-11, 15 leu2-3, 112 LYS2 trp1-1 ura3-1 can1-100*	provided by S.R. Wente (Strawn *et al.*, 2004)
SWY2885	*MATa/α myc-loxP-nup57△GLFG/myc-loxP-nup57△GLFG t7-loxP-nup49△GLFG/t7-loxP-nup49△GLFG ade2-1::ADE2/ade2-1::ADE2 his3/his3 leu2/leu2 LYS2/lys2 trp1-1/TRP1 ura3/ura3 can1-100/can1-100*	provided by S.R. Wente (Strawn *et al.*, 2004)
SWY2930	*MATα t7-loxP-nup49△GLFG flag-loxP-nsp1△FxFG-△FG ade2-1::ADE2 his3-11, 15 leu2-3, 112 lys2 TRP1 ura3-1 can1-100*	provided by S.R. Wente (Strawn *et al.*, 2004)
SWY2934	*MATa myc-loxP-nup57△GLFG flag-loxP-nsp1△FxFG-△FG ade2-1::ADE2 his3-11, 15 leu2-3, 112 lys2 TRP1 ura3-1 can1-100*	provided by S.R. Wente (Strawn *et al.*, 2004)
YMR18	*myc-loxP-nup57△GLFG/myc-loxP-nup57△GLFG t7-loxP-nup49△GLFG/t7-loxP-nup49△GLFG NSP1/△nsp1::HIS3*	SWY2885
YMR26.69	*myc-loxP-nup57△GLFG t7-loxP-nup49△GLFG △nsp1::HIS3 + pMR69 (NSP1 NUP49 NUP57 URA3 CEN)*	YMR18
YMR26.109	*myc-loxP-nup57△GLFG t7-loxP-nup49△GLFG △nsp1::HIS3 + pMR109 (ADH1promotor NSP1 URA3 CENmut)*	YMR18
YMR27	*myc-loxP-nup57△GLFG flag-loxP-nsp1△FXFG-△FG △nup49::HIS + pMR62 (ADH1promotor NUP49 URA3 CEN)*	SWY2934
YMR28	*t7-loxP-nup49△GLFG flag-loxP-nsp1△FXFG-△FG △nup57::HIS + pMR63 (ADH1promotor NUP57 URA3 CEN)*	SWY2930
YMR29	*MATα △nsp1::HIS3 ade2-1::ADE2 his3-11, 15 leu2-3, 112 LYS2 trp1-1 ura3-1 can1-100 + pSF234 (ADH1promotor nsp1△FG (△2-605) URA3 CEN)*	SWY2284
YMR30	*MATα △nup49::HIS3 ade2-1::ADE2 his3-11, 15 leu2-3, 112 LYS2 trp1-1 ura3-1 can1-100 + pMR62 (ADH1promotor NUP49 URA3 CEN)*	SWY2284

Continued on next page

Strain	Relevante genotype	Parental strain / Reference
	Table 4.1 – *Continued from previous page*	
YMR31	*MATα Δnup57::HIS3 ade2-1::ADE2 his3-11, 15 leu2-3, 112 LYS2 trp1-1 ura3-1 can1-100* + pMR63 (*ADH1promotor NUP57 URA3 CEN*)	SWY2284
YMR35	*MATa Δade2 his3-11, 15 leu2-3, 112 LYS2 trp1-1 ura3 can1-100*	SFY401
YMR36	*Δnsp1::HIS3-ADE2* + pMR61 (*ADH1promotor NSP1 URA3 CEN*)	YMR35
YMR37	*Δnup1::URA3-ADE2*	YMR35
YMR38	*Δnup2::URA3-ADE2*	YMR35
YMR39	*Δnup42::URA3-ADE2*	YMR35
YMR40	*Δnup60::URA3-ADE2*	YMR35
YMR41	*Δnup49::HIS3-ADE2* + pMR62 (*ADH1promotor NUP49 URA3 CEN*)	YMR35
YMR42	*Δnup57::HIS3-ADE2* + pMR63 (*ADH1promotor NUP57 URA3 CEN*)	YMR35
YMR43	*Δnup145::HIS3-ADE2* + pSF1126 (*ADH1promotor NUP145 URA3 CEN*)	YMR35
YMR44	*Δnup100::URA3-ADE2*	YMR35
YMR45	*Δnup116::HIS3-ADE2* + pSF1127 (*ADH1promotor NUP116 URA3 CEN*)	YMR35
YMR46	*Δnup159::HIS3-ADE2* + pSF1128 (*ADH1promotor NUP159 URA3 CEN*)	YMR35
YMR47	*nup42ΔFG(Δ4-364)*	YMR39
YMR48	*nup1ΔFG(Δ382-888)*	YMR37
YMR49	*nup1ΔFG(Δ384-1043)*	YMR37
YMR50	*nup42ΔFG(Δ4-364) Δnup1::URA3-ADE2*	YMR47
YMR51	*nup42ΔFG(Δ4-364) Δnup2::URA3-ADE2*	YMR47
YMR52	*nup42ΔFG(Δ4-364) Δnup60::URA3-ADE2*	YMR47
YMR53	*nup42ΔFG(Δ4-364) Δnup100::URA3-ADE2*	YMR47
YMR54	*Δnsp1::HIS3-ADE2* + pMR109 (*ADH1promotor NSP1 URA3 CENmut*)	YMR35
YMR55	*Δnup49::HIS3-ADE2* + pMR114 (*ADH1promotor NUP49 URA3 CENmut*)	YMR35
YMR56	*Δnup57::HIS3-ADE2* + pMR115 (*ADH1promotor NUP57 URA3 CENmut*)	YMR35
YMR57	*Δnup145::HIS3-ADE2* + pMR116 (*ADH1promotor NUP145 URA3 CENmut*)	YMR35
YMR58	*Δnup116::HIS3-ADE2* + pMR117 (*ADH1promotor NUP116 URA3 CENmut*)	YMR35
YMR60	*nup1ΔFG(Δ382-888) Δnup2::URA3-ADE2*	YMR48
YMR61	*nup1ΔFG(Δ382-888) Δnup42::URA3-ADE2*	YMR48
YMR62	*nup1ΔFG(Δ382-888) Δnup60::URA3-ADE2*	YMR48
YMR63	*nup1ΔFG(Δ382-888) Δnup100::URA3-ADE2*	YMR48
YMR64	*nsp1ΔFG(Δ3-602) nup57ΔFG(Δ2-223) nup145ΔFG(Δ10-209)*	YMR108
YMR65	*nup1ΔFG(Δ384-1043) Δnup42::URA3-ADE2*	YMR49
YMR66	*nup100ΔFG(Δ2-576) nup145ΔFG(Δ10-209) nsp1::NSP1-GLEBS*[a]	YMR116
YMR67	*nup1ΔFG(Δ384-1043) Δnup100::URA3-ADE2*	YMR49

Strain	Relevante genotype	Parental strain / Reference
	Table 4.1 – *Continued from previous page*	
YMR68	*nsp1ΔFG*(Δ3-602) *nup57ΔFG*(Δ2-223) *nup145ΔFG*(Δ10-209) Δ*nup49::HIS3-ADE2* + pMR114 (*ADH1promotor NUP49 URA3 CENmut*)	YMR64
YMR69	*nup60ΔFG*(Δ397-512)	YMR40
YMR70	*nsp1::NSP1-GLEBS*[b]	YMR35
YMR71	*nup1ΔFG*(Δ382-888) *nup2ΔFG*(Δ189-556)	YMR60
YMR72	*nup49ΔFG*(Δ2-236)	YMR55
YMR73	*nsp1::NSP1-GLEBS*[b] Δ*nup116::HIS3-ADE2* + pMR117 (*ADH1promotor NUP116 URA3 CENmut*)	YMR70
YMR74	*nsp1::NSP1-GLEBS*[b] *nup100ΔFG*(Δ2-576)	YMR70
YMR75	*nsp1::NSP1-GLEBS*[b] *nup145ΔFG*(Δ10-209)	YMR102
YMR76	*nup1ΔFG*(Δ382-1043) *nup42ΔFG*(Δ4-364)	YMR65
YMR77	*nsp1::NSP1-GLEBS*[b] *nup145ΔFG*(Δ10-209) *nup116ΔFG*(Δ2-714)	YMR75
YMR78	*nsp1ΔFG*(Δ3-602) *nup49ΔFG*(Δ2-236) *nup145ΔFG*(Δ10-209) Δ*nup57::HIS3-ADE2* + pMR115 (*ADH1promotor NUP57 URA3 CENmut*)	YMR120
YMR79	*nup1ΔFG*(Δ382-888) *nup42ΔFG*(Δ4-364)	YMR50
YMR80	*nup49ΔFG*(Δ2-236) Δ*nup100::URA3-ADE2*	YMR72
YMR81	*nsp1ΔFG*(Δ3-602) *nup49ΔFG*(Δ2-236) *nup100ΔFG*(Δ2-576) Δ*nup57::HIS3-ADE2* + pMR115 (*ADH1promotor NUP57 URA3 CENmut*)	YMR118
YMR82	*nsp1ΔFG*(Δ3-602) *nup49ΔFG*(Δ2-236) *nup100ΔFG*(Δ2-576) Δ*nup145::HIS3-ADE2* + pMR116 (*ADH1promotor NUP145 URA3 CENmut*)	YMR118
YMR83	*nsp1ΔFG*(Δ3-602) *nup49ΔFG*(Δ2-236) *nup57ΔFG*(Δ2-223) Δ*nup100::HIS3-ADE2* + pMR151 (*ADH1promotor NUP100 URA3 CENmut*)	YMR119
YMR84	*nsp1ΔFG*(Δ3-602) *nup49ΔFG*(Δ2-236) *nup100ΔFG*(Δ2-576) Δ*nup116::HIS3-ADE2* + pMR117 (*ADH1promotor NUP116 URA3 CENmut*)	YMR118
YMR85	*nsp1ΔFG*(Δ3-602) *nup49ΔFG*(Δ2-236) *nup57ΔFG*(Δ2-223) Δ*nup145::HIS3-ADE2* + pMR116 (*ADH1promotor NUP145 URA3 CENmut*)	YMR119
YMR86	*nup60ΔFG*(Δ397-512) Δ*nup2::URA3-ADE2*	YMR69
YMR87	*nup60ΔFG*(Δ397-512) Δ*nup42::URA3-ADE2*	YMR69
YMR88	*nup60ΔFG*(Δ397-512) Δ*nup100::URA3-ADE2*	YMR69
YMR89	*nup1ΔFG*(Δ382-888) *nup2ΔFG*(Δ189-556) Δ*nup42::URA3-ADE2*	YMR71
YMR90	*nup1ΔFG*(Δ382-888) *nup2ΔFG*(Δ189-556) Δ*nup60::URA3-ADE2*	YMR71
YMR91	*nup1ΔFG*(Δ382-888) *nup2ΔFG*(Δ189-556) Δ*nup100::URA3-ADE2*	YMR71
YMR92	*nup1ΔFG*(Δ382-1043) *nup42ΔFG*(Δ4-364) Δ*nup100::URA3-ADE2*	YMR76
YMR93	*nup1ΔFG*(Δ382-888) *nup42ΔFG*(Δ4-364) Δ*nup2::URA3-ADE2*	YMR79
YMR94	*nup1ΔFG*(Δ382-888) *nup42ΔFG*(Δ4-364) Δ*nup60::URA3-ADE2*	YMR79
YMR95	*nup1ΔFG*(Δ382-888) *nup42ΔFG*(Δ4-364) Δ*nup100::URA3-ADE2*	YMR79

Continued on next page

Strain	Relevante genotype	Parental strain / Reference
	Table 4.1 – Continued from previous page	
YMR96	$nup1\Delta FG(\Delta382\text{-}1043)$ $nup42\Delta FG(\Delta4\text{-}364)$ $\Delta nup60::URA3\text{-}ADE2$	YMR76
YMR97	$nup49\Delta FG(\Delta2\text{-}236)$ $\Delta nsp1::HIS3\text{-}ADE2$ + pMR109 (*ADH1promotor NSP1 URA3 CENmut*)	YMR72
YMR98	$nup49\Delta FG(\Delta2\text{-}236)$ $\Delta nup159::HIS3\text{-}ADE2$ + pMR118 (*ADH1promotor NUP159 URA3 CENmut*)	YMR72
YMR99	$nup49\Delta FG(\Delta2\text{-}236)$ $\Delta nup145::HIS3\text{-}ADE2$ + pMR116 (*ADH1promotor NUP145 URA3 CENmut*)	YMR72
YMR100	$nsp1\Delta FG(\Delta3\text{-}602)$	YMR35
YMR101	$nup57\Delta FG(\Delta2\text{-}223)$ H107Q	YMR35
YMR102	$nup145\Delta FG(\Delta10\text{-}209)$	YMR35
YMR103	$nup49\Delta FG(\Delta2\text{-}236)$ $nup145\Delta FG(\Delta10\text{-}209)$	YMR72
YMR104	$nsp1\Delta FG(\Delta3\text{-}602)$ $nup57\Delta FG(\Delta2\text{-}223)$	YMR100
YMR105	$nsp1\Delta FG(\Delta3\text{-}602)$ $nup145\Delta FG(\Delta10\text{-}209)$	YMR100
YMR106	$nsp1\Delta FG(\Delta3\text{-}602)$ $nup49\Delta FG(\Delta2\text{-}236)$	YMR72
YMR107	$nup49\Delta FG(\Delta2\text{-}236)$ $nup57\Delta FG(\Delta2\text{-}223)$	YMR72
YMR108	$nup57\Delta FG(\Delta2\text{-}223)$ $nup145\Delta FG(\Delta10\text{-}209)$	YMR102
YMR109	$nup49\Delta FG(\Delta2\text{-}236)$ $nup57\Delta FG(\Delta2\text{-}223)$ $nup145\Delta FG(\Delta10\text{-}209)$	YMR103
YMR110	$nup49\Delta FG(\Delta2\text{-}236)$ $nup145\Delta FG(\Delta10\text{-}209)$ $\Delta nsp1::HIS3\text{-}ADE2$ + pMR109 (*ADH1promotor NSP1 URA3 CENmut*)	YMR103
YMR111	$nup49\Delta FG(\Delta2\text{-}236)$ $nup145\Delta FG(\Delta10\text{-}209)$ $\Delta nup57::HIS3\text{-}ADE2$ + pMR115 (*ADH1promotor NUP57 URA3 CENmut*)	YMR103
YMR112	$nsp1\Delta FG(\Delta3\text{-}602)$ $nup145\Delta FG(\Delta10\text{-}209)$ $\Delta nup49::HIS3\text{-}ADE2$ + pMR114 (*ADH1promotor NUP49 URA3 CENmut*)	YMR105
YMR113	$nup49\Delta FG(\Delta2\text{-}236)$ $nup57\Delta FG(\Delta2\text{-}223)$ $nup145\Delta FG(\Delta10\text{-}209)$ $\Delta nsp1::HIS3\text{-}ADE2$ + pMR109 (*ADH1promotor NSP1 URA3 CENmut*)	YMR109
YMR114	$nsp1\Delta FG(\Delta3\text{-}602)$ $nup145\Delta FG(\Delta10\text{-}209)$ $\Delta nup57::HIS3\text{-}ADE2$ + pMR115 (*ADH1promotor NUP57 URA3 CENmut*)	YMR105
YMR115	$nsp1\Delta FG(\Delta3\text{-}602)$ $nup100\Delta FG(\Delta2\text{-}576)$	YMR100
YMR116	$nup100\Delta FG(\Delta2\text{-}576)$ $nup145\Delta FG(\Delta10\text{-}209)$	YMR102
YMR117	$nsp1\Delta FG(\Delta3\text{-}602)$ $nup57\Delta FG(\Delta2\text{-}223)$ $nup100\Delta FG(\Delta2\text{-}576)$	YMR115
YMR118	$nsp1\Delta FG(\Delta3\text{-}602)$ $nup49\Delta FG(\Delta2\text{-}236)$ $nup100\Delta FG(\Delta2\text{-}576)$	YMR106
YMR119	$nsp1\Delta FG(\Delta3\text{-}602)$ $nup49\Delta FG(\Delta2\text{-}236)$ $nup57\Delta FG(\Delta2\text{-}223)$	YMR106
YMR120	$nsp1\Delta FG(\Delta3\text{-}602)$ $nup49\Delta FG(\Delta2\text{-}236)$ $nup145\Delta FG(\Delta10\text{-}209)$	YMR103
YMR121	$nup49\Delta FG(\Delta2\text{-}236)$ $nup57\Delta FG(\Delta2\text{-}223)$ $nup145\Delta FG(\Delta10\text{-}209)$ $\Delta nup100::HIS3\text{-}ADE2$ + pMR151 (*ADH1promotor NUP100 URA3 CENmut*)	YMR109
YMR122	$nsp1\Delta FG(\Delta3\text{-}602)$ $nup49\Delta FG(\Delta2\text{-}236)$ $nup100\Delta FG(\Delta2\text{-}576)$ $nup145\Delta FG(\Delta10\text{-}209)$	YMR118
YMR123	$nsp1\Delta FG(\Delta3\text{-}602)$ $nup49\Delta FG(\Delta2\text{-}236)$ $nup57\Delta FG(\Delta2\text{-}223)$ $nup100\Delta FG(\Delta2\text{-}576)$	YMR118
YMR124	$nsp1\Delta FG(\Delta3\text{-}602)$ $nup49\Delta FG(\Delta2\text{-}236)$ $nup57\Delta FG(\Delta2\text{-}223)$ $nup100\Delta FG(\Delta2\text{-}576)$ $\Delta nup116::HIS3\text{-}ADE2$ + pMR117 (*ADH1promotor NUP116 URA3 CENmut*)	YMR123

Strain	Relevante genotype	Parental strain / Reference
	Table 4.1 – *Continued from previous page*	
YMR125	$nsp1\Delta FG(\Delta 3\text{-}602)$ $nup49\Delta FG(\Delta 2\text{-}236)$ $nup100\Delta FG(\Delta 2\text{-}576)$ $nup145\Delta FG(\Delta 10\text{-}209)$ $\Delta nup57{::}HIS3\text{-}ADE2$ + pMR115 (*ADH1promotor NUP57 URA3 CENmut*)	YMR122
YMR127	$nsp1{::}NSP1\text{-}GLEBS$[b] $nup100\Delta FG(\Delta 2\text{-}576)$ $\Delta nup116{::}HIS3\text{-}ADE2$ + pMR117 (*ADH1promotor NUP116 URA3 CENmut*)	YMR74
YMR128	$nsp1{::}NSP1\text{-}GLEBS$[b] $nup145\Delta FG(\Delta 10\text{-}209)$ $nup116\Delta FG(\Delta 2\text{-}714)$ $\Delta nup100{::}HIS3\text{-}ADE2$ + pMR151 (*ADH1promotor NUP100 URA3 CENmut*)	YMR77

"CEN mut" indicates a vector with mutated centromere region. See 4.1.10 for details.

[a] The GLEBS domain of Nup116p (amino acids 105-175) (Bailer *et al.*, 1998) was inserted into the FG domain of Nsp1p between amino acids 271 and 273. The insertion resulted in the following exact amino acid sequence:

Nsp1p 1-271 + KL + Nup116p 105-175 + GLR + Nsp1p 273-823.

[b] In this strain the GLEBS domain insertion resulted in the following exact amino acid sequence:

Nsp1p 1-271 + KL + Nup116p 105-175 + GLR + Nsp1p 273-602 + T + Nsp1p 603-823.

4.1.9 Oligonucleotides

Oligonucleotides were synthesized by Sigma-Aldrich (St. Louis, MO, USA), Eurofins MWG GmbH (Ebersberg, Germany), or BioSpring GmbH (Frankfurt a. M., Germany).

4.1.10 Plasmids

Plasmids were generated as described in section 4.2.1. Plasmids characterized with "mutated *CEN*" or "*CEN*mut" originate from the pRS416 plasmid backbone. In these plasmids, the centromere region was mutated to result in a less mitotically stable replication plasmid by deleting the 24 base pairs between the *Pml*I and the *Swa*I endonuclease recognition sites of the *ARSH4* sequence.

The plasmid backbone "pRS402mod" originates from pRS402 but carries additional the *URA3* gene sub-cloned from pRS406.

Plasmids named pSF were kindly provided by Steffen Frey.

The following upstream and downstream regions were used as promotor and terminator regions respectively:

	Promotor (bp before start codon)	Terminator (bp after stop codon)
ADH1	433	-
NUF2	-	306
NSP1	488	441
NUP	563	401
NUP2	439	595
NUP42	500	303
NUP49	698	298
NUP57	456	395
NUP60	561	525
NUP100	300	300
NUP116	585	425
NUP145	416	406
NUP159	616	721

Plasmids used in FOA Assays are listed in table 4.2. All other plasmids used in this study are listed in table 4.3.

Table 4.2: Plasmids used in FOA Assays Plasmids listed in this table originate from pRS415 (*CEN LEU2 Amp*). All genes are flanked by the endogenous promotor and terminator regions according to the coded anchor domain.

Plasmid	Insert	Coded protein sequence
pMR001	Nsp1-anchor	Nsp1p 1-2 + GSTQA + 603-823
pMR002	Nsp1-FGs Nsp1-anchor	Nsp1p 1-2 + GS + 2-602 + T + 603-823
pMR003	Nup100-FGs Nsp1-anchor	Nsp1p 1-2 + GS + Nup100p 2-580 + T + Nsp1p 603-823
pMR004	Nup116-FGs Nsp1-anchor	Nsp1p 1-2 + GS + Nup116p 2-725 + A + Nsp1p 603-823
pMR005	Nup1-FxFGs Nsp1-anchor	Nsp1p 1-2 + GS + Nup1p 384-888 + T + Nsp1p 603-823
pMR006	Nup2-FxFGs Nsp1-anchor	Nsp1p 1-2 + GS + Nup2p 189-527 + T + Nsp1p 603-823
pMR015	Nup49-GLFG Nsp1-anchor	Nsp1p 1-2 + GS + Nup49p 2-236 + T + Nsp1p 603-823
pMR016	Nup57-GLFG Nsp1-anchor	Nsp1p 1-2 + GS + Nup57p 2-223 + A + Nsp1p 603-823
pMR019	Nup145N-GLFG Nsp1anchor	Nsp1p 1-2 + GS + Nup145Np 10-209 + A + Nsp1p 603-823
pMR020	Nup42-FG Nsp1anchor	Nsp1p 1-2 + GS + Nup42p 4-364 + A + Nsp1p 603-823
pMR021	Nsp1	Nsp1p wild type
pMR023	empty	-
pMR024	Nup159-FG Nsp1anchor	Nsp1p 1-2 + GS + Nup159p 464-876 + A + Nsp1p 603-823
pMR025	Nup60-FxF Nsp1anchor	Nsp1p 1-2 + GS + Nup60p 397-512 + A + Nsp1p 603-823
pMR060	Nup57anchor-Scar (myc loxP)	MCEQKLISEEDLTSTTLNITSYNVCYTKLLGDIRST + Nup57p 224-541
pMR068	Nup49anchor-Scar (T7 loxP)	MMASMTGGQQMGTSTTLNITSYNVCYTKLLGDIRST + Nup49p 237-472
pMR070	Nup49anchor	MFGSTQAS + Nup49p 237-472
pMR071	Nup57anchor	M GSTQAS + Nup57p 224-541
pMR076	Nup100	Nup100p wild type

Continued on next page

Plasmid	Insert	Coded protein sequence
pMR082	Nup116	Nup116p wild type
pMR084	Citrulin-Nsp1anchor	NGSTQAS + Citrulin + GSGP + Nsp1p 603-823
pMR085	Citrulin-Nup49anchor	MFGSTQAS + Citrulin + GSGPS + Nup49p 237-472
pMR086	Citrulin-Nup57anchor	M GSTQAS + Citrulin + Nup57p 224-541
pMR087	Nsp1FG-Citrulin-Nsp1anchor	Nsp1p 1-2 + GS + Nsp1p 2-602 + TS + Citrulin + GSGP + Nsp1p 603-823
pMR088	Nup49GLFG-Citrulin-Nup49anchor	MFGS + Nup49p 2-236 + TS + Citrulin + GSGPS + Nup49p 237-472
pMR089	Nup57GLFG-Citrulin-Nup57anchor	MNGS + Nup57p 2-223 + AS + Citrulin + GSGPS + Nup57p 224-541
pMR110	Nup100GLFG-Citrulin-Nsp1anchor	MNGS + Nup100p 2-580 + TS + Citrulin + GSGP + Nsp1p 603-823
pMR111	Nup100GLFG-Citrulin-Nup49anchor	MFGS + Nup100p 2-580 + TS + Citrulin + GSGPS + Nup49p 237-472
pMR112	Nup100GLFG-Citrulin-Nup57anchor	MNGS + Nup100p 2-580 + TS + Citrulin + GSGPS + Nup57p 224-541
pMR136	Nup100anchor	Nup100p 1 + GSTQAS + Nup100p 571-959
pMR155	Nup49-GLFG Nup100anchor	Nup100p 1 + GS + Nup49p 2-236 + TS + Nup100p 571-959
pMR156	Nup57-GLFG Nup100anchor	Nup100p 1 + GS + Nup57p 2-223 + AS + Nup100p 571-959
pMR157	Nsp1-FG Nup100anchor	Nup100p 1 + GS + Nsp1p 2-602 + TS + Nup100p 571-959
pMR160	Nup1-FxFG Nup100anchor	Nup100p 1 + GS + Nup1p 384-888 + TS + Nup100p 571-959
pMR161	Nup2-FxFG Nup100anchor	Nup100p 1 + GS + Nup2p 189-527 + TS + Nup100p 571-959
pMR162	Nup100-GLFG Nup100anchor	Nup100p 1 + GS + Nup100p 2-580 + TS + Nup100p 571-959
pMR163	Nup116-GLFG Nup100anchor	Nup100p 1 + GS + Nup116p 2-725 + TS + Nup100p 571-959
pMR164	Nup42-FG Nup100anchor	Nup100p 1 + GS + Nup42p 4-364 + AS + Nup100p 571-959
pMR165	Nup60-FG Nup100anchor	Nup100p 1 + GS + Nup60p 397-512 + AS + Nup100p 571-959
pMR166	Nup145N-GLFG Nup100anchor	Nup100p 1 + GS + Nup145 10-209 + AS + Nup100p 571-959
pMR167	Nup159-FG Nup100anchor	Nup100p 1 + GS + Nup159 464-876 + AS + Nup100p 571-959
pMR195	Nup49-GLFG Nup49anchor	MFGS + Nup49p 2-236 + TS + Nup49p 237-472
pMR202	Nup100-GLFG Nup49anchor	MFGS + Nup100p 2-580 + TS + Nup49p 237-472
pMR216	Nup49-GLFG Nup57anchor	MNGS + Nup49p 2-236 + TS + Nup57p 224-541
pMR217	Nup57-GLFG Nup57anchor	MNGS + Nup57p 2-223 + AS + Nup57p 224-541
pMR218	Nsp1-FG Nup57anchor	MNGS + Nsp1p 2-602 + TS + Nup57p 224-541
pMR223	Nup100-GLFG Nup57anchor	MNGS + Nup100p 2-580 + TS + Nup57p 224-541
pMR224	Nup116-GLFG Nup57anchor	MNGS + Nup116p 2-725 + AS + Nup57p 224-541
pMR227	Nup145N-GLFG Nup57anchor	MNGS + Nup145Np 10-209 + AS + Nup57p 224-541
pMR279	GLEBS-Nup116anchor	Nup116p 1-6 + 140-175 + GLRSTQT + Nup116p 715-1113
pMR283	Nsp1FG-GLEBS-FSFG-Nsp1anchor	Nsp1p 1-271 + KL + Nup116p 105-175 + GLR + Nsp1p 273-602 + T + 603-823
pMR293	clean Nsp1 anchor	Nsp1p 1-2+603-823
pMR294	clean Nup49 anchor	Nup49p 1 + 237-472
pMR295	clean Nup57 anchor	Nup57p 1 + 224-541
pMR299	Nup57GLFG-Nup49GLFG Nsp1anchor	Nsp1p 1-2+GS+ Nup57 2-233+FMG+ Nup49 2-236+T+ Nsp1p 603-823

Continued on next page

Table 4.2 – *Continued from previous page*

Plasmid	Insert	Coded protein sequence
pMR300	Nup57GLFG-Nsp1FG-Nup49GLFG Nsp1anchor	Nsp1p 1-2+GS+Nup57 2-233+FMG+Nsp1p 2-601+FMG+Nup49 2-236+T+Nsp1p 603-823
pMR306	Nup100FG-Nup49FG Nsp1anchor	Nsp1p 1-2+GS+Nup100p 2-580+T+Nup49 23-236+T+Nsp1p 603-823
pMR307	Nup116FG-Nup49FG Nsp1anchor	Nsp1p 1-2+GS+Nup116p 2-725+A+Nup49 23-236+T+Nsp1p 603-823
pMR311	Nup116anchor	Nup116p 1-6 + SAFTGGLT + Nup116p 715-1113
pMR313	Nup49-GLFG Nup116anchor	Nup116p 1-6 + S + Nup49p 2-236 + T + Nup116p 715-1113
pMR314	Nup57-GLFG Nup116anchor	Nup116p 1-6 + S + Nup57p 2-223 + A + Nup116p 715-1113
pMR315	Nsp1-FG Nup116anchor	Nup116p 1-6 + S + Nsp1p 2-602 + T + Nup116p 715-1113
pMR316	Nup100-GLFG Nup116anchor	Nup116p 1-6 + S + Nup100p 2-580 + T + Nup116p 715-1113
pMR317	Nup145N-GLFG Nup116anchor	Nup116p 1-6 + S + Nup145 10-209 + A + Nup116p 715-1113
pMR336	clean Nup116anchor	M + Nup116p 715-1113
pMR372	4xNup145FG Nsp1anchor	MGSTS + 3x(Nup145Np 10-209 + AS) + Nup145 10-209 + A + Nsp1p 603-823
pMR373	4xNup145FG Nup100anchor	MGSTS + 4x (Nup145Np 10-209 + AS) + Nup100p 571-959
pMR374	4xNup145FG Nup116anchor	Nup116p 1-6 + STS + 3x(Nup145Np 10-209 + AS) + Nup145 10-209 + A + Nup116p 715-1113
pMR398	Nup100FG-Nterm-short1	MGS + Nup100p 2-107 + TS + Nup100p 571-959
pMR399	Nup100FG-Nterm-short2	MGS + Nup100p 2-199 + S + Nup100p 571-959
pMR400	Nup100FG-Nterm-short3	MGS + Nup100p 2-296 + TS + Nup100p 571-959
pMR401	Nup100FG-Nterm-short4	MGS + Nup100p 2-403 + S + Nup100p 571-959
pMR402	Nup100FG-Nterm-short5	MGS + Nup100p 2-501 + Nup100p 571-959
pMR403	Nup100FG-Cterm-short1	M + Nup100p 107-580 + TS + Nup100p 571-959
pMR404	Nup100FG-Cterm-short2	MGS + Nup100p 200-580 + TS + Nup100p 571-959
pMR405	Nup100FG-Cterm-short3	MG + Nup100p 297-580 + TS + Nup100p 571-959
pMR406	Nup100FG-Cterm-short4	M + Nup100p 404-580 + TS + Nup100p 571-959
pMR407	Nup100FG-Cterm-short5	MG + Nup100p 501-580 + TS + Nup100p 571-959
pMR408	Nup1FxFG Nup116anchor	Nup116p 1-6 + S + Nup1p 384-888 + T + Nup116p 715-1113
pMR409	Nup2FxFG Nup116anchor	Nup116p 1-6 + S + Nup2p 189-527 + T + Nup116p 715-1113
pMR410	Nup42FG Nup116anchor	Nup116p 1-6 + S + Nup42p 4-364 + A + Nup116p 715-1113
pMR411	Nup159FG Nup116anchor	Nup116p 1-6 + S + Nup159p 464-876 + A + Nup116p 715-1113
pMR412	Nup60FG Nup116anchor	Nup116p 1-6 + S + Nup60p 397-512 + A + Nup116p 715-1113
pSF1191	Nup116 ΔGLEBS	Nup116p 1-109 + 167-1113
pSF1196	NUP116 ΔGLFG174-715-Spacer	Nup116p 1-175 + 16x(NSGSGTGSSG) + T + Nup116p 715-1113

Table 4.3: Additional plasmids used in this study Plasmids listed in this table originate from pRS415 (*CEN LEU2 Amp*).

Plasmid	Insert	Promotor	Terminator	Backbone	Marker
pMR061	*NSP1*	*ADH1*	*NUF2*	pRS316	*URA3 Amp*
pMR062	*NUP49*	*ADH1*	*NUF2*	pRS316	*URA3 Amp*
pMR063	*NUP57*	*ADH1*	*NUF2*	pRS316	*URA3 Amp*

Plasmid	Insert	Promotor	Terminator	Backbone	Marker
Table 4.3 – *Continued from previous page*					
pMR069	*NSP1 NUP49 NUP57*	endogenous		pRS416	*URA3 Amp*
pMR092	knockIn *nup49ΔFG (Δ2-236)*	*NUP49*		pBlueScript	*Amp*
pMR096	knockIn *nup1ΔFG (Δ382-888)*	*NUP1*		pBlueScript	*Amp*
pMR097	knockIn *nup1Δ (Δ384-1043)*	*NUP1*		pBlueScript	*Amp*
pMR098	knockIn *nup2ΔFG (Δ189-556)*	*NUP2*		pBlueScript	*Amp*
pMR099	knockIn *nup42ΔFG (Δ4-364)*	*NUP42*		pBlueScript	*Amp*
pMR100	knockIn *nup60ΔFG (Δ397-512)*	*NUP60*		pBlueScript	*Amp*
pMR109	*NSP1*	*ADH1*	*NUF2*	CENmut	*URA3 Amp*
pMR114	*NUP49*	*ADH1*	*NUF2*	CENmut	*URA3 Amp*
pMR115	*NUP57*	*ADH1*	*NUF2*	CENmut	*URA3 Amp*
pMR116	*NUP145*	*ADH1*	*NUF2*	CENmut	*URA3 Amp*
pMR117	*NUP116*	*ADH1*	*NUF2*	CENmut	*URA3 Amp*
pMR139	loopOut *nsp1ΔFG (Δ3-602)*	*NSP1*		pRS402mod	*URA3 ADE2 Amp*
pMR141	loopOut *nup57ΔFG (Δ2-223)*	*NUP57*		pRS402mod	*URA3 ADE2 Amp*
pMR142	loopOut *nup145ΔFG (Δ10-209)*	*NUP145*		pRS402mod	*URA3 ADE2 Amp*
pMR143	loopOut *nup100ΔFG (Δ2-576)*	*NUP100*		pRS402mod	*URA3 ADE2 Amp*
pMR151	*NUP100*	*ADH1*	*NUF2*	CENmut	*URA3 Amp*
pMR288	loopOut *nsp1FG-GLEBS-FSFG-nsp1anchor*	*NSP1*		pRS402mod	*URA3 ADE2 Amp*
pMR326	loopOut *nup116ΔFG (Δ2-714)*	*NUP116*		pRS402mod	*URA3 ADE2 Amp*
pSF0234	*nsp1ΔN (Δ2-605)*	*ADH1*	*NUF2*	pRS316	*URA3 Amp*
pSF1126	*NUP145*	*ADH1*	*NUF2*	pRS416	*URA3 Amp*
pSF1127	*NUP116*	*ADH1*	*NUF2*	pRS416	*URA3 Amp*
pSF1128	*NUP159*	*ADH1*	*NUF2*	pRS416	*URA3 Amp*

4.2 Methods

4.2.1 Standard Methods in Molecular Biology

All standard methods in Molecular Biology were performed on the basis of Sambrook and Russell (2001) with modifications as described in this section.

4.2.1.1 Polymerase Chain Reaction (PCR)

Specific DNA fragments can be amplified from template DNA by polymerase chain reaction (PCR)(Mullis *et al.*, 1986). Use of synthesized primers enables the introduction of endonuclease restriction sites at both ends of the generated DNA fragment for subsequent cloning steps. Oligonucleotide synthesis of primers was performed by Sigma-Aldrich (desalted oligonucleotides were used, if not stated otherwise).

In general, a 100μL reaction mixture for PCR was composed as described below:

$x\mu$L	Template DNA solution (approximately 50-100ng)
10μL	2,5mM dNTP-mix (containing 2,5mM of dGTP, dATP, dTTP, dCTP respectively)
1μL	100μM forward primer
1μL	100μM reverse primer
1μL	DNA polymerase
10μL	$10\times$ polymerase buffer

fill with H_2O to a total volume of 20μL

The polymerase and its buffer were chosen according to requirements: PfuS polymerase tripple mix (100ng/μL PfuS DNA polymerase, 15ng/μL Pab pyrophosphatase, 2,5ng/μL Pab dUTPase; produced in the department by S. Frey) was used for general cloning, whereas Tth polymerase mix (100ng/μL Tth DNA polymerase, 15ng/μL Pab pyrophosphatase; produced in the department by S. Frey) was used for colony PCR reactions (see 4.2.1.7 or 4.2.2.7).

PCR reactions were performed in a SensoQuest lab cycler, programmed with needed temperatures and durations, outlined here for a typical reaction with PfuS polymerase:

Initial denaturation step

98℃	2min

Amplification cycles (30-35 cycles)

98℃	30sec
$t_{annealing}$	30sec
72℃	$t_{amplification}$

Completion step

72℃	5 min
10℃	∞

$t_{annealing}$ stands for the average annealing temperature of a specific primer pair calculated by Oligo software and $t_{amplification}$ represents the duration of amplification, depending on the expected sequence length and amplification rate of the DNA polymerase (estimated to

be ∼30sec/kb for PfuS- and ∼40-60sec/kb for Tth DNA Polymerase). In reactions were Tth DNA polymerase was used, denaturing temperature was lowered to 94℃.

4.2.1.2 Mutagenesis Polymerase Chain Reaction

Mutagenesis PCR allows (i) to delete a small part of a gene, (ii) to exchange single amino acids coded in a gene, or (iii) to introduce base pairs coding for additional amino acids. For this purpose PCR primers were designed that amplify the entire plasmid of interest. The changes originate from non-complementary base pairs of the primers. Apart from that the primers were complementary to the regions to be modified. For mutagenesis PCR HPLC-purified and phosphorylated primers were ordered. A PCR reaction with PfuS DNA polymerase was performed as described in 4.2.1.1. After the reaction, the PCR product was precipitated by addition of one volume isopropanol to the PCR reaction mixture followed by 10min of centrifugation (table-top centrifuge, 13000rpm) at room temperature. The supernatant was removed and the resulting pellet was resuspended in $30\mu L$ digestion mix ($2510\mu L$ H_2O, $3\mu L$ NEB buffer 4, $2\mu L$ DpnI (20 U/μL)) for digestion of the methylated template plasmid. The digestion reaction was incubated for 1-2h at 37℃. Subsequently, the mix was purified by DNA gel purification (4.2.1.4) and ligated overnight at 16℃ (4.2.1.5). 1-2μL of the ligated PCR product reaction was transformed into *E. coli* (4.2.1.6) and plated on selective medium.

4.2.1.3 DNA Gel Electrophoresis

Corresponding to their size, double stranded DNA fragments can be separated by their migration behavior in an agarose matrix exposed to an electric field. This method was used to separate, analyse and purify DNA fragments created by PCR or restriction digestion. Depending on the size of the expected DNA fragments, 0,8% - 3% (w/v) of agarose was dissolved in TAE buffer by heating. For visualization of DNA, the intercalating dye ethidium bromide (EtBr) was added to a final concentration of ∼0,5μg/mL. The resulting gel solution was poured into custom-made gel slides. After solidification, the gel was transferred into a custom-made electrophoresis chamber and a DNA marker of known size (1kb DNA ladder, Fermentas) as well as DNA samples mixed with 1:10 (v/v) Orange G DNA loading buffer were loaded to the gel. Electrophoresis was carried out at ∼160V for approximately 30min. DNA was detected by direct examination of the gel in UV light with Intas Gel Documentation System (Intas Science Imaging Instruments GmbH, Göttingen, Germany).

4.2.1.4 Purification of DNA fragments from Agarose Gel and Concentration Determination

After DNA gel electrophoresis, separated DNA fragments were cut out from the gel and purified with the Zymoclean Gel DNA recovery kit (Zymo Research, CA, USA) according to manufacturer's instructions.

DNA concentrations were determined with a NanoDrop ND-2000 spectrophotometer.

4.2.1.5 Enzymatic Restriction Digestion & Ligation of DNA

All restriction endonucleases were purchased from NEB (New England Biolabs, Beverly, MA, USA). Digestion reactions were carried out according to manufacturer's instructions and at least 2-fold excess of enzyme was used for 1h digestions at 37℃. For over night digestion at 37℃ the amount of restriction endonucleases was decreased.

Ligations were performed using the T4 ligase (100ng/μL; produced in the department by S. Frey). Ligation reaction mix was set up as follows:

$x\mu$L $\sim$ 30fmol Vector DNA ($\sim$20ng/kb)
$x\mu$L $\sim$ 60fmol Insert DNA ($\sim$40ng/kb)
1μL   T4 DNA ligase
10μL   10$\times$ ligation buffer
fill with H$_2$O to a total volume of 10μL

To reduce religation reactions of the vector, DNA was dephosphorylated for 30min at 37℃ with 1μL FastAP (Fermentas, Glen Burnie, Maryland, USA) prior to ligation. As a negative control and to evaluate the relative efficiency of a ligation reaction, digested and dephosphorylated vector was incubated without addition of inserts.

The ligation reaction mix was mixed, shortly spined down in a table-top centrifuge and incubated for 30min at 37℃ for sticky-end ligations or overnight at 16℃ for blunt-end ligations. Afterwards 1μL of ligation reaction mix was introduced into *Escherichia coli* cells by electroporation (4.2.1.6).

4.2.1.6 Transformation of *Escherichia coli* with DNA

For electroporation, 45μL electro-competent *Escherichia coli* cell solution (prepared in the department by G. Kopp) was mixed in an electroporation cuvette (BioRad, Burlington, USA) with 1μL of DNA ligation reaction mix or $\sim$50ng of plasmid DNA. Electroporation

was performed in a GenePulser™ device (BioRad, Burlington, USA) according to manufacturer's instructions. Afterwards cells were recovered in 1mL 2YT medium supplemented with 0,2% glucose without antibiotics and incubated for 45min at 37℃ in a Thermomixer comfort (Eppendorf, Germany) agitating with 1300rpm. Cells were subsequently plated on selective agar plates containing an appropriate antibiotic (100μg/mL Ampicillin or 25μg/mL Kanamycin) and incubated overnight at 37℃.

4.2.1.7 Colony PCR with *Escherichia coli* cells

A variation of the PCR method (4.2.1.1) was used to screen for correct cloning constructs after transformation of *Escherichia coli* cells. Instead of using purified DNA, living cells were added as a template. For this purpose a colony was picked and thoroughly resuspended in 50μL of medium. 1μL of the resulting cell suspension was added to 19μL PCR reaction mixture (see 4.2.1.1). Tth polymerase mix (100ng/μL Tth DNA polymerase, 15ng/μL Pab pyrophosphatase; produced in the department by S. Frey) was used for colony-PCR. The PCR reaction was followed by analysis via agarose gel electrophoresis (4.2.1.3). In case of a positive result, the remaining cell suspension was used to inoculate a culture for DNA purification.

4.2.1.8 Plasmid DNA Purification from *Escherichia coli*

Plasmid DNA from *Escherichia coli* was purified with the assistance of G. Kopp at analytical scale using the NucleoSpin® Plasmid Mini kit (Macherey Nagel, Germany) or at preparative scale using NucleoBond® Xtra Midi kit (Macherey Nagel, Germany) according to the manufacturer's instructions.

2mL of 2YT medium containing appropriate antibiotics were inoculated for analytical purification while 250mL of 2YT medium were used for preparative purification. The cultures were incubated over night at 37℃.

4.2.1.9 DNA Sequencing

DNA sequencing reactions of plasmids or purified DNA fragments generated by PCR were performed by Seqlab-Sequence Laboratories Göttingen GmbH. The results were analyzed with SeqMan Software.

4.2.2 Methods in *Saccharomyces cerevisiae* Genetics

4.2.2.1 General Culture and Storage of *Saccharomyces cerevisiae*

Strains were cultured at 30℃ or, if necessary, at 25℃ either in YPD medium or in SD-medium, selecting for the appropriate auxotrophy marker.

Growth of liquid cultures was monitored by measuring the optical density at 600nm (OD_{600}) with a Eppendorf BioPhotometer plus.

For long-term storage, glycerol culture stocks were prepared. To do so, 1mL of a culture grown to stationary phase was mixed with 800μL of sterile glycerol (86% (v/v)) and directly stored at -80℃.

4.2.2.2 Transformation of *Saccharomyces cerevisiae* with DNA

The transformation procedure was based on a protocol developed by Gietz *et al.* (1995) and was applied as follows: A 10mL pre-culture of the strain to be transformed was grown overnight ($\sim$16h) or for up to 40h to stationary phase ($OD_{600} \gtrsim 2$). It was then used to inoculate a 25mL culture to an OD_{600} of $\sim$0,1. This main culture was incubated until grown to an OD_{600} between 0,5 and 0,8. Cells were harvested by centrifugation (5min, room temperature, 4500rpm, Swing-out rotor 75006445 in Thermo Scientific Multifuge 3L-R), washed once in 20mL sterile H_2O, once in 10mL LiAc/TE-solution, and resuspended in 100μL LiAc/TE-solution. 1μg of transformation DNA, 8μL denatured salmon sperm DNA solution ($\sim$10mg/mL), and 500μL PEG/LiAc/TE-solution were added to the cells and mixed by vortexing thoroughly. Cells were incubated for at least 1h at 25℃ (up to 3h) and heat-shocked for 20min at 42℃.

200μL of this mix were plated on selection agar plates and incubated at 25℃. When linear dsDNA was transformed, the remaining mix was shortly centrifuged and the PEG supernatant was removed. Pelleted cells were resuspended in 300μL sterile H_2O and plated as well.

4.2.2.3 Genomic Gene Deletion

Genomic genes were deleted by transformation of cells with PCR-generated gene replacement cassettes (figure 4.1A). A gene replacement cassette for gene deletion consisted of two marker genes (*HIS3* or *URA3* in addition to *ADE2*) that were flanked by sequences homologous to the 5'-UTR and 3'-UTR of the target gene, respectively. Employment of the *ADE2* marker allowed for additional selection via red/white screening.

In case that the targeted gene was essential, a rescue vector had been transformed before

deletion. To avoid targeting of a gene replacement cassette to the vector, the *ADH1* promotor was chosen as a 5'-UTR for the rescue construct, whereas the 3'-UTR of the gene was replaced by the *NUF2* 3'-UTR. See table 4.4 for a summary of gene deletion cassettes used in this study.

To verify genomic gene deletion, the genomic locus was analyzed by PCR with primers annealing up- and downstream of the region where homologous recombination occurred.

Table 4.4: Gene deletion cassettes generated by PCR

Deletion cassette	Template	Primer	Rescue vector
NSP1::HIS3-ADE2	pSF1198	SF1110 & SF1111	pMR109
NUP1::URA3-ADE2	pSF1197	SF1090 & SF1091	/
NUP2::URA3-ADE2	pSF1177	SF1092 & SF1093	/
NUP42::URA3-ADE2	pSF1178	SF1094 & SF1095	/
NUP60::URA3-ADE2	pSF1179	SF1096 & SF1097	/
NUP49::HIS3-ADE2	pSF1200	SF1098 & SF1099	pMR62 or pMR114
NUP57::HIS3-ADE2	pSF1201	SF1100 & SF1101	pMR63 or pMR115
NUP145::HIS3-ADE2	pSF1202	SF1102 & SF1103	pSF1126 or pMR116
NUP100::URA3-ADE2	pSF1180	SF1104 & SF1105	/
NUP100::HIS3-ADE2	pMR152	SF1104 & SF1105	pMR151
NUP116::HIS3-ADE2	pSF1203	SF1106 & SF1107	pSF1127 or pMR117
NUP159::HIS3-ADE2	pSF1204	SF1108 & SF1109	pSF1128 or pMR118
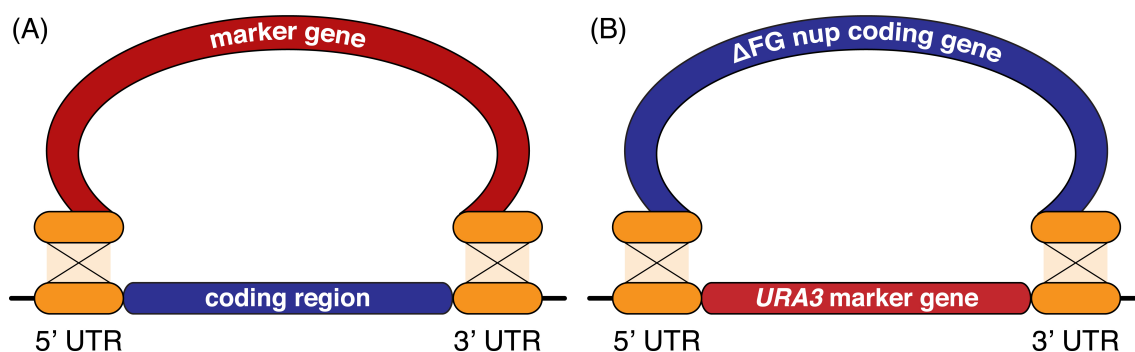
Figure 4.1: Principle of gene deletion and gene insertion via replacement. (A) A selectable marker gene is targeted to the gene of interest by flanking regions, which are homologous to the 5'-UTR and 3'-UTR of the coding region of the target gene. The marker gene is then integrated by homologous recombination and replaces the coding region of the gene of interest. (B) A similar strategy can be applied to integrate a gene coding a ΔFG nucleoporin mutant. To do so, the coding sequence is previously deleted by replacement with the *URA3* marker gene. Insertion of the ΔFG mutant coding gene via homologous recombination results then in cells that are no longer sensitive to FOA (see 4.2.2.9 for details of resistance).

4.2.2.4 Genomic Deletion of FG Domains

Two strategies were applied to genomically delete FG repeat domains of nucleoporins. First, as depicted in figure 4.1 B, a strategy similar to that used for genomic gene deletions was pursued. For this purpose, the nucleoporin gene was previously disrupted by a gene replacement cassette containing the *URA3* marker gene. In case of an essential nucleoporin, the replacement cassette contained the *HIS3* marker gene and the according rescue vector coded the *URA3* marker. Such a strain was then transformed with a second gene replacement cassette (see table 4.5). This cassette contained a gene, which coded for a ΔFG form of the nucleoporin and was flanked by the endogenous UTRs responsible for targeting the cassette to the genomic locus. Replacement cassettes were generated by restriction digestion of the appropriate plasmid. After transformation, cells were incubated in YPD medium over night before counter selection on FOA plates was performed.

Resulting colonies were screened by colony PCR. To further verify correct insertion of the gene replacement cassette and to rule out any unwanted mutation, the genomic locus was amplified by PCR with primers annealing up- and downstream of the regions of homologous recombination and the resulting PCR product was sequenced.

For unknown reasons, this strategy was only successful for some nucleoporin genes. Therefore a second strategy was applied: The genes coding for ΔFG forms of the nucleoporins including their flanking region were cloned into yeast integration vectors (pRS400 series by Sikorski and Hieter, 1989; Christianson *et al.*, 1992) containing the *URA3* and the *ADE2* marker gene. The resulting vectors were linearized by restriction digestion with an endonuclease recognizing a unique target site within the coding region of the nucleoporin gene (see table 4.5).

A vector prepared in this way was then transformed and cells that integrated the vector were selected via plating on CSM-Ura. A successful integration event, i.e. a "loop-in" event, resulted in two copies of the nucleoporin gene at the genomic locus: a wild type and a ΔFG coding allele (figure 4.2 B, page82), respectively. To allow the occurrence of a "loop-out" event (figure 4.2 C), a colony was grown for two days in ∼5mL YPD liquid medium. 5-20μL of this culture were plated on FOA plates and incubated until colonies were visible. Since the "loop-out" event could result in either a wild type or a ΔFG coding version of the gene being present at the locus, resulting colonies were screened by colony PCR. To verify the exclusive presence of the ΔFG allele, genomic DNA was prepared and the genomic locus was amplified by PCR with primers annealing up- and downstream of

the recombination regions. The resulting PCR product was sequenced in order to rule out any unwanted mutation of the coding sequence.

Table 4.5: Constructs for the insertion of mutated nucleoporin genes

Construct	Strategy	Plasmid	Restriction with
nup49∆FG (∆2-236)	Gene insertion via replacement	pMR92	*Not*I & *Xho*I
nup1∆FG (∆382-888)	Gene insertion via replacement	pMR96	*Pvu*I & *Pvu*II & *Eco*RV
nup1∆FG (∆384-1043)	Gene insertion via replacement	pMR97	*Pvu*I & *Pvu*II & *Eco*RV
nup2∆FG (∆189-556)	Gene insertion via replacement	pMR98	*Nsp*I & *Xho*I
nup42∆FG (∆4-364)	Gene insertion via replacement	pMR99	*Acc*I & *Ahd*I
nup60∆FG (∆397-512)	Gene insertion via replacement	pMR100	*Acc*I & *Eco*RI
nsp1∆FG (∆3-602)	Gene domain deletion via loop-in loop-out	pMR139	*Sna*BI
nup57∆FG (∆2-223)	Gene domain deletion via loop-in loop-out	pMR141	*Bsi*WI
nup145∆FG (∆10-209)	Gene domain deletion via loop-in loop-out	pMR142	*Sna*BI
nup100∆FG (∆2-576)	Gene domain deletion via loop-in loop-out	pMR143	*Bmg*BI
nup116∆FG (∆2-714)	Gene domain deletion via loop-in loop-out	pMR326	*Eco*RI
NSP1-GLEBS-fusion construct[a]	Gene domain deletion via loop-in loop-out	pMR288	*Sfo*I

[a] The GLEBS domain of Nup116p (amino acids 105-175) (Bailer *et al.*, 1998) was inserted into the FG domain of Nsp1p between amino acids 271 and 273. The construct codes for the following exact amino acid sequence: Nsp1p 1-271 + KL + Nup116p 105-175 + GLR + Nsp1p 273-602 + T + Nsp1p 603-823.

4.2.2.5 Preparation of Genomic DNA from *Saccharomyces cerevisiae*

Yeast genomic DNA was prepared using the YeaStar™ Genomic DNA kit (Zymo Research, CA, USA) according to the manufacturer's instructions. DNA was eluted in 70μL H_2O.

4.2.2.6 Preparation of Plasmid DNA from *Saccharomyces cerevisiae*

A modified protocol of Singh and Weil (2002) was employed to isolate plasmid DNA from *Saccharomyces cerevisiae* as described below. Solutions and columns of the NucleoSpin® Plasmid Mini kit (Macherey Nagel, Germany) were used.

Cells from a 10mL overnight culture were collected by centrifugation and resuspended in 250μL solution A1. To digest the cell wall, 5μL R-Zymolyase™(1000U/mL; Zymo Research, CA, USA) was added. The mix was thoroughly vortexed and incubated for at least 45min (overnight incubation is possible as well) at 37℃. Cell lysis was then accomplished by addition of 250μL solution A2 followed by a gentle inversion of the reaction tube and incubation at room temperature. After 10min 300μL solution A3 were added and the mix was centrifuged (10min, room temperature, 14.000rpm, Eppendorf table top centrifuge).
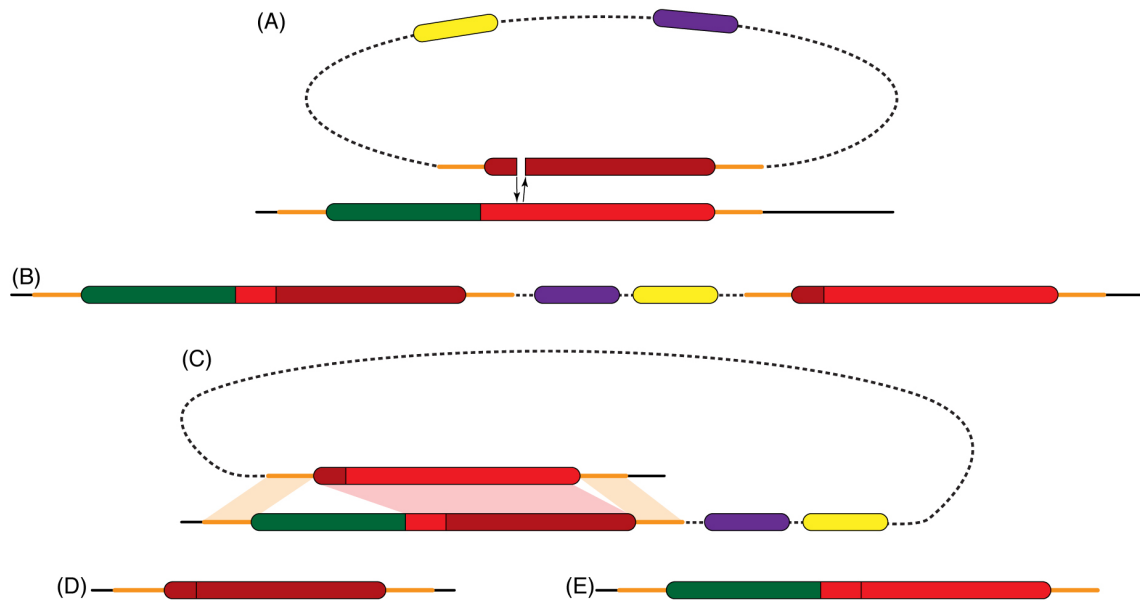
Figure 4.2: Principle of gene domain deletion via loop-in loop-out. (A) Yeast integration vectors are linearized within the coding region of the nucleoporin (red) lacking the FG domain (shown in green for the genomic gene). Non-coding homologous regions are depicted in orange. After transformation, the linearized vector can integrate into the genomic locus as shown in (B) resulting in two copies of the nucleoporin gene (with and without the FG domain, respectively). These are separated by the sequence originating from the yeast integration vector (dashed line, marker genes in yellow and purple, respectively). (C) Due to sequence homology, a loop-out event can occur and recombination can eventuate at any part of the homologous regions, so that the loop-out event can have two different overall results: (D) either recombination occurs in the 5'-UTR (orange) finally resulting in the deletion of the FG domain coding sequence or (E) a wild type situation is restored.

The supernatant was applied to a column via a short centrifugation step. The column was afterwards washed twice with 500μL prewarmed ($\sim$50℃) solution AW and 600μL solution A4 respectively. 50μL H_2O were added and DNA was eluted after 1min incubation at room temperature by centrifugation for 30sec.

4.2.2.7 Colony PCR with *Saccharomyces cerevisiae* cells

Screening of positive clones after transformation of DNA was facilitated by colony PCR, which avoids the need of DNA purification for characterisation. As distinguished from standard PCR (4.2.1.1) whole cells were used as PCR template. Colonies to be tested were picked from a agar plate and resuspended in 25μL digestion buffer containing 50mM Tris (pH8,5) and 50U/mL R-Zymolyase™(Zymo Research, CA, USA). Directly after resuspending the cells, 1μL of the suspension was spotted on fresh agar medium to allow cell growth of the potentially positive clones. The remaining suspension was incubated overnight in an Eppendorf Thermomixer plus at 37℃ with 1300rpm agitation to digest cell walls.

The next day the thermomixer was heated to 95℃ for 10min to denature proteins and thereby lyse the cells. To collect condensed water from the lid of the reaction tubes, the tubes were briefly centrifuged before 1μL of the supernatant was used as a template for the PCR reaction with Tth DNA Polymerase (see 4.2.1.1 for PCR mix and conditions).

4.2.2.8 Sporulation & Tetrad Dissection

Diploid strains were sporulated by growing them first for three days on YPD plates and for further 10 to 16 days on sporulation plates at 25℃. Sporulation was monitored by light-microscopic observation with an Olympus BX50 (Kassir and Simchen, 1991). To detach the wall of the ascus from the spores, tetrads were scratched from the sporulation plate with a sterile inoculating loop. After suspension in 500μL H_2O supplemented with 10μL β-D-glucuronidase/arylsulfatase from *Helix pomatia* (Roche Diagnostics, Mannheim, Germany), tetrads were briefly mixed and incubated for exactly 8min at room temperature (Johnston and Mortimer, 1959). 5-10μL of the suspension were streaked at the edge of a YPD plate. Segregation of the four spores of a tetrad was carried out using a micromanipulator (Singer MSM System Series 300). Dissected spores were allowed to grow for $\sim$7 days at 25℃ before growth behaviour on several selection media was observed.

4.2.2.9 FOA Complementation Assay

This assay allows to monitor the complementation strength of a mutated allele versus the wild type allele of an essential gene.

Crucial for this assay is the cytotoxic effect of the pyrimidine analog 5-fluoro-orotic acid (FOA) in strains bearing a functional *URA3* gene. The *URA3* gene product orotidine-5'-phosphate decarboxylase converts FOA into the toxic compound 5-fluorouracil (Boeke *et al.*, 1984). For this reason wild type yeast cells or cells containing a plasmid coded *URA3* gene are unable to grow on medium containing FOA.

To analyse the complementation strength of a mutated gene, a strain is used, in which an essential gene of interest is coded only by a plasmid containing the *URA3* selection marker gene. This strain is transformed with a second plasmid coding for the mutated allele of the essential gene. If both alleles are functional, cells forfeit one of the two plasmids by a random process. When plated on FOA containing medium, only those cells are able to grow, in which the mutated allele of the gene can complement for the loss of the wild type gene.

The assay was performed as follows: A strain of interest containing a plasmid with the *URA3* selection marker was grown in CSM-Ura medium for up to two days and was then transformed as described in 4.2.2.2 with a second plasmid containing the *LEU2* selection marker. Transformants were selected on double selective plates (CSM-Ura-Leu) to avoid spontaneous mutations of the *URA3* gene. To allow for loss of the *URA3* coding plasmid, a single colony was picked, resuspended in 3mL CSM-Leu medium, and incubated at 25℃ until the culture reached stationary phase (in general after $\sim$40h for strains with multiple FG repeat domain deletions).

Using this culture, cells were diluted in sterile H_2O to yield 1mL with an OD_{600} of 0,6. Ten-fold dilution series of this OD_{600} 0,6 culture were prepared in a 96 well plate (TPP, Trasadingen, Switzerland) and spotted on FOA containing plates, YPD plates, and CSM-Leu plates with a multi channel pipette (Eppendorf research pro). The plates were incubated at 25℃. Pictures of plates were acquired after two to 14 days by scanning with an Epson Perfection V700 Photo Scanner using "Epson Scan" Software (Version 3.28A) set to produce 8bit grayscale images with 400dpi.

4.2.2.10 Temperature Sensitivity Assay

To assay growth properties at a range of temperatures, strains were incubated in 3mL YPD medium at 25℃ until the culture reached stationary phase. Using this culture, cells were diluted in YPD to yield 1mL with an OD_{600} of 0,6. Ten-fold dilution series of this OD_{600} 0,6 culture were prepared in a 96 well plate (TPP, Trasadingen, Switzerland) and spotted on four YPD plates with a multi channel pipette (Eppendorf research pro). The plates were incubated at 16℃, 25℃, 30℃, and 37℃ respectively. Pictures of the plates were acquired after two to 14 days by scanning with an Epson Perfection V700 Photo Scanner using "Epson Scan" Software (Version 3.28A) set to produce 8bit grayscale images with 400dpi.

4.2.3 Confocal Microscopy

Proteins were genetically fused to Citrine (Griesbeck *et al.*, 2001), an enhanced version of the yellow fluorescent protein, to study their intracellular localization. Cells expressing Citrine fusion proteins were grown to stationary phase and 5μL of the culture were directly loaded on Superfrost UltraPlus microscope slides (Menzel GmbH, Braunschweig, Germany). Confocal images were acquired with a Leica SP5 confocal laser scanning microscope equipped with a $20\times$ or $63\times$ immersion objective (Leica, Wetzlar, Germany).

Bibliography

Ader, C., Frey, S., Maas, W., Schmidt, H. B., Görlich, D., and Baldus, M. (2010). Amyloid-like interactions within nucleoporin FG hydrogels. *Proc Natl Acad Sci USA*, 107(14):6281–5.

Aitchison, J. D., Blobel, G., and Rout, M. P. (1995a). Nup120p: a yeast nucleoporin required for NPC distribution and mRNA transport. *J Cell Biol*, 131(6 Pt 2):1659–75.

Aitchison, J. D. and Rout, M. P. (2012). The yeast nuclear pore complex and transport through it. *Genetics*, 190(3):855–83.

Aitchison, J. D., Rout, M. P., Marelli, M., Blobel, G., and Wozniak, R. W. (1995b). Two novel related yeast nucleoporins Nup170p and Nup157p: complementation with the vertebrate homologue Nup155p and functional interactions with the yeast nuclear pore-membrane protein Pom152p. *J Cell Biol*, 131(5):1133–48.

Akey, C. W. and Goldfarb, D. S. (1989). Protein import through the nuclear pore complex is a multistep process. *J Cell Biol*, 109(3):971–82.

Akey, C. W. and Radermacher, M. (1993). Architecture of the Xenopus nuclear pore complex revealed by three-dimensional cryo-electron microscopy. *J Cell Biol*, 122(1):1–19.

Alber, F., Dokudovskaya, S., Veenhoff, L. M., Zhang, W., Kipper, J., Devos, D., Suprapto, A., Karni-Schmidt, O., Williams, R., Chait, B. T., Sali, A., and Rout, M. P. (2007). The molecular architecture of the nuclear pore complex. *Nature*, 450(7170):695–701.

Bahr, G. and Beermann, W. (1954). The fine structure of the nuclear membrane in the larval salivary gland and midgut of Chironomus. *Exp Cell Res*, 6(2):519–22.

Baï, S. W., Rouquette, J., Umeda, M., Faigle, W., Loew, D., Sazer, S., and Doye, V. (2004). The fission yeast Nup107-120 complex functionally interacts with the small GTPase Ran/Spi1 and is required for mRNA export, nuclear pore distribution, and proper cell division. *Mol Cell Biol*, 24(14):6379–92.

Bailer, S. M., Balduf, C., and Hurt, E. (2001). The Nsp1p carboxy-terminal domain is organized into functionally distinct coiled-coil regions required for assembly of nucleoporin subcomplexes and nucleocytoplasmic transport. *Mol Cell Biol*, 21(23):7944–55.

Bailer, S. M., Balduf, C., Katahira, J., Podtelejnikov, A., Rollenhagen, C., Mann, M., Pante, N., and Hurt, E. (2000). Nup116p associates with the Nup82p-Nsp1p-Nup159p nucleoporin complex. *J Biol Chem*, 275(31):23540–8.

Bailer, S. M., Siniossoglou, S., Podtelejnikov, A., Hellwig, A., Mann, M., and Hurt, E. (1998). Nup116p and Nup100p are interchangeable through a conserved motif which constitutes a docking site for the mRNA transport factor Gle2p. *EMBO J*, 17(4):1107–19.

Bayliss, R., Leung, S. W., Baker, R. P., Quimby, B. B., Corbett, A. H., and Stewart, M. (2002a). Structural basis for the interaction between NTF2 and nucleoporin FxFG repeats. *EMBO J*, 21(12):2843–53.

Bayliss, R., Littlewood, T., and Stewart, M. (2000). Structural basis for the interaction between FxFG nucleoporin repeats and importin-beta in nuclear trafficking. *Cell*, 102(1):99–108.

Bayliss, R., Littlewood, T., Strawn, L. A., Wente, S. R., and Stewart, M. (2002b). GLFG and FxFG nucleoporins bind to overlapping sites on importin-beta. *J Biol Chem*, 277(52):50597–606.

Bayliss, R., Ribbeck, K., Akin, D., Kent, H. M., Feldherr, C. M., Görlich, D., and Stewart, M. (1999). Interaction between NTF2 and xFxFG-containing nucleoporins is required to mediate nuclear import of RanGDP. *Journal of Molecular Biology*, 293(3):579–93.

Beck, M., Förster, F., Ecke, M., Plitzko, J. M., Melchior, F., Gerisch, G., Baumeister, W., and Medalia, O. (2004). Nuclear pore complex structure and dynamics revealed by cryoelectron tomography. *Science (New York, NY)*, 306(5700):1387–90.

Beck, M., Lučić, V., Förster, F., Baumeister, W., and Medalia, O. (2007). Snapshots of nuclear pore complexes in action captured by cryo-electron tomography. *Nature*, 449(7162):611–615.

Bednenko, J., Cingolani, G., and Gerace, L. (2003). Importin beta contains a COOH-terminal nucleoporin binding region important for nuclear transport. *J Cell Biol*, 162(3):391–401.

Belanger, K. D., Kenna, M. A., Wei, S., and Davis, L. I. (1994). Genetic and physical interactions between Srp1p and nuclear pore complex proteins Nup1p and Nup2p. *J Cell Biol*, 126(3):619–30.

Belgareh, N., Snay-Hodge, C., Pasteau, F., Dagher, S., Cole, C. N., and Doye, V. (1998). Functional characterization of a Nup159p-containing nuclear pore subcomplex. *Mol Biol Cell*, 9(12):3475–92.

Belov, G. A., Lidsky, P. V., Mikitas, O. V., Egger, D., Lukyanov, K. A., Bienz, K., and Agol, V. I. (2004). Bidirectional increase in permeability of nuclear envelope upon poliovirus infection and accompanying alterations of nuclear pores. *J Virol*, 78(18):10166–77.

Ben-Efraim, I. and Gerace, L. (2001). Gradient of increasing affinity of importin beta for nucleoporins along the pathway of nuclear import. *J Cell Biol*, 152(2):411–7.

Boeke, J. D., LaCroute, F., and Fink, G. R. (1984). A positive selection for mutants lacking orotidine-5'-phosphate decarboxylase activity in yeast: 5-fluoro-orotic acid resistance. *Mol Gen Genet*, 197(2):345–6.

Brohawn, S. G., Leksa, N. C., Spear, E. D., Rajashankar, K. R., and Schwartz, T. U. (2008). Structural evidence for common ancestry of the nuclear pore complex and vesicle coats. *Science (New York, NY)*, 322(5906):1369–73.

Brohawn, S. G., Partridge, J. R., Whittle, J. R. R., and Schwartz, T. U. (2009). The nuclear pore complex has entered the atomic age. *Structure*, 17(9):1156–68.

Brown, J. A., Bharathi, A., Ghosh, A., Whalen, W., Fitzgerald, E., and Dhar, R. (1995). A mutation in the Schizosaccharomyces pombe rae1 gene causes defects in poly(A)+ RNA export and in the cytoskeleton. *J Biol Chem*, 270(13):7411–9.

Chadrin, A., Hess, B., Roman, M. S., Gatti, X., Lombard, B., Loew, D., Barral, Y., Palancade, B., and Doye, V. (2010). Pom33, a novel transmembrane nucleoporin required for proper nuclear pore complex distribution. *J Cell Biol*, 189(5):795–811.

Chial, H. J., Rout, M. P., Giddings, T. H., and Winey, M. (1998). Saccharomyces cerevisiae Ndc1p is a shared component of nuclear pore complexes and spindle pole bodies. *J Cell Biol*, 143(7):1789–800.

Christianson, T. W., Sikorski, R. S., Dante, M., Shero, J. H., and Hieter, P. (1992). Multifunctional yeast high-copy-number shuttle vectors. *Gene*, 110(1):119–22.

Cordes, V. C., Reidenbach, S., Rackwitz, H. R., and Franke, W. W. (1997). Identification of protein p270/Tpr as a constitutive component of the nuclear pore complex-attached intranuclear filaments. *J Cell Biol*, 136(3):515–29.

Cronshaw, J. M., Krutchinsky, A. N., Zhang, W., Chait, B. T., and Matunis, M. J. (2002). Proteomic analysis of the mammalian nuclear pore complex. *J Cell Biol*, 158(5):915–27.

D'Angelo, M. A. and Hetzer, M. W. (2008). Structure, dynamics and function of nuclear pore complexes. *Trends in Cell Biology*, 18(10):456–66.

Davis, L. I. and Blobel, G. (1987). Nuclear pore complex contains a family of glycoproteins that includes p62: glycosylation through a previously unidentified cellular pathway. *Proc Natl Acad Sci USA*, 84(21):7552–6.

Davis, L. I. and Fink, G. R. (1990). The NUP1 gene encodes an essential component of the yeast nuclear pore complex. *Cell*, 61(6):965–78.

de Castillia, C. S., Blobel, G., and Rout, M. P. (1999). Proteins connecting the nuclear pore complex with the nuclear interior. *J Cell Biol*, 144(5):839–55.

Denning, D., Mykytka, B., Allen, N. P., Huang, L., Burlingame, A., and Rexach, M. (2001). The nucleoporin Nup60p functions as a Gsp1p-GTP-sensitive tether for Nup2p at the nuclear pore complex. *J Cell Biol*, 154(5):937–50.

Denning, D. P., Patel, S. S., Uversky, V., Fink, A. L., and Rexach, M. (2003). Disorder in the nuclear pore complex: the FG repeat regions of nucleoporins are natively unfolded. *Proc Natl Acad Sci USA*, 100(5):2450–5.

Denning, D. P. and Rexach, M. F. (2007). Rapid evolution exposes the boundaries of domain structure and function in natively unfolded FG nucleoporins. *Mol Cell Proteomics*, 6(2):272–82.

Denning, D. P., Uversky, V., Patel, S. S., Fink, A. L., and Rexach, M. (2002). The Saccharomyces cerevisiae nucleoporin Nup2p is a natively unfolded protein. *J Biol Chem*, 277(36):33447–55.

Devos, D., Dokudovskaya, S., Alber, F., Williams, R., Chait, B. T., Sali, A., and Rout, M. P. (2004). Components of coated vesicles and nuclear pore complexes share a common molecular architecture. *PLoS Biol*, 2(12):e380.

Dilworth, D. J., Suprapto, A., Padovan, J. C., Chait, B. T., Wozniak, R. W., Rout, M. P., and Aitchison, J. D. (2001). Nup2p dynamically associates with the distal regions of the yeast nuclear pore complex. *J Cell Biol*, 153(7):1465–78.

Eisele, N. B., Frey, S., Piehler, J., Görlich, D., and Richter, R. P. (2010). Ultrathin nucleoporin phenylalanine-glycine repeat films and their interaction with nuclear transport receptors. *EMBO Rep*, 11(5):366–72.

Fabre, E., Boelens, W. C., Wimmer, C., Mattaj, I. W., and Hurt, E. C. (1994). Nup145p is required for nuclear export of mRNA and binds homopolymeric RNA in vitro via a novel conserved motif. *Cell*, 78(2):275–89.

Fabre, E. and Hurt, E. (1997). Yeast genetics to dissect the nuclear pore complex and nucleocytoplasmic trafficking. *Annu Rev Genet*, 31:277–313.

Fabre, E., Schlaich, N. L., and Hurt, E. C. (1995). Nucleocytoplasmic trafficking: what role for repeated motifs in nucleoporins? *Cold Spring Harb Symp Quant Biol*, 60:677–85.

Feldherr, C. M. (1962). The nuclear annuli as pathways for nucleocytoplasmic exchanges. *J Cell Biol*, 14(1):65.

Fernandez-Martinez, J., Phillips, J., Sekedat, M. D., Diaz-Avalos, R., Velazquez-Muriel, J., Franke, J. D., Williams, R., Stokes, D. L., Chait, B. T., Sali, A., and Rout, M. P. (2012). Structure-function mapping of a heptameric module in the nuclear pore complex. *J Cell Biol*, 196(4):419–34.

Feuerbach, F., Galy, V., Trelles-Sticken, E., Fromont-Racine, M., Jacquier, A., Gilson, E., Olivo-Marin, J.-C., Scherthan, H., and Nehrbass, U. (2002). Nuclear architecture and spatial positioning help establish transcriptional states of telomeres in yeast. *Nature Cell Biology*, 4(3):214–21.

Field, M. C. and Dacks, J. B. (2009). First and last ancestors: reconstructing evolution of the endomembrane system with ESCRTs, vesicle coat proteins, and nuclear pore complexes. *Current opinion in cell biology*, 21(1):4–13.

Finlay, D. R. and Forbes, D. J. (1990). Reconstitution of biochemically altered nuclear pores: transport can be eliminated and restored. *Cell*, 60(1):17–29.

Fontoura, B. M., Blobel, G., and Matunis, M. J. (1999). A conserved biogenesis pathway for nucleoporins: proteolytic processing of a 186-kilodalton precursor generates Nup98 and the novel nucleoporin, Nup96. *J Cell Biol*, 144(6):1097–112.

Frey, S. and Görlich, D. (2007). A saturated FG-repeat hydrogel can reproduce the permeability properties of nuclear pore complexes. *Cell*, 130(3):512–23.

Frey, S. and Görlich, D. (2009). FG/FxFG as well as GLFG repeats form a selective permeability barrier with self-healing properties. *The EMBO Journal*, 28(17):2554–67.

Frey, S., Richter, R. P., and Görlich, D. (2006). FG-rich repeats of nuclear pore proteins form a three-dimensional meshwork with hydrogel-like properties. *Science (New York, NY)*, 314(5800):815–7.

Fried, H. and Kutay, U. (2003). Nucleocytoplasmic transport: taking an inventory. *Cell Mol Life Sci*, 60(8):1659–88.

Gall, J. G. (1967). Octagonal nuclear pores. *J Cell Biol*, 32(2):391–9.

Giaever, G., Chu, A. M., Ni, L., Connelly, C., Riles, L., Véronneau, S., Dow, S., Lucau-Danila, A., Anderson, K., André, B., Arkin, A. P., Astromoff, A., El-Bakkoury, M., Bangham, R., Benito, R., Brachat, S., Campanaro, S., Curtiss, M., Davis, K., Deutschbauer, A., Entian, K.-D., Flaherty, P., Foury, F., Garfinkel, D. J., Gerstein, M., Gotte, D., Güldener, U., Hegemann, J. H., Hempel, S., Herman, Z., Jaramillo, D. F., Kelly, D. E., Kelly, S. L., Kötter, P., LaBonte, D., Lamb, D. C., Lan, N., Liang, H., Liao, H., Liu, L., Luo, C., Lussier, M., Mao, R., Menard, P., Ooi, S. L., Revuelta, J. L., Roberts, C. J., Rose, M., Ross-Macdonald, P., Scherens, B., Schimmack, G., Shafer, B., Shoemaker, D. D., Sookhai-Mahadeo, S., Storms, R. K., Strathern, J. N., Valle, G., Voet, M., Volckaert, G., yun Wang, C., Ward, T. R., Wilhelmy, J., Winzeler, E. A., Yang, Y., Yen, G., Youngman, E., Yu, K., Bussey, H., Boeke, J. D., Snyder, M., Philippsen, P., Davis, R. W., and Johnston, M. (2002). Functional profiling of the Saccharomyces cerevisiae genome. *Nature*, 418(6896):387–91.

Gietz, R. D., Schiestl, R. H., Willems, A. R., and Woods, R. A. (1995). Studies on the transformation of intact yeast cells by the LiAc/SS-DNA/PEG procedure. *Yeast*, 11(4):355–60.

Goldstein, A. L., Snay, C. A., Heath, C. V., and Cole, C. N. (1996). Pleiotropic nuclear defects associated with a conditional allele of the novel nucleoporin Rat9p/Nup85p. *Mol Biol Cell*, 7(6):917–34.

Gomez-Ospina, N., Morgan, G., Giddings, T. H., Kosova, B., Hurt, E., and Winey, M. (2000). Yeast nuclear pore complex assembly defects determined by nuclear envelope reconstruction. *J Struct Biol*, 132(1):1–5.

Görlich, D. and Kutay, U. (1999). Transport between the cell nucleus and the cytoplasm. *Annu. Rev. Cell. Dev. Biol.*, 15:607–60.

Gorsch, L. C., Dockendorff, T. C., and Cole, C. N. (1995). A conditional allele of the novel repeat-containing yeast nucleoporin RAT7/NUP159 causes both rapid cessation of mRNA export and reversible clustering of nuclear pore complexes. *J Cell Biol*, 129(4):939–55.

Grandi, P., Doye, V., and Hurt, E. C. (1993). Purification of NSP1 reveals complex formation with 'GLFG' nucleoporins and a novel nuclear pore protein NIC96. *EMBO J*, 12(8):3061–71.

Grandi, P., Schlaich, N., Tekotte, H., and Hurt, E. C. (1995). Functional interaction of Nic96p with a core nucleoporin complex consisting of Nsp1p, Nup49p and a novel protein Nup57p. *EMBO J*, 14(1):76–87.

Griesbeck, O., Baird, G. S., Campbell, R. E., Zacharias, D. A., and Tsien, R. Y. (2001). Reducing the environmental sensitivity of yellow fluorescent protein. Mechanism and applications. *J Biol Chem*, 276(31):29188–94.

Griffis, E. R., Xu, S., and Powers, M. A. (2003). Nup98 localizes to both nuclear and cytoplasmic sides of the nuclear pore and binds to two distinct nucleoporin subcomplexes. *Mol Biol Cell*, 14(2):600–10.

Grote, M., Kubitscheck, U., Reichelt, R., and Peters, R. (1995). Mapping of nucleoporins to the center of the nuclear pore complex by post-embedding immunogold electron microscopy. *J Cell Sci*, 108 (Pt 9):2963–72.

Gustin, K. E. and Sarnow, P. (2001). Effects of poliovirus infection on nucleo-cytoplasmic trafficking and nuclear pore complex composition. *EMBO J*, 20(1-2):240–9.

Gustin, K. E. and Sarnow, P. (2002). Inhibition of nuclear import and alteration of nuclear pore complex composition by rhinovirus. *J Virol*, 76(17):8787–96.

Hetzer, M. W., Walther, T. C., and Mattaj, I. W. (2005). Pushing the envelope: Structure, Function, and Dynamics of the Nuclear Periphery. *Annu. Rev. Cell. Dev. Biol.*, 21(1):347–380.

Hinshaw, J. E., Carragher, B. O., and Milligan, R. A. (1992). Architecture and design of the nuclear pore complex. *Cell*, 69(7):1133–41.

Ho, A. K., Shen, T. X., Ryan, K. J., Kiseleva, E., Levy, M. A., Allen, T. D., and Wente, S. R. (2000). Assembly and preferential localization of Nup116p on the cytoplasmic face of the nuclear pore complex by interaction with Nup82p. *Mol Cell Biol*, 20(15):5736–48.

Hodel, A. E., Hodel, M. R., Griffis, E. R., Hennig, K. A., Ratner, G. A., Xu, S., and Powers, M. A. (2002). The three-dimensional structure of the autoproteolytic, nuclear pore-targeting domain of the human nucleoporin Nup98. *Molecular Cell*, 10(2):347–58.

Hurt, E. C. (1988). A novel nucleoskeletal-like protein located at the nuclear periphery is required for the life cycle of Saccharomyces cerevisiae. *The EMBO Journal*, 7(13):4323–34.

Hurwitz, M. E., de Castillia, C. S., and Blobel, G. (1998). Two yeast nuclear pore complex proteins involved in mRNA export form a cytoplasmically oriented subcomplex. *Proc Natl Acad Sci USA*, 95(19):11241–5.

Iovine, M. K., Watkins, J. L., and Wente, S. R. (1995). The GLFG repetitive region of the nucleoporin Nup116p interacts with Kap95p, an essential yeast nuclear import factor. *J Cell Biol*, 131(6 Pt 2):1699–713.

Iovine, M. K. and Wente, S. R. (1997). A nuclear export signal in Kap95p is required for both recycling the import factor and interaction with the nucleoporin GLFG repeat regions of Nup116p and Nup100p. *J Cell Biol*, 137(4):797–811.

Isgro, T. A. and Schulten, K. (2005). Binding dynamics of isolated nucleoporin repeat regions to importin-beta. *Structure*, 13(12):1869–79.

Johnston, J. and Mortimer, R. (1959). Use of snail digestive juice in isolation of yeast spore tetrads. *J Bacteriol*, 78:292.

Jovanovic-Talisman, T., Tetenbaum-Novatt, J., McKenney, A. S., Zilman, A., Peters, R., Rout, M. P., and Chait, B. T. (2009). Artificial nanopores that mimic the transport selectivity of the nuclear pore complex. *Nature*, 457(7232):1023–7.

Kassir, Y. and Simchen, G. (1991). Monitoring meiosis and sporulation in Saccharomyces cerevisiae. *Meth Enzymol*, 194:94–110.

Kenna, M. A., Petranka, J. G., Reilly, J. L., and Davis, L. I. (1996). Yeast N1e3p/Nup170p is required for normal stoichiometry of FG nucleoporins within the nuclear pore complex. *Mol Cell Biol*, 16(5):2025–36.

Kiseleva, E., Allen, T. D., Rutherford, S., Bucci, M., Wente, S. R., and Goldberg, M. W. (2004). Yeast nuclear pore complexes have a cytoplasmic ring and internal filaments. *J Struct Biol*, 145(3):272–88.

Kiseleva, E., Goldberg, M. W., Allen, T. D., and Akey, C. W. (1998). Active nuclear pore complexes in Chironomus: visualization of transporter configurations related to mRNP export. *J Cell Sci*, 111 (Pt 2):223–36.

Kölling, R., Nguyen, T., Chen, E. Y., and Botstein, D. (1993). A new yeast gene with a myosin-like heptad repeat structure. *Mol Gen Genet*, 237(3):359–69.

Kosova, B., Panté, N., Rollenhagen, C., and Hurt, E. (1999). Nup192p is a conserved nucleoporin with a preferential location at the inner site of the nuclear membrane. *J Biol Chem*, 274(32):22646–51.

Kowalczyk, S. W., Kapinos, L., Blosser, T. R., Magalhães, T., van Nies, P., Lim, R. Y. H., and Dekker, C. (2011). Single-molecule transport across an individual biomimetic nuclear pore complex. *Nature nanotechnology*, 6(7):433–8.

Kubitscheck, U., Grünwald, D., Hoekstra, A., Rohleder, D., Kues, T., Siebrasse, J. P., and Peters, R. (2005). Nuclear transport of single molecules: dwell times at the nuclear pore complex. *J Cell Biol*, 168(2):233–43.

Laurell, E., Beck, K., Krupina, K., Theerthagiri, G., Bodenmiller, B., Horvath, P., Aebersold, R., Antonin, W., and Kutay, U. (2011). Phosphorylation of Nup98 by multiple kinases is crucial for NPC disassembly during mitotic entry. *Cell*, 144(4):539–50.

Lim, R. Y. H., Fahrenkrog, B., Koser, J., Schwarz-Herion, K., Deng, J., and Aebi, U. (2007). Nanomechanical Basis of Selective Gating by the Nuclear Pore Complex. *Science*, 318(5850):640–643.

Lim, R. Y. H., Huang, N.-P., Köser, J., Deng, J., Lau, K. H. A., Schwarz-Herion, K., Fahrenkrog, B., and Aebi, U. (2006). Flexible phenylalanine-glycine nucleoporins as entropic barriers to nucleocytoplasmic transport. *Proc Natl Acad Sci USA*, 103(25):9512–7.

Lusk, C. P., Makhnevych, T., Marelli, M., Aitchison, J. D., and Wozniak, R. W. (2002). Karyopherins in nuclear pore biogenesis: a role for Kap121p in the assembly of Nup53p into nuclear pore complexes. *J Cell Biol*, 159(2):267–78.

Lutzmann, M., Kunze, R., Buerer, A., Aebi, U., and Hurt, E. (2002). Modular self-assembly of a Y-shaped multiprotein complex from seven nucleoporins. *EMBO J*, 21(3):387–97.

Lutzmann, M., Kunze, R., Stangl, K., Stelter, P., Tóth, K. F., Böttcher, B., and Hurt, E. (2005). Reconstitution of Nup157 and Nup145N into the Nup84 complex. *J Biol Chem*, 280(18):18442–51.

Madrid, A. S., Mancuso, J., Cande, W. Z., and Weis, K. (2006). The role of the integral membrane nucleoporins Ndc1p and Pom152p in nuclear pore complex assembly and function. *J Cell Biol*, 173(3):361–71.

Makio, T., Stanton, L. H., Lin, C.-C., Goldfarb, D. S., Weis, K., and Wozniak, R. W. (2009). The nucleoporins Nup170p and Nup157p are essential for nuclear pore complex assembly. *J Cell Biol*, 185(3):459–73.

Meinema, A. C., Laba, J. K., Hapsari, R. A., Otten, R., Mulder, F. A. A., Kralt, A., van den Bogaart, G., Lusk, C. P., Poolman, B., and Veenhoff, L. M. (2011). Long unfolded linkers facilitate membrane protein import through the nuclear pore complex. *Science (New York, NY)*, 333(6038):90–3.

Miao, L. and Schulten, K. (2009). Transport-related structures and processes of the nuclear pore complex studied through molecular dynamics. *Structure*, 17(3):449–59.

Miao, M., Ryan, K. J., and Wente, S. R. (2006). The integral membrane protein Pom34p functionally links nucleoporin subcomplexes. *Genetics*, 172(3):1441–57.

Milles, S. and Lemke, E. A. (2011). Single molecule study of the intrinsically disordered FG-repeat nucleoporin 153. *Biophys J*, 101(7):1710–9.

Mincer, J. S. and Simon, S. M. (2011). Simulations of nuclear pore transport yield mechanistic insights and quantitative predictions. *Proc Natl Acad Sci USA*, 108(31):E351–8.

Mohr, D., Frey, S., Fischer, T., Güttler, T., and Görlich, D. (2009). Characterisation of the passive permeability barrier of nuclear pore complexes. *The EMBO Journal*, 28(17):2541–53.

Moussavi-Baygi, R., Jamali, Y., Karimi, R., and Mofrad, M. R. K. (2011). Brownian dynamics simulation of nucleocytoplasmic transport: a coarse-grained model for the functional state of the nuclear pore complex. *PLoS Comput Biol*, 7(6):e1002049.

Mullis, K., Faloona, F., Scharf, S., Saiki, R., Horn, G., and Erlich, H. (1986). Specific enzymatic amplification of DNA in vitro: the polymerase chain reaction. *Cold Spring Harb Symp Quant Biol*, 51 Pt 1:263–73.

Murphy, R., Watkins, J. L., and Wente, S. R. (1996). GLE2, a Saccharomyces cerevisiae homologue of the Schizosaccharomyces pombe export factor RAE1, is required for nuclear pore complex structure and function. *Mol Biol Cell*, 7(12):1921–37.

Nagy, V., Hsia, K.-C., Debler, E. W., Kampmann, M., Davenport, A. M., Blobel, G., and Hoelz, A. (2009). Structure of a trimeric nucleoporin complex reveals alternate oligomerization states. *Proc Natl Acad Sci USA*, 106(42):17693–8.

Nehrbass, U., Rout, M. P., Maguire, S., Blobel, G., and Wozniak, R. W. (1996). The yeast nucleoporin Nup188p interacts genetically and physically with the core structures of the nuclear pore complex. *J Cell Biol*, 133(6):1153–62.

Neumann, N., Lundin, D., and Poole, A. M. (2010). Comparative genomic evidence for a complete nuclear pore complex in the last eukaryotic common ancestor. *PLoS ONE*, 5(10):e13241.

Onischenko, E., Stanton, L. H., Madrid, A. S., Kieselbach, T., and Weis, K. (2009). Role of the Ndc1 interaction network in yeast nuclear pore complex assembly and maintenance. *J Cell Biol*, 185(3):475–91.

Onischenko, E. and Weis, K. (2011). Nuclear pore complex-a coat specifically tailored for the nuclear envelope. *Current opinion in cell biology*, 23(3):293–301.

Osmani, A. H., Davies, J., Liu, H.-L., Nile, A., and Osmani, S. A. (2006). Systematic deletion and mitotic localization of the nuclear pore complex proteins of Aspergillus nidulans. *Mol Biol Cell*, 17(12):4946–61.

Ovechkina, Y., Maddox, P., Oakley, C. E., Xiang, X., Osmani, S. A., Salmon, E. D., and Oakley, B. R. (2003). Spindle formation in Aspergillus is coupled to tubulin movement into the nucleus. *Mol Biol Cell*, 14(5):2192–200.

Paine, P. L. and Feldherr, C. M. (1972). Nucleocytoplasmic exchange of macromolecules. *Exp Cell Res*, 74(1):81–98.

Paine, P. L., Moore, L. C., and Horowitz, S. B. (1975). Nuclear envelope permeability. *Nature*, 254(5496):109–14.

Palmer, B. R. and Marinus, M. G. (1994). The dam and dcm strains of Escherichia coli–a review. *Gene*, 143(1):1–12.

Park, N., Katikaneni, P., Skern, T., and Gustin, K. E. (2008). Differential targeting of nuclear pore complex proteins in poliovirus-infected cells. *J Virol*, 82(4):1647–55.

Patel, S. S., Belmont, B. J., Sante, J. M., and Rexach, M. F. (2007). Natively unfolded nucleoporins gate protein diffusion across the nuclear pore complex. *Cell*, 129(1):83–96.

Peters, R. (2005). Translocation through the nuclear pore complex: selectivity and speed by reduction-of-dimensionality. *Traffic*, 6(5):421–7.

Peters, R. (2009). Translocation through the nuclear pore: Kaps pave the way. *Bioessays*, 31(4):466–77.

Powers, M. A., Macaulay, C., Masiarz, F. R., and Forbes, D. J. (1995). Reconstituted nuclei depleted of a vertebrate GLFG nuclear pore protein, p97, import but are defective in nuclear growth and replication. *J Cell Biol*, 128(5):721–36.

Priore, V. D., Heath, C., Snay, C., MacMillan, A., Gorsch, L., Dagher, S., and Cole, C. (1997). A structure/function analysis of Rat7p/Nup159p, an essential nucleoporin of Saccharomyces cerevisiae. *J Cell Sci*, 110 (Pt 23):2987–99.

Pritchard, C. E., Fornerod, M., Kasper, L. H., and van Deursen, J. M. (1999). RAE1 is a shuttling mRNA export factor that binds to a GLEBS-like NUP98 motif at the nuclear pore complex through multiple domains. *J Cell Biol*, 145(2):237–54.

Radu, A., Moore, M. S., and Blobel, G. (1995). The peptide repeat domain of nucleoporin Nup98 functions as a docking site in transport across the nuclear pore complex. *Cell*, 81(2):215–22.

Ratner, G. A., Hodel, A. E., and Powers, M. A. (2007). Molecular Determinants of Binding between Gly-Leu-Phe-Gly Nucleoporins and the Nuclear Pore Complex. *Journal of Biological Chemistry*, 282(47):33968–33976.

Reichelt, R., Holzenburg, A., Buhle, E. L., Jarnik, M., Engel, A., and Aebi, U. (1990). Correlation between structure and mass distribution of the nuclear pore complex and of distinct pore complex components. *J Cell Biol*, 110(4):883–94.

Ribbeck, K. and Görlich, D. (2001). Kinetic analysis of translocation through nuclear pore complexes. *EMBO J*, 20(6):1320–30.

Ribbeck, K. and Görlich, D. (2002). The permeability barrier of nuclear pore complexes appears to operate via hydrophobic exclusion. *EMBO J*, 21(11):2664–71.

Rout, M. P., Aitchison, J. D., Magnasco, M. O., and Chait, B. T. (2003). Virtual gating and nuclear transport: the hole picture. *Trends in Cell Biology*, 13(12):622–8.

Rout, M. P., Aitchison, J. D., Suprapto, A., Hjertaas, K., Zhao, Y., and Chait, B. T. (2000). The yeast nuclear pore complex: composition, architecture, and transport mechanism. *J Cell Biol*, 148(4):635–51.

Rout, M. P. and Blobel, G. (1993). Isolation of the yeast nuclear pore complex. *J Cell Biol*, 123(4):771–83.

Rout, M. P. and Wente, S. R. (1994). Pores for thought: nuclear pore complex proteins. *Trends in Cell Biology*, 4(10):357–65.

Saavedra, C. A., Hammell, C. M., Heath, C. V., and Cole, C. N. (1997). Yeast heat shock mRNAs are exported through a distinct pathway defined by Rip1p. *Genes Dev*, 11(21):2845–56.

Sambrook, J. and Russell, D. W. (2001). Molecular Cloning: A Laboratory Manual. *Cold Spring Harbor Laboratory Press, NY*, (3).

Sauer, B. (1987). Functional expression of the cre-lox site-specific recombination system in the yeast Saccharomyces cerevisiae. *Mol Cell Biol*, 7(6):2087–96.

Sauer, B. (1998). Inducible gene targeting in mice using the Cre/lox system. *Methods*, 14(4):381–92.

Schlaich, N. L., Häner, M., Lustig, A., Aebi, U., and Hurt, E. C. (1997). In vitro reconstitution of a heterotrimeric nucleoporin complex consisting of recombinant Nsp1p, Nup49p, and Nup57p. *Mol Biol Cell*, 8(1):33–46.

Schrader, N., Stelter, P., Flemming, D., Kunze, R., Hurt, E., and Vetter, I. R. (2008). Structural basis of the nic96 subcomplex organization in the nuclear pore channel. *Molecular Cell*, 29(1):46–55.

Sherman, F. (2002). Getting started with yeast. *Meth Enzymol*, 350:3–41.

Sikorski, R. S. and Hieter, P. (1989). A system of shuttle vectors and yeast host strains designed for efficient manipulation of DNA in Saccharomyces cerevisiae. *Genetics*, 122(1):19–27.

Singh, M. V. and Weil, P. A. (2002). A method for plasmid purification directly from yeast. *Anal Biochem*, 307(1):13–7.

Siniossoglou, S., Lutzmann, M., Santos-Rosa, H., Leonard, K., Mueller, S., Aebi, U., and Hurt, E. (2000). Structure and assembly of the Nup84p complex. *J Cell Biol*, 149(1):41–54.

Siniossoglou, S., Wimmer, C., Rieger, M., Doye, V., Tekotte, H., Weise, C., Emig, S., Segref, A., and Hurt, E. C. (1996). A novel complex of nucleoporins, which includes Sec13p and a Sec13p homolog, is essential for normal nuclear pores. *Cell*, 84(2):265–75.

Snow, C. M., Senior, A., and Gerace, L. (1987). Monoclonal antibodies identify a group of nuclear pore complex glycoproteins. *J Cell Biol*, 104(5):1143–56.

Souza, C. P. C. D., Osmani, A. H., Hashmi, S. B., and Osmani, S. A. (2004). Partial nuclear pore complex disassembly during closed mitosis in Aspergillus nidulans. *Curr Biol*, 14(22):1973–84.

Stelter, P., Kunze, R., Flemming, D., Höpfner, D., Diepholz, M., Philippsen, P., Böttcher, B., and Hurt, E. (2007). Molecular basis for the functional interaction of dynein light chain with the nuclear-pore complex. *Nat Cell Biol*, 9(7):788–96.

Stoffler, D., Feja, B., Fahrenkrog, B., Walz, J., Typke, D., and Aebi, U. (2003). Cryo-electron tomography provides novel insights into nuclear pore architecture: implications for nucleocytoplasmic transport. *Journal of Molecular Biology*, 328(1):119–30.

Strawn, L. A., Shen, T., Shulga, N., Goldfarb, D. S., and Wente, S. R. (2004). Minimal nuclear pore complexes define FG repeat domains essential for transport. *Nat Cell Biol*, 6(3):197–206.

Stutz, F., Kantor, J., Zhang, D., McCarthy, T., Neville, M., and Rosbash, M. (1997). The yeast nucleoporin rip1p contributes to multiple export pathways with no essential role for its FG-repeat region. *Genes Dev*, 11(21):2857–68.

Stutz, F., Neville, M., and Rosbash, M. (1995). Identification of a novel nuclear pore-associated protein as a functional target of the HIV-1 Rev protein in yeast. *Cell*, 82(3):495–506.

Suelmann, R., Sievers, N., and Fischer, R. (1997). Nuclear traffic in fungal hyphae: in vivo study of nuclear migration and positioning in Aspergillus nidulans. *Mol Microbiol*, 25(4):757–69.

Teixeira, M. T., Siniossoglou, S., Podtelejnikov, S., Bénichou, J. C., Mann, M., Dujon, B., Hurt, E., and Fabre, E. (1997). Two functionally distinct domains generated by in vivo cleavage of Nup145p: a novel biogenesis pathway for nucleoporins. *EMBO J*, 16(16):5086–97.

Terry, L. J. and Wente, S. R. (2007). Nuclear mRNA export requires specific FG nucleoporins for translocation through the nuclear pore complex. *J Cell Biol*, 178(7):1121–32.

Terry, L. J. and Wente, S. R. (2009). Flexible gates: dynamic topologies and functions for FG nucleoporins in nucleocytoplasmic transport. *Eukaryotic Cell*, 8(12):1814–27.

Thomas, J. H. and Botstein, D. (1986). A gene required for the separation of chromosomes on the spindle apparatus in yeast. *Cell*, 44(1):65–76.

Wälde, S. and Kehlenbach, R. H. (2010). The Part and the Whole: functions of nucleoporins in nucleocytoplasmic transport. *Trends in Cell Biology*, 20(8):461–9.

Weirich, C. S., Erzberger, J. P., Berger, J. M., and Weis, K. (2004). The N-terminal domain of Nup159 forms a beta-propeller that functions in mRNA export by tethering the helicase Dbp5 to the nuclear pore. *Molecular Cell*, 16(5):749–60.

Wente, S. R. and Blobel, G. (1993). A temperature-sensitive NUP116 null mutant forms a nuclear envelope seal over the yeast nuclear pore complex thereby blocking nucleocytoplasmic traffic. *J Cell Biol*, 123(2):275–84.

Wente, S. R. and Blobel, G. (1994). NUP145 encodes a novel yeast glycine-leucine-phenylalanine-glycine (GLFG) nucleoporin required for nuclear envelope structure. *J Cell Biol*, 125(5):955–69.

Wente, S. R., Rout, M. P., and Blobel, G. (1992). A new family of yeast nuclear pore complex proteins. *J Cell Biol*, 119(4):705–23.

Whittle, J. R. R. and Schwartz, T. U. (2009). Architectural nucleoporins Nup157/170 and Nup133 are structurally related and descend from a second ancestral element. *Journal of Biological Chemistry*, 284(41):28442–52.

Wimmer, C., Doye, V., Grandi, P., Nehrbass, U., and Hurt, E. C. (1992). A new subclass of nucleoporins that functionally interact with nuclear pore protein NSP1. *EMBO J*, 11(13):5051–61.

Winey, M., Hoyt, M. A., Chan, C., Goetsch, L., Botstein, D., and Byers, B. (1993). NDC1: a nuclear periphery component required for yeast spindle pole body duplication. *J Cell Biol*, 122(4):743–51.

Wischnitzer, S. (1958). An electron microscope study of the nuclear envelope of amphibian oocytes. *J Ultrastruct Res*, 1(3):201–22.

Wozniak, R. W., Blobel, G., and Rout, M. P. (1994). POM152 is an integral protein of the pore membrane domain of the yeast nuclear envelope. *J Cell Biol*, 125(1):31–42.

Yamada, J., Phillips, J. L., Patel, S., Goldfien, G., Calestagne-Morelli, A., Huang, H., Reza, R., Acheson, J., Krishnan, V. V., Newsam, S., Gopinathan, A., Lau, E. Y., Colvin, M. E., Uversky, V. N., and Rexach, M. F. (2010). A bimodal distribution of two distinct categories of intrinsically disordered structures with separate functions in FG nucleoporins. *Mol Cell Proteomics*, 9(10):2205–24.

Yang, Q., Rout, M., and Akey, C. (1998). Three-dimensional architecture of the isolated yeast nuclear pore complex: functional and evolutionary implications. *Molecular Cell*, 1(2):223–234.

Yang, W. (2011). 'Natively unfolded' nucleoporins in nucleocytoplasmic transport: Clustered or evenly distributed? *Nucleus (Austin, Tex)*, 2(1):10–16.

Yang, W. and Musser, S. M. (2006). Nuclear import time and transport efficiency depend on importin beta concentration. *J Cell Biol*, 174(7):951–61.

Yoshida, K., Seo, H.-S., Debler, E. W., Blobel, G., and Hoelz, A. (2011). Structural and functional analysis of an essential nucleoporin heterotrimer on the cytoplasmic face of the nuclear pore complex. *Proc Natl Acad Sci USA*, 108(40):16571–6.

Zabel, U., Doye, V., Tekotte, H., Wepf, R., Grandi, P., and Hurt, E. C. (1996). Nic96p is required for nuclear pore formation and functionally interacts with a novel nucleoporin, Nup188p. *J Cell Biol*, 133(6):1141–52.

Zeitler, B. and Weis, K. (2004). The FG-repeat asymmetry of the nuclear pore complex is dispensable for bulk nucleocytoplasmic transport in vivo. *J Cell Biol*, 167(4):583–90.

Abbreviations

aa	Amino acid
ATP	Adenosine triphosphate
bp	Base pairs
BSA	Bovine serum albumin
dATP	Deoxyadenosine triphosphate
dCTP	Deoxycytosine triphosphate
dGTP	Deoxyguanosine triphosphate
DID	Dynein light chain interacting domain
DMSO	Dimethylsulfoxide
DNA	Deoxyribonucleic acid
dpi	Dots per inch
DTT	Dithiothreitol
dTTP	Deoxythymidine triphosphate
EDTA	Ethylenediaminetetraacetic acid
FG	Phenylalanine-glycine
FOA	5'-Fluoroorotic Acid
GLEBS	Gle2p binding site
hr	Hour(s)
min	Minute(s)
mRNA	Messenger ribonucleic acid
N-	Amino-
NE	Nuclear envelope
NPC	Nuclear pore complex
NRM	Nucleoporin RNA-binding motif
NTR	Nuclear transport receptor
nup	Nucleoporin
OD	Optical density at 600nm
PCR	Polymerase chain reaction
rpm	Rounds per minute
RT	Room temperature
SDS	Sodium dodecyl sulphate
sec	Second(s)
Tris	Tris(hydroxymethyl)aminomethane
v/v	Volume/volume
w/v	Weight/volume